

Testing and evaluating non-extractive  
sampling platforms to assess deep-water  
rocky reef ecosystems on the  
continental shelf

Jan Seiler

BSc (Applied Marine Biology)



Submitted in fulfilment of the requirements for the Degree of Doctor  
of Philosophy, in the CSIRO-UTAS PhD Program in Quantitative  
Marine Science  
at University of Tasmania.

---

Institute for Marine and Antarctic Studies, University of Tasmania  
January 16, 2013

---

---

---

## Statement of Declaration

I declare that this thesis contains no material which has been accepted for a degree or diploma by the University or any other institution, except by way of background information and duly acknowledged in the thesis, and to the best of my knowledge and belief no material previously published or written by another person except where due acknowledgement is made in the text of the thesis, nor does the thesis contain any material that infringes copyright.

The publishers of the papers comprising Chapters 3 and 5 hold the copyright for that content, and access to the material should be sought from the respective journals. The remaining non published content of the thesis may be made available for loan and limited copying and communication in accordance with the *Copyright Act 1968*.

Jan Seiler



---

## Abstract

Traditional extractive sampling methods, such as netting and trawling, to assess benthic species diversity, size and abundance are unable to sample complex hard substrates, e.g., rocky reefs. This inability led to the development of alternative non-extractive sampling platforms, such as digital stills and video cameras mounted onto stationary or moving platforms. This thesis examined two moving platforms, autonomous underwater vehicle (AUV) and towed video platform and one stationary platform, stereo baited underwater video systems (BUVS). These platforms were used as sampling tools to assess reef fish diversity, size distribution and absolute and relative abundance in complex deep-water (30 – 100 m) rocky reefs in temperate Australia (Tasmania). Each platform was evaluated with respect to their efficiency and reliability within a sustainable resource management framework. A novel feature extraction routine, using colour, texture, patch-gap summaries and rugosity, to semi-automatically classify AUV images into habitat classes is proposed. Here, the randomForest classification tree algorithm was used to assign habitat classes to images after initial training (i.e., 500 images annotated by a trained human expert). Classifier accuracy was assessed using this human scored image set. Habitat prediction accuracy was 84% (with a kappa statistic of 0.793).

The evaluation of stereo BUVS as a tool to inventory and monitor deep-water temperate reef fish diversity can inform resource managers of advantages and

---

disadvantages of this particular sampling platform. Species richness and relative abundance across different survey sites over two years were investigated. In addition, stereophotogrammetric fish length estimation of two commercially important species, striped trumpeter (*Latris lineata*) and blue-throated wrasse (*Notolabrus tetricus*), were utilised to set a benchmark for future reference and compared to line-fishing (*L. lineata*) and trapping data (*N. tetricus*).

All three platforms were compared to evaluate their ability to assess reef fish diversity and abundance. Sample variability for each tool was assessed statistically and synergy between platforms proposed. The cost-effectiveness of each platform was assessed qualitatively.

An assessment of the size and abundance distribution of the ocean perch *Helicolenus percooides* was conducted using photographic records taken by the AUV. Stereophotogrammetric size estimates were converted into biomass and examined with respect to depth and habitat types. Habitat preferences of adult and juvenile ocean perch were also investigated. The results suggest that AUV *Sirius* is a mature survey platform in complex hard substratum environments. The utility of this non-extractive sampling tool in a fisheries context is discussed.

Non-extractive imagery-yielding sampling platforms provide useful alternatives when sampling complex environments. Data quality, derived from imagery, is benefitting from rapidly developing technology, e.g., high-definition video and megapixel digital cameras. Non-extractive methods provide the only means to sample marine protected areas. Advantages and disadvantages of each platform are now readily accessible to advise resource management agencies.

---

---

---

# Contents

<b>Statement of Declaration</b>	<b>i</b>
<b>Abstract</b>	<b>iii</b>
<b>Contents</b>	<b>vii</b>
<b>List of Figures</b>	<b>xv</b>
<b>List of Tables</b>	<b>xvii</b>
<b>Statement of co-author contributions</b>	<b>xix</b>
<b>Acknowledgements</b>	<b>xxiii</b>
<b>1 Introduction</b>	<b>1</b>
1.1 In a nutshell . . . . .	1
1.2 Sustainable resource management – a fisheries example . . . . .	1
1.3 Australia’s recent EBM history . . . . .	3
1.4 Consequences of adopting EBM . . . . .	4
1.5 Current EBM challenges . . . . .	5
1.6 Solutions – thesis objectives . . . . .	7
1.7 Thesis outcomes and future research . . . . .	12

---

<b>2</b>	<b>Data acquisition</b>	<b>17</b>
2.1	Introduction . . . . .	17
2.2	Study area . . . . .	18
2.3	Bathymetric mapping . . . . .	20
2.4	Autonomous Underwater Vehicle . . . . .	20
2.4.1	AUV camera calibration . . . . .	21
2.4.2	AUV sampling design . . . . .	23
2.4.3	AUV image annotation . . . . .	24
2.5	Baited Underwater Video Systems . . . . .	25
2.5.1	BUVS design and components . . . . .	26
2.5.2	BUVS camera calibration . . . . .	28
2.5.3	BUVS sampling design . . . . .	29
2.5.4	BUVS video annotation . . . . .	32
2.6	Towed video platform . . . . .	34
2.6.1	Towed video sampling design . . . . .	34
2.6.2	Towed video annotation . . . . .	36
<b>3</b>	<b>Image-based continental shelf habitat mapping using novel automated data extraction techniques</b>	<b>39</b>
3.1	Abstract . . . . .	39
3.2	Introduction . . . . .	40

---

3.3	Methods . . . . .	44
3.3.1	Study area . . . . .	44
3.3.2	Data acquisition . . . . .	45
3.3.3	Automated feature extraction . . . . .	46
3.3.4	Modified hue-saturation values (HSV) . . . . .	47
3.3.5	Local binary pattern (LBP) . . . . .	49
3.3.6	Patch-gap summaries . . . . .	50
3.3.7	Deriving rugosity . . . . .	52
3.3.8	Manual image scoring . . . . .	52
3.3.9	Random forests classifier training and evaluation . . . . .	53
3.4	Results . . . . .	58
3.4.1	Prediction accuracy . . . . .	58
3.4.2	Predictor importance . . . . .	59
3.4.3	Confusion matrices . . . . .	60
3.4.4	$\chi^2$ and permutation . . . . .	62
3.4.5	Multi-dimensional scaling and proximity . . . . .	65
3.4.6	Habitat mapping . . . . .	66
3.5	Discussion . . . . .	69

---

<b>4</b>	<b>Beyond diver's depth: evaluating stereo baited underwater video systems as a tool to monitor deep-water temperate reef fish assemblages on the continental shelf</b>	<b>75</b>
4.1	Abstract . . . . .	75
4.2	Introduction . . . . .	76
4.2.1	Individual species abundances of reef fish assemblages . . . . .	80
4.2.2	Size structure of two commercial species . . . . .	81
4.2.3	Improving estimates of relative abundance . . . . .	82
4.2.4	Power analysis . . . . .	82
4.3	Material and Methods . . . . .	84
4.3.1	Composition of reef fish assemblages . . . . .	86
4.3.2	Individual species abundances of reef fish assemblages . . . . .	89
4.3.3	Size structure of two commercial species . . . . .	90
4.3.4	Improving estimates of relative abundance . . . . .	91
4.3.5	Power analysis . . . . .	93
4.4	Results . . . . .	95
4.4.1	Composition of reef fish assemblages . . . . .	95
4.4.2	Individual species abundances of reef fish assemblages . . . . .	99
4.4.3	Size structure of two commercial species obtained by photogrammetric length estimation . . . . .	101
4.4.4	Improving estimates of relative abundance . . . . .	108

---

4.4.5	Power analysis . . . . .	110
4.5	Discussion . . . . .	114
4.5.1	Composition of reef fish assemblages . . . . .	114
4.5.2	Individual species abundances of reef fish assemblages . . . . .	117
4.5.3	Size structure of two commercial species obtained by photogrammetric length estimation . . . . .	118
4.5.4	Improving estimates of relative abundance . . . . .	121
4.5.5	Power analysis . . . . .	125
4.6	Conclusion . . . . .	126
<b>5</b>	<b>Assessing size, abundance and habitat preferences of the ocean perch <i>Helicolenus percoides</i> using a AUV-borne stereo camera system</b>	<b>127</b>
5.1	Abstract . . . . .	127
5.2	Introduction . . . . .	128
5.3	Material and Methods . . . . .	131
5.3.1	Field Sampling . . . . .	131
5.3.2	Data acquisition and processing . . . . .	133
5.3.3	Statistical analysis . . . . .	137
5.4	Results . . . . .	142
5.4.1	Measurement precision . . . . .	142
5.4.2	Habitat association and spatial autocorrelation . . . . .	142
5.4.3	Fish occurrence, length and biomass . . . . .	143
5.4.4	Habitat preferences . . . . .	148
5.5	Discussion . . . . .	151
5.5.1	Distribution and size composition of <i>H. percoides</i> across habitat types . . . . .	151
5.5.2	Improving efficiency and quality of image-based data . . . . .	154
5.5.3	Utility of AUV <i>Sirius</i> for fishery assessments . . . . .	157

---

<b>6</b>	<b>A continental shelf deep-water temperate reef fish assemblage recorded by three different non-extractive image-yielding platforms – a comparison</b>	<b>161</b>
6.1	Abstract . . . . .	161
6.2	Introduction . . . . .	162
6.3	Materials and methods . . . . .	165
6.3.1	Study area and sites . . . . .	165
6.3.2	Sampling platforms . . . . .	166
6.3.3	Data analysis . . . . .	170
6.4	Results . . . . .	172
6.4.1	Species richness and total number of individuals . . . . .	172
6.4.2	Individual species abundances . . . . .	178
6.5	Discussion . . . . .	186
6.5.1	Platform strengths and weaknesses . . . . .	187
6.5.2	To bait, or not to bait . . . . .	192
6.5.3	Dissecting assemblage composition – platform-specific species detection . . . . .	195
6.5.4	Future research . . . . .	195
6.5.5	Concluding remarks . . . . .	196
<b>7</b>	<b>Discussion and conclusion</b>	<b>197</b>
7.1	Summary of achievements . . . . .	197

---

7.1.1	Introduction . . . . .	197
7.1.2	Mapping marine habitats – essential information for sustainable resource management . . . . .	198
7.1.3	Beyond diver’s depth – assessing reef-fish assemblages using baited underwater video systems . . . . .	200
7.1.4	Collecting fisheries-independent stock assessment data using a stereo-vision AUV . . . . .	201
7.1.5	Observing deep-water temperate rocky reef fish assemblages on the continental shelf using three non-extractive sampling platforms . . . . .	202
7.1.6	Utilising non-extractive imagery-yielding samplers in an ecosystem-based management context . . . . .	203
7.2	Future research . . . . .	205
7.2.1	AUV . . . . .	205
7.2.2	BUVS . . . . .	208
7.2.3	Size selectivity . . . . .	210
7.3	Summary . . . . .	211

<b>References</b>	<b>213</b>
-------------------	------------

---

---

## List of Figures

1.1	Schema diagram elucidating thesis structure . . . . .	15
2.1	Study area location . . . . .	19
2.2	Autonomous Underwater Vehicle schematic . . . . .	23
2.3	Schematic of BUVS unit . . . . .	28
2.4	Calibration cube . . . . .	30
2.5	Schematic of towed video system . . . . .	35
3.1	Study area off O'Hara Bluff with superimposed AUV transect . . . . .	45
3.2	Schematic illustrating the concept of Local Binary Patterns (LBP) . . . . .	50
3.3	Example images for each habitat class . . . . .	55
3.4	Comparison of different predictors . . . . .	59
3.5	Predictor importance . . . . .	61
3.6	Frequency of occurrence of observed and predicted habitat classes . . . . .	64
3.7	Multi-dimensional scaling plot of the proximity matrix . . . . .	67
3.8	Colour-coded observed and predicted habitat classes . . . . .	68
4.1	Map depicting BUVS deployments . . . . .	85
4.2	Two-dimensional nMDS plot of inshore and offshore fish assemblages . . . . .	97

---

4.3	Spearman’s ranked correlation coefficient $\rho$ for complexity measures and fish assemblage composition . . . . .	98
4.4	Species accumulation curve against estimates . . . . .	100
4.5	Size and weight frequency histogram of striped trumpeter . . . . .	104
4.6	Size frequency histogram of blue-throated wrasse . . . . .	106
4.7	<i>N. tetricus</i> by depth probability . . . . .	107
4.8	Barplot of fit and line plot of statistical power . . . . .	112
4.9	Line plot of statistical power and sample size . . . . .	113
5.1	AUV dive locations . . . . .	132
5.2	Calibration chequerboard . . . . .	135
5.3	PhotoMeasure user interface . . . . .	137
5.4	Histogram of measurement error . . . . .	143
5.5	Correlograms with 95% point-wise bootstrap confidence intervals . . .	144
5.6	Mean biomass in gram of <i>H. percooides</i> by habitat . . . . .	145
5.7	GLMM predicted probabilities of <i>H. percooides</i> presence per image . .	147
5.8	Histograms of <i>H. percooides</i> length and weight . . . . .	148
5.9	Habitat preference index by habitat . . . . .	150
5.10	Percentage of juveniles and adult fish by habitat . . . . .	151
6.1	AUV, BUVS, towed video sampling locations . . . . .	167
6.2	Barplot of mean species richness and total number of individuals at each site for each platform . . . . .	179
6.3	Barplot of selected mean species abundance at each site for each platform . . . . .	181
6.4	nMDS plot based on fourth-root transformed species composition . .	183
6.5	nMDS plot based on species presence/absence . . . . .	184
6.6	Species accumulation curve for each platform . . . . .	186

---

## List of Tables

2.1	List of AUV specifications and sensors . . . . .	22
2.2	Habitat types scored during AUV image annotation with brief description . . . . .	25
3.1	Overview of extracted image features and brief description . . . . .	48
3.2	Habitat class code, habitat class, brief habitat description and frequency of occurrence . . . . .	54
3.3	Confusion matrix for habitat classification prediction . . . . .	63
4.1	Habitat complexity measures derived from DEM with definition and references . . . . .	88
4.2	Total species richness estimates . . . . .	99
4.3	Species and common names and total <i>MaxN</i> count of the five most numerous fish species in the BUVS data set . . . . .	99
4.4	Negative binomial GLM results comparing fish abundance between inshore and offshore sites . . . . .	102
4.5	<i>MaxN</i> and <i>N</i> comparison <i>L. lineata</i> . . . . .	109
4.6	<i>MaxN</i> and <i>N</i> comparison <i>N. tetricus</i> . . . . .	111
4.7	Distribution and parameters $\mu$ and $k$ used in the power analysis for the three species . . . . .	113
5.1	ANOVA results for <i>H. percoides</i> biomass in response to habitat . . . . .	148
6.1	Species list . . . . .	174

---

6.2	ANOVA results for species richness and abundance in response to site and platform . . . . .	178
6.3	Univariate ANOVA results for <i>C. lepidoptera</i> and <i>P. psittaculus</i> $\ln(x + 1)$ transformed abundance data in response to site and platform.	181
6.4	GLMs parameter estimates for untransformed <i>Helicolenus percoides</i> and <i>Nemadactylus macropterus</i> counts . . . . .	182
6.5	PERMANOVA results based on Bray-Curtis dissimilarity of fourth-root transformed relative abundance and presence/absence data. The two factors P and S refer to platform and site, respectively. . . . .	183

---

## Statement of co-author contributions

Chapters 3 and 5 of this thesis have been accepted for publication in peer-reviewed journals. Research design and implementation, data analysis, interpretation of results and manuscript preparation were the sole responsibility of the research candidate in consultation with supervisors and with input from specialist contributors.

The following people and institutions contributed to the publication of work undertaken as part of this thesis:

Jan Seiler (University of Tasmania)

Ariell Friedman and Daniel Steinberg (University of Sydney)

Dr Alan Williams (CSIRO)

Dr Neville Barrett and Dr Neil Holbrook (University of Tasmania)

Author details and their roles:

The candidate was the primary author for the publication “Image-based continental shelf habitat mapping using novel automated data extraction techniques”

---

(Continental Shelf Research, doi.10.1016/j.csr.2012.06.003), located in chapter 3. Ariell Friedman and Daniel Steinberg extracted additional image features to extent the suite of predictors for the random forests model. Dr Alan Williams, Dr Neville Barrett and Dr Neil Holbrook provided advice on approaches to habitat mapping and commented the manuscript.

Jan Seiler (University of Tasmania)

Dr Alan Williams (CSIRO)

Dr Neville Barrett (University of Tasmania)

Author details and their roles:

The candidate was the primary author for the publication “Assessing size, abundance and habitat preferences of the Ocean perch *Helicolenus percooides* using a AUV-borne stereo camera system” (Fisheries Research, doi:10.1016/j.fishres.2012.06.011), located in chapter 5. Dr Alan Williams and Dr Neville Barrett provided advice on approaches to assess benthic reef fish stocks and commented the manuscript.

We the undersigned agree with the above stated “proportion of work undertaken” for each of the above published (or submitted) peer-reviewed manuscripts contributing to this thesis:

---

Signed:

---

Neville Barrett

Supervisor

IMAS

University of Tasmania

Head of School

IMAS

University of Tasmania



---

## Acknowledgements

This work has been funded through the Commonwealth Environment Research Facilities (CERF) program, an Australian Government initiative supporting world class, public good research. The CERF Marine Biodiversity Hub is a collaborative partnership between the University of Tasmania, CSIRO Wealth from Oceans Flagship, Geoscience Australia, Australian Institute of Marine Science and Museum Victoria. Logistic support for the AUV *Sirius*, used for this project, was provided by the Australian Centre for Field Robotics at the University of Sydney and the Integrated Marine Observing System (IMOS) - which collectively represents nationally distributed equipment and data-information services. The assistance and support of the following people is greatly appreciated; Colin Buxton and Justin Hulls (Institute for Marine and Antarctic Studies, UTas), Stefan Williams, Oscar Pizzaro, Michael Jakuba, Duncan Mercer and George Powell (University of Sydney) and Matthew Francis and Jac Gibson (R/V *Challenger* crew). Richard Coleman (Australian Research Council) initiated the use of the AUV in Tasmanian waters. The gridded bathymetric dataset was collected and processed by Geoscience Australia.

## Chapter

# 1 Introduction

### 1.1 In a nutshell

Continental shelves provide more than 90% per cent of the world's fisheries landings and for 3 billion people, fish constitutes 15% of their animal protein intake per capita (FAO, 2010). Rocky reefs are highly productive and an ecologically important component of continental shelves due to their high species numbers and habitat diversity (Taylor, 1998). Sustainable management of finite resources on the continental shelf requires efficient and preferably non-extractive methods to assess and monitor these assets. This thesis tests and evaluates three novel non-extractive methods to sample marine resources with respect to efficiency and applicability to current managerial needs such as habitat mapping and fisheries and conservation management.

### 1.2 Sustainable resource management – a fisheries example

Traditional single-species fisheries management has often been ineffective as it ignores ecosystem components of the target species such as habitat, predators and prey (Pikitch et al., 2004). Over the past decade many nations adopted an alternative management approach that strives to sustain healthy marine ecosystems

---

and the fisheries they support (Pikitch et al., 2004). This alternative is called the Ecosystem-Based Fisheries Management (EBFM) or the ecosystem approach to fisheries (Garcia et al., 2003). Ecosystem-based management (EBM) is not exclusive to fisheries but finds application in contemporary ocean and living marine resource management (Murawski, 2007). According to Pikitch et al. (2004) EBFM should (i) avoid degradation of ecosystems, as measured by indicators of environmental quality and system status; (ii) minimize the risk of irreversible change to natural assemblages of species and ecosystem processes; (iii) obtain and maintain long-term socioeconomic benefits without compromising the ecosystem; (iv) generate knowledge of ecosystem processes sufficient to understand the likely consequences of human actions. Where knowledge is insufficient, robust and precautionary fishery management measures that favour the ecosystem should be adopted (Pikitch et al., 2004). The central piece of legislation in Australia to address these four points is the Environment Protection and Biodiversity Conservation Act 1999 (EPBC). The EPBC Act provides a legal framework to protect and manage nationally and internationally important flora, fauna and ecological communities (DSEWPC, 2012). This includes measures to mitigate threats through global warming, i.e., sea-level rise (to protect reef-forming corals) and increased occurrences of severe weather events (cyclones and droughts) and reducing river pollution and sediment loads in rivers (both are factors that affect mangrove forest and coral reef ecosystem health; Rogers (1990); Fabricius et al. (2005)). Under the EPBC Act, the Australian Government identified a network of marine reserves to halt the decline in biodiversity and implemented marine bioregional planning. Commonwealth Marine Reserves (CMR)

form part of this network with the following activities still allowed: recreational and commercial fishing, marine tourism, charter boat operations (fishing), recreational boating, mining and oil and gas activities and port development and shipping. Protection of CMRs is provided by fishing gear restrictions, gear with no or little impact on the benthic fauna, control over the extent of fishing activities, environmental assessments before commencing mining and port development and licensing for tourism and charter boat operators.

### **1.3 Australia's recent EBM history**

“Australia aims to realise its international commitments as a signatory to the Convention on Biological Diversity through the significant expansion of its existing MPA network throughout Australia's Exclusive Economic Zone (EEZ) by 2012” (DSEWPC, 2012). This expansion is achieved through the establishment of a National Representative System of Marine Protected Areas (NRSMPA). “The primary goal of the NRSMPA is to establish and manage a comprehensive, adequate and representative system of marine protected areas to contribute to the long-term ecological viability of marine and estuarine systems, to maintain ecological processes and systems, and to protect Australia's biological diversity at all levels” (DSEWPC, 2012). One of the secondary NRSMPA objectives is to provide scientific reference sites. These reference sites provide a benchmark against which the effects of human impacts in unprotected areas can be compared.

---

## 1.4 Consequences of adopting EBM

Currently,  $\sim 880,000 \text{ km}^2$  or 10% of Australia's EEZ, excluding the Australian Antarctic Territory are part of the NRSMPA (DSEWPC, 2012). However, only a fraction of this area, usually areas in State coastal water and parts of the Great Barrier Reef, has been inventoried or was subjected to baseline MPA monitoring to capture the variability of natural processes. Actual knowledge of what the NRSMPA comprise is so poorly known, that surveys of the Australian continental shelf and slope typically find that 30 – 50% of the decapod species sampled are new to science (Poore et al., 2008). Protected areas within the NRSMPA need to contribute to the representativeness, comprehensiveness or adequacy of the national system which, given the poor knowledge of what the areas actually comprise, is a challenging prospect. This only highlights the difficulties encountered during the planning phase regardless of meeting the 2012 target. Once established [NRSMPA], the Environment Protection and Biodiversity Conservation Act requires an annual environmental performance report. Currently, surveys of State managed marine reserves provide the most comprehensive knowledge of continental shelf habitats and therefore allow CAR (Comprehensive Adequate and Representative) principles to be fully implemented. Consequently, adopting ecosystem-based management (EBM) requires solutions to address (1) rapid resource and habitat mapping, (2) baseline data to evaluate management strategies and (3) regular monitoring techniques. With respect to habitat mapping in an EBM context, it is not sufficient to identify habitat types and quantify their distribution (see EBFM management objective (iv))

above). Rather, EBFM should generate knowledge of ecosystem processes such as fish-habitat associations and inter-habitat relationships.

## 1.5 Current EBM challenges

Qualitative and quantitative data are a prerequisite for managing coastal marine resources. This knowledge is fundamental during the planning phase (inventory) as well as after implementation (monitoring). Underwater visual census (UVC) techniques are the most commonly used methods for monitoring biotic change in coastal MPAs [Marine Protected Areas] (Barrett and Buxton, 2002). UVC is a diver-based sampling method. Despite its [UVC] popularity it is ineffective in sampling most managed fishing grounds and reserves; UVC is restricted to water depths, that are safe for SCUBA divers ( $< 30$  m). To address the critical need for efficient sampling tools without depth restrictions, the Marine Biodiversity Hub funded by the Commonwealth Environmental Research Facilities program tested and integrated, relatively new survey technologies such as multibeam sonar, underwater video and autonomous underwater vehicle (AUV) imagery (Bax, 2011; Brown et al., 2011; Kostylev et al., 2001). Desirable characteristics of these new sampling tools include being quantitative, non-extractive and suitable for monitoring, i.e., cost-effective and able to return to the exact sampling location for subsequent surveys. Marine habitat maps are fundamental prerequisites for scientific fisheries management and monitoring environmental changes and anthropogenic impacts on benthic habitats (Kostylev et al., 2001; Diaz et al., 2004; Halpern et al., 2008; Hobday et al., 2011). Currently, only 12.5% of Australia's marine territory has been

---

bathymetrically mapped (Bax, 2011). This territory does not exceed 200 nautical miles from the baseline, i.e., low water line along the coast, unless the geological continental shelf extends beyond the 200 nm limit. Hence, the continental shelf and slope, abyssal plains, canyons and other submarine features can occur within this geologically arbitrary 200 nm limit. Current notable mapping coverage include almost all MPAs in Australia, Cape Nelson, Victoria (Rattray et al., 2009) and the Hopkins site in Victoria (Ierodiaconou et al., 2007). The aforementioned habitat maps are based on multibeam sonar data (bathymetry and acoustic backscatter) and fine-scale ground-truthing data using video imagery of the seafloor. Although sonar data in isolation can provide coarse habitat maps using morphometric feature classification (Lucieer and Pederson, 2008) they cannot provide ecologically more meaningful maps of kelp forest, sponge garden or coral reef extent (Wilson et al., 2007). Morphometric feature classification is based on nearest neighbour statistics on gridded bathymetry data. For example, by examining relationships between neighbouring grid cells and the central grid cell in a  $3 \times 3$  window an algorithm developed by Wood (1996) classifies each cell into one of six feature (habitat) classes: plains, passes, ridges, peaks, channels or pits. However, the creation of ecologically more meaningful habitat maps relies on the combination of bathymetric data and fine-scale data obtained from grab samplers, sediment cores or imagery (ground-truthing). In recent years multibeam sonar backscatter analysis has provided some insight to the nature of seabed features such as hard or soft substratum (Hasan et al., 2012). Both techniques in conjunction with ground-truthing, either extractive or image-based, provide the foundation to develop models that predict seafloor habitats

(Kostylev et al., 2001). Processing fine-scale ( $\sim 1 \text{ m}^2$ ) samples is time-consuming and resource-intensive. This processing stage is often considered the proverbial bottleneck during map production. However, this extraction of information is essential to acquire qualitative and quantitative data using fine-scale imagery.

## 1.6 Solutions – thesis objectives

As part of the Marine Biodiversity Hub this study tested and evaluated imagery-yielding samplers that are non-extractive and quantitative. An advantageous characteristic of imagery-yielding samplers is the permanent record and auxiliary information contained in the imagery, e.g., the target species AND its environment. Testing and evaluation was conducted under the following criteria: (1) cost-effectiveness with respect to collecting an inventory of habitats and monitoring fragile and/or protected environments, applicability to existing needs, e.g., fisheries-independent stock assessment, MPA planning and monitoring and habitat mapping. Three different sampling tools were tested to address several challenges with respect to the current EBM challenges outlined above.

**Advanced habitat mapping techniques – chapter 3 (Seiler et al., doi.10.1016/j.csr.2012.06.003)**

Almost 90% of Australia’s EEZ remains to be bathymetrically mapped. However, within this 200 nm EEZ there are several geological features, such as the continental slope, seamounts, abyssal plains and canyons that are less well known than the

continental shelf. Currently, multibeam echo sounders (MBES) are the only means to efficiently fathom Australia's continental shelves, especially areas with high conservation value such as Australia's MPAs. Most notable areas that were mapped using scientific multibeam echo sounders are Jervis Bay, NSW (Anderson et al., 2009) and the Freycinet and Huon Commonwealth Marine Reserves, TAS (Nichol et al., 2009). However, the resolution and information provided by MBES alone is insufficient at the habitat scale – the scale at which EBM [ecosystem-based management] operates. At the habitat scale (area that comprises ecologically linked multi-species assemblages, such as kelp, invertebrates and fish in a kelp forest habitat), imagery-yielding samplers are the only means of mapping benthic habitats on hard substrates such as sponge gardens or kelp forests on rocky reef (Copeland et al., 2011). However, there are examples where Regional Marine Planning is based on geomorphic features, such as continental rise, pinnacle, canyon, terrace, trench/trough, etc, which are derived from grid-based terrain analysis using multibeam bathymetry data (Harris et al., 2003). Two dominant methods of producing marine habitat maps of hard substrates are currently in use (i) seafloor images (point samples) combined with continuous interpreted MBES data and (ii) transect or full-area photographic surveys. The former uses machine-learning algorithms to establish relationships between topographic attributes, obtained from terrain analysis using digital elevation models (MBES data), and distinct habitat classes, annotated seafloor images, to predict habitat distribution outside the photographed area (Rattray et al., 2009). The latter, photographic surveys, are solely based on imagery collected by the sampler (Singh et al., 2004b). Both methods

require annotation of imagery by a trained expert, which is time-consuming and often subjective. A widely used habitat classification scheme based on substratum type, requires classification based on a primary ( $> 50\%$  coverage) and secondary ( $> 20\%$  coverage) substratum type (Greene et al., 1995). Subjectivity, or observer bias, can cause coverage estimates to differ by 20% (personal communication Mark Green, CSIRO). However, image annotation time can be significantly reduced and observer bias eliminated using computer vision techniques. By combining several computer vision techniques, such as edge and scene detection, assigning habitat classes to images based on image content can be automated. Once the automation routine is set up it only takes a few seconds to classify additional images thereby increasing statistical power and precision (Purser et al., 2009). Chapter 3 describes a method to automatically classify seafloor images into habitats based on a training data set.

#### **Effective sampling beyond diver's depths – chapter 4**

Underwater visual census is commonly used to monitor temperate marine protected areas (Barrett and Buxton, 2002). However, high quality optical surveys are needed to monitor MPAs beyond the range of safe SCUBA diving operations (Singh et al., 2004a). For example, only 6% of the Great Barrier Reef Marine Park can be safely monitored using SCUBA (Cappo et al., 2003). However, within depth ranges encountered on continental shelves, remote or tethered camera platforms are free from depth restrictions and serve as reliable samplers in deeper depths ( $> 30$  m). Nevertheless, these platforms need to be tested and evaluated whether they provide

data quality as good, or better than those provided by SCUBA divers in shallow depths. Assis et al. (2007) found that their towed video platform could assess a larger protected area with respect to number of observed elasmobranch species and individuals within the same time compared to UVC. However, Colton and Swearer (2010) found that UVC recorded more individuals (fish species), higher richness at species and family level than Baited Underwater Video Systems (BUVS). Chapter 4 tested the hypothesis whether BUVS are an equivalent to underwater visual census in deeper waters with respect to reef-fish assemblage composition, species richness and abundance and size structure. Further chapter objectives include a test whether a new relative abundance index based on stereophotogrammetric fish length measurements to identify individuals by length is superior to the current relative abundance standard  $MaxN$  – maximum number of individuals of species  $x$  in videoframe  $y$  and to develop a novel statistical approach to conduct power analysis using count data, for which the common assumption of normality do not apply.

**Non-extractive fisheries-independent stock assessment – chapter 5**  
(Seiler et al., doi:10.1016/j.fishres.2012.06.011)

Traditional fishery resource assessment methods using extractive trawl gear are unable to sample rocky substratum and are prone to underestimate the biomass of species having partial or strong association with rocky reefs. The ocean perch *Helicolenus percooides*, a species with strong association with rocky reefs was sampled most frequently using trawls compared to traps and gill nets (Williams

and Bax, 2001). Non-extractive imagery-yielding alternatives, that can sample rocky substratum include manned submersibles (Yoklavich et al., 2000) and autonomous underwater vehicles (Tolimieri et al., 2008). Tolimieri et al. (2008) report rosethorn rockfish (*Sebastes helvomaculatus*) densities and habitat preferences over different substrata, i.e., rock, sand and mud in depth ranging from 100 – 300 m based on digital images taken by an AUV. One major advantage of camera platforms over trawl gear is the ability to observe species-habitat interactions. For example, trawl gear usually samples several kilometers of seafloor, thereby traversing several habitat types, however, the trawl catch comprises only fish and bycatch and provides no information as to where a particular fish was caught. In contrast, images capture fish in their natural environment and therefore allow species-habitat investigations. Chapter 5 details the use of the stereo-camera onboard the autonomous underwater vehicle *Sirius* to collect fisheries-independent complementary data, such as abundance, size structure and habitat preferences of the ocean perch *Helicolenus percoides*. More specifically, I tested the hypothesis whether annotated, geo-referenced digital images taken by the AUV *Sirius* can provide data required for ocean perch stock assessments under constraints of spatial autocorrelation and untrawlable terrain, i.e. rocky reefs.

### **Efficiency testing three non-extractive samplers – chapter 6**

Several non-extractive samplers are available to resource managers to inventory and monitor protected or restricted marine areas. From a resource management perspective these samplers should be cost-effective, easy to deploy and applicable

to various management objectives. One management objective, to halt the decline of biodiversity, encompasses enumeration of individuals (abundance) and species (species richness). In order to halt or reverse biodiversity decline an understanding of fish assemblage distribution over various spatial and temporal scales is essential. BUVS studies in three marine parks in New South Wales, Australia by Malcolm et al. (2007) found that total species richness of fish assemblages did not follow the latitudinal gradient phenomenon and that the temporal component (5 yr) is small compared to the spatial component. Other imagery-yielding platforms such as towed video and AUVs are potentially useful to assess temporal and spatial differences in fish assemblage composition. Chapter 6 tests three non-extractive imagery-yielding samplers and their ability to efficiently assess abundance and diversity of fish assemblages on temperate rocky reefs.

## **1.7 Thesis outcomes and future research**

The schema diagram in Fig. 1.1 shows various research question presented in this thesis to address EBM needs and requirements such as resource maps, cost-effective monitoring methods and management regime performance measures. The results in this thesis show that several challenges, sustainable resource management agencies are currently facing, such as effective habitat mapping, non-extractive fisheries-independent benthic reef fish stock and biodiversity assessments, can be solved using the methods presented in this thesis. Automated extraction of image features enables semi-automated habitat mapping using imagery collected by the AUV *Sirius*. Given the limited knowledge of marine habitat distributions below safe SCUBA

diving depths and Australia's pledge to sustainable resource management, which includes habitats, AUVs, such as *Sirius*, in conjunction with automation routines can significantly curtail processing time to produce habitat maps. An assessment of size, abundance and habitat preference that can potentially complement fisheries-independent ocean perch *H. percooides* stock assessments is presented in this thesis, which showed the value of non-extractive imagery-yielding samplers (e.g., AUV *Sirius*) compared to traditional fishing techniques (e.g., bottom trawls). With respect to benthic reef fish, AUV imagery is free from sampling gear bias (size selectivity) and AUVs can be deployed over rugged terrain, inaccessible to trawl gear. This positive outcome is likely to encourage resource managers to adopt sophisticated non-extractive sampling techniques (i.e., AUVs, BUVS and towed video). The Convention on Biological Diversity (United Nations, 1992) defines sustainable use as; resource use without a long-term decline in biodiversity. Trends in biodiversity can only be detected using reliable sampling platforms within a monitoring framework. With respect to temperate reef fish biodiversity below safe SCUBA diving depths, chapter 4 showed that BUVS are efficient and reliable samplers to monitor assemblage composition (i.e., species richness and abundance). Although, BUVS have been used to assess fish diversity in the tropics (Great Barrier Reef Biodiversity Assessment), its use in temperate deep-water reef environments is sparse. South-eastern Australia, including Tasmania, is one of the fastest warming regions in the southern hemisphere (Ridgway, 2007; Johnson et al., 2011) and it is anticipated that BUVS will be the preferred method of assessing flow-on effects to reef fish communities in this area.

Although some solutions to current sustainable resource management challenges in Australia are presented in this thesis, other challenges remain to be solved. The biggest problem since the inception of baited video systems, unknown sample volume, needs more attention. Visible sampling volume can now be determined using stereophotogrammetry (i.e., calculating the point cloud volume using x-y-z coordinates), however, bait plume dispersal in rugged terrain remains elusive. Major improvements have been made to model sewage outfall plumes and coral larval dispersal using computational fluid dynamics (Wild-Allen et al., 2010) and it is likely that the same models can be applied to model bait plume dispersal.

Although, my results showed how applying computer vision routines can expedite the process of habitat mapping, another branch of computer vision – object recognition – could further expedite image processing. However, object recognition of fish, invertebrates and macroalgae in their natural environment is still in its early stages and needs further research (Gobi, 2010).

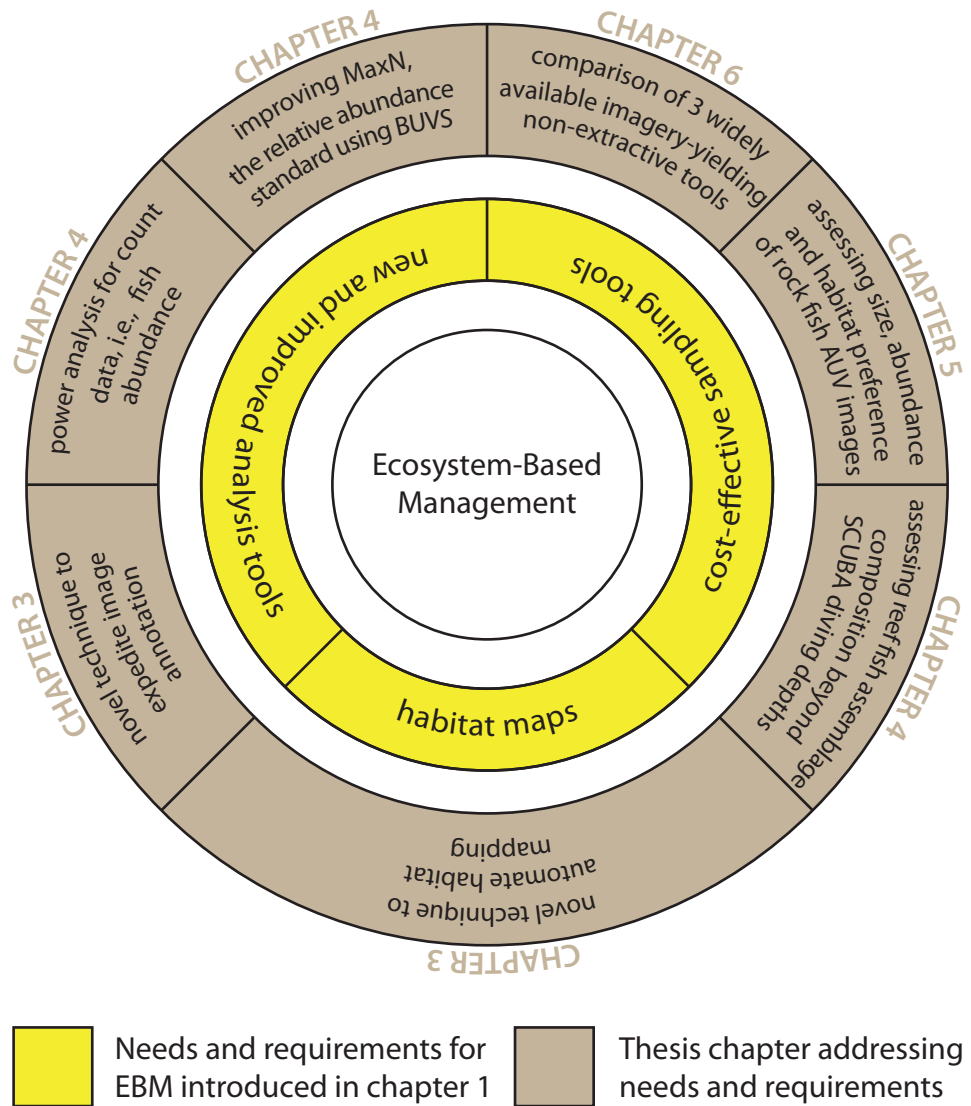


Figure 1.1: Schema diagram elucidating how research questions address ecosystem based management needs and requirements.



---

## Chapter

# 2

## Data acquisition

### 2.1 Introduction

Sampling conducted during this thesis was under the auspices of the Commonwealth Environmental Research Facilities funded Marine Biodiversity Hub. The majority of data were collected during three surveys using R/V *Challenger*. Survey one was conducted 13 – 26 June 2008, survey two 6 – 14 October 2008 and survey three 23 February – 14 March 2009. All surveys were conducted in south-east Tasmanian waters, Tasmanian, Australia. “The purpose of field surveys in the Surrogates Program [program within the Marine Biodiversity Hub] is to collect high-resolution, accurately co-located physical and biological data to enable the robust testing of a range of physical parameters as surrogates of patterns of benthic biodiversity at relatively fine spatial scales” (Nichol et al., 2009). This chapter describes three non-extractive, imagery-yielding sampling platforms used during this candidature. The three sampling platforms below surveyed the same reef complexes Fig. 2.1.

- (i) Autonomous Underwater Vehicle (AUV)
- (ii) towed video system
- (iii) Baited Underwater Video System (BUVS)

---

AUV and the towed video system were deployed using R/V *Challenger*. BUVS were deployed using small (6 m) boats. The basic design and components are described for each platform. BUVS and the towed video system recorded digital video footage and the AUV recorded digital still images. BUVS and AUV were equipped with a stereo camera setup and provided photogrammetric length measurements of objects in the imagery. BUVS deployment locations were chosen based on known habitat types derived from annotated AUV images. Towed video transects were placed to overlap AUV mission tracks and to cover roughly the same areal extent.

## 2.2 Study area

The study area stretched over some 50 km of coastline in south-eastern Tasmania between High Yellow Bluff and the Hippolyte Rocks (Fig. 2.1). Despite being a popular recreational SCUBA dive destination, little was known about the benthic assemblages below diver's depths (< 30 m). The "Peninsula Mapping Region" (Barrett et al., 2001) has a dominantly easterly aspect, high vertical cliffs, deepwater reefs (to 100 m depth) and medium to high wave exposure 2.1. Key ecological features down to the 40 m depth contour were mapped during the SEAMAP ([www.seamap.imas.utas.edu.au/](http://www.seamap.imas.utas.edu.au/)) project using a range of towed video surveys Barrett et al. (2001). Geologically the coastline is composed of dolerite, sedimentary rock and to a lesser extent granite, i.e., the Sisters, see Fig. 2.1 (Barrett et al., 2001).

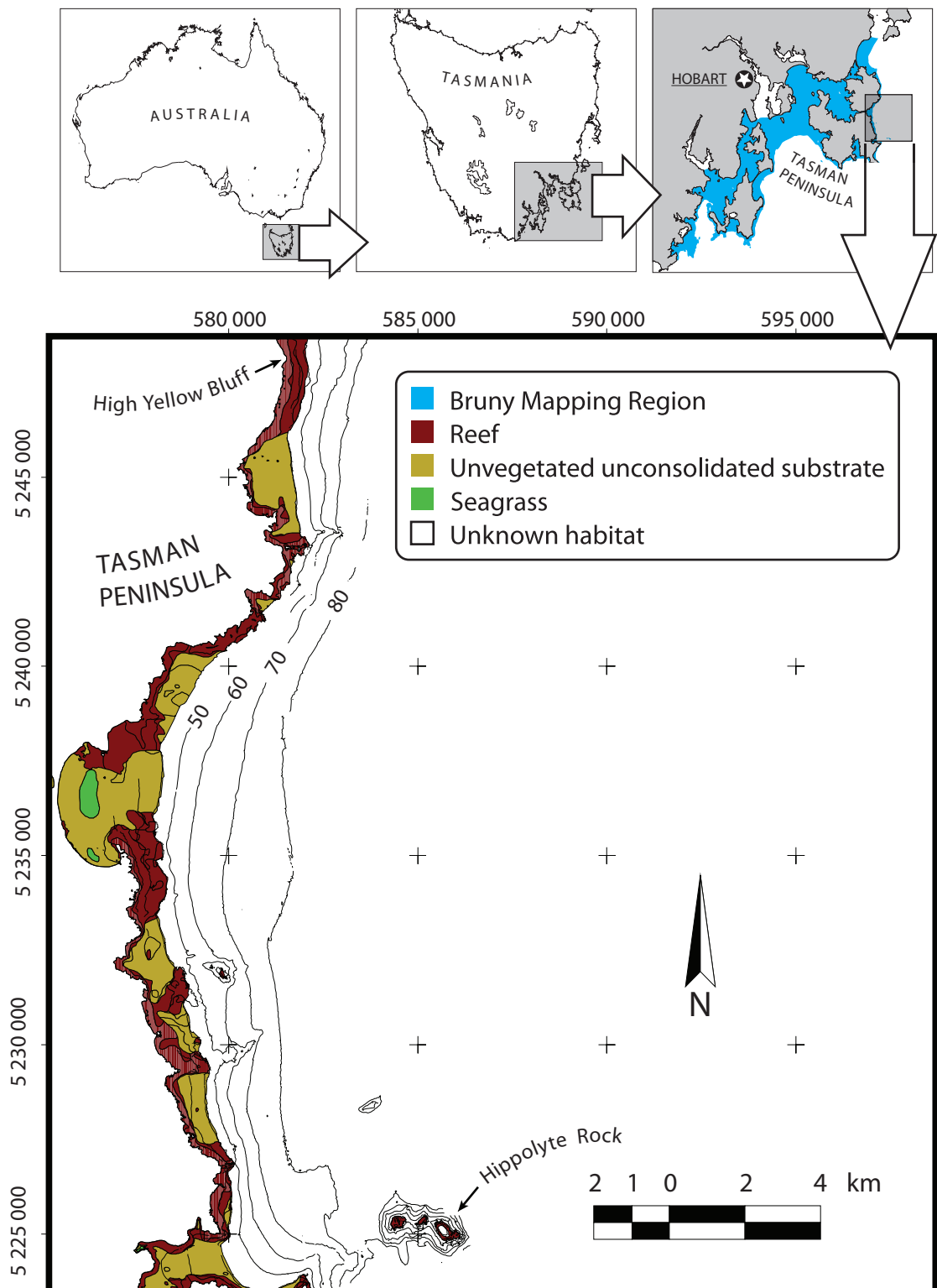


Figure 2.1: Location of study area (High Yellow Bluff to Hippolyte Rock). Extent of Bruni Mapping Region (Barrett et al. (2001)) highlighted in blue. Habitats from shoreline to 40 m depth contour according to [www.seamap.imas.utas.edu.au](http://www.seamap.imas.utas.edu.au). Depth contours from multibeam bathymetric data in meters. Projection: UTM, Zone 55G, CM 147 degrees E.

---

## 2.3 Bathymetric mapping

A ship-borne Simrad EM3002(D) 300 kHz multibeam echo sounder (MBES) in single transducer mode was used for bathymetric mapping from 13 – 26 June 2008 (Nichol et al., 2009). The Applanix Position and Orientation system (Applanix Corporation) collected motion referencing and navigation data. Geographical position during the survey was recorded using the C-Nav GPS system (C-Nav World DGNS). Vessel survey speed in inshore and shallow water areas was 5 knots and 10 knots in deeper offshore waters. Multibeam data were corrected for tides and vessel motion using CARIS Hips and Sips v6.1 software (CARIS). The final raster digital elevation model had a resolution of  $2 \times 2$  m.

## 2.4 Autonomous underwater vehicle

The Autonomous Underwater Vehicle (AUV) *Sirius*, operated by the Australian Centre for Field Robotics at the University of Sydney, sampled benthic fauna by means of digital photography. *Sirius* was a modified version of the SeaBED AUV (Singh et al. 2004) built by the Woods Hole Oceanographic Institution (Fig. 2.2). This ocean-going survey AUV was designed to be passively stable in pitch and roll. Stability was achieved by two torpedo-like components joined by turbulence-reducing vertical struts. The upper component consisted of flotation bodies and the electronics housing, giving the AUV positive buoyancy and the lower component contained the various sensors and batteries. The overall dimensions of the AUV were 2.0 m (length)  $\times$  1.5 m (height)  $\times$  1.5 m (width). Its weight, depending

on payload, was  $\sim 200$  kg. The vehicle was rated to 700 m depth. Yaw, forward and backward movement was controlled by a pair of aft-facing thrusters. Vertical (depth) movement was accomplished by one vertical thruster. Geographical vehicle positioning on the surface was accomplished using GPS. Navigation underwater was achieved using a Doppler velocity log, inertial measurement unit, ultra-short baseline acoustic positioning system, pressure sensor and compass. For an exhaustive list of all vehicle specifications and sensors see Table 2.1. The AUV's ability to 'hover' facilitated a virtually constant altitude of 2 m above the seafloor which equated to an image footprint of  $1.6 \times 1.3$  m ( $\sim 2$  m<sup>2</sup>). Average image area was 2.04 m<sup>2</sup> ( $\pm 0.09$  SD). The relatively slow 'flying' speed of the AUV is  $\sim 0.4$  m/s. A pair of downward-looking Pixelfly HiRes ( $1360 \times 1024$  pixels) digital cameras took images at a one second interval. Two strobes, one situated at the front and the other at the back of the AUV, synchronously illuminated the field of view.

#### 2.4.1 AUV camera calibration

The stereo camera setup was calibrated to ensure precise photogrammetric measurements. Images of an object with known dimension were recorded using the stereo camera setup in a circular pool filled with seawater. This object was a printed chequerboard-pattern laminated to a  $80 \times 80$  mm stiff perspex board. The photogrammetric bundle adjustment package CAL (Seager, 2009c) was used to derive a set of constants specifying the coordinate system of the stereo camera unit (datum). The resultant parameters were necessary for photogrammetric length, area or volume estimation of objects using the PhotoMeasure software package (Seager,

Table 2.1: List of AUV specifications and sensors

**Vehicle Specifications**

Depth rating	700 m
Size	2.0 m (L) $\times$ 1.5 m (H) $\times$ 1.5 m (W)
Mass	200 kg, depending on payload
Maximum Speed	1.2 m/s
Batteries	1.5 kWh Li-ion pack
Propulsion	3 $\times$ 150 W brushless DC thrusters

**Navigation**

Attitude/Heading	Tilt ( $\pm 0.5^\circ$ ), Compass ( $\pm 2^\circ$ )
Depth	Paroscientific pressure sensor (0.01 %)
Velocity	RDI Navigator ADCP (1 - 2 mm/s)
Altitude	RDI Navigator
USBL	TrackLink 1500 HA (0.2 m range, $0.25^\circ$ )
GPS	Ashtech A12

**Optical Sensing**

Camera	Stereo Prosilica 12bit $1360 \times 1024$ CCD
Lighting	2 $\times$ 2.8 J strobe
Separation	$\sim 1$ m between camera and strobe

**Acoustic Sensing**

Multibeam sonar	Imagenex DeltaT 837 Profiling 260 kHz
Imaging sonar	Tritech Seaking (optional)
Obstacle Avoidance	Imagenex 852 Echo Sounder

**Other Sensors**

CTD	Seabird 37SBI
Fluorometers	Wetlabs Ecopuck (chlorophyll <i>a</i> , CDOM, scattering red)
dissolved oxygen	Aanderaa Optode

**Communications**

Radio Frequency	Freewave 900kHz radio + ethernet
Acoustic Modem	TrackLink 1500 HA modem

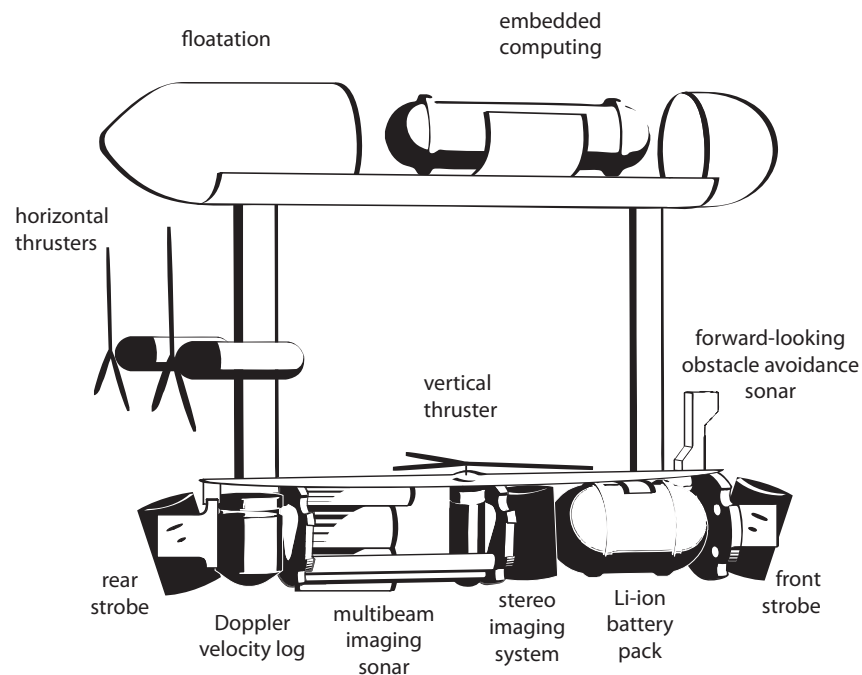


Figure 2.2: Labelled schematic of Autonomous Underwater Vehicle and its components. Note: Top and bottom hull cover removed for clarity.

2009a).

#### 2.4.2 AUV sampling design

The AUV sampled rocky reefs from 6 – 14 October 2008 with the support of R/V *Challenger* (Nichol et al., 2009). Total transect length was  $\sim 60$  km (16 dives). Individual AUV dives were haphazardly placed on prominent deep-water rocky reefs (25 – 100 m depth) emphasising on rocky reefs as well as transition zones between reef and adjacent sandy areas. Transect placement was based on visual assessments of sun-illuminated geoTIFF files from a previous multibeam survey (Nichol et al., 2009). The intersecting survey pattern (Fig. 5.1) was necessary to maintain high spatial accuracy (positional error is in the centimetre range). In a monitoring context

---

it is anticipated that the AUV is sampling the same transect during each survey. This survey pattern reduced positional error, introduced by dead-reckoning and sensor inaccuracies, by using the simultaneous localisation and mapping (SLAM) technique. SLAM re-navigated the estimated vehicle trajectories (Williams et al., 2008b) based on matching images (intersections).

### 2.4.3 AUV image annotation

AUV images were manually annotated, recording habitat type and mobile megafauna, e.g., fishes, echinoderms, crustaceans and molluscs. Eleven habitat types in three subgroups, hard and soft substrate and transition zones are described in Table 2.2. Annotation was based on the dominating ( $> 50\%$ ) visible feature within the image irrespective whether it is a physical and biological structuring component. For example, although it is a fair assumption that the macroalga *Ecklonia radiata* resides on hard substrate, images containing *E. radiata* were classified as ECKLONIA (provided *E. radiata* cover was  $> 50\%$ ). During habitat scoring only changes in habitat type were recorded. For example, if image 1 – 100 depicted habitat type *sand* and image 101 - 120 depicted habitat type *high relief reef*, there would be only two records; image 1 - sand, image 101 - high relief reef. The remaining images, 2 – 100 and 102 – 120, were automatically labelled based on its predecessor's label using a MATLAB script. Species identification was based on identification guides (Gomon et al., 2008; Edgar, 1997) and expert advice from leading taxonomists. Each image was recorded with a unique date and time stamp. This date and time stamp linked an image to auxiliary data such as geo-position,

depth, salinity, temperature, etc.

Table 2.2: Habitat types scored during AUV image annotation with brief description

habitat type	description
Caulerpa	macroalgae, <i>Caulerpa spp.</i> , covering more than 50% of the rocky seafloor
Ecklonia	macroalga <i>Ecklonia radiata</i> covering more than 50% of the rocky seafloor
high relief reef	rocky reef, elevation change more than 20 cm (within image)
low relief reef	rocky reef, elevation change less than 20 cm (within image)
coarse sand	coarse sand with small pebbles and gravel
pebble and tuft	coarse sand with small pebbles and gravel dominated by bryozoan tuft
sand	fine sand
screw shell rubble	screw shells, <i>Maoricolpus roseus</i> , covering more than 50% of the sandy seafloor (within image)
screw shell rubble/sand	screw shells covering less than 50% of the sandy seafloor
patch reef	patches of rocky reef within sand
reef-sand ecotone	rocky reef edge, transition to/from sand

## 2.5 Baited underwater video system

Although, underwater photography is almost as old as photography itself (Norton, 2000), baited underwater video systems were first deployed in 1996 by Willis and Babcock (2000). Their downward-looking (vertical) camera design was subsequently changed to a forward-looking (horizontal) camera design, culminating in stereo BUVS pioneered by Harvey and Shortis (1996). BUVS are primarily used to assess fish assemblage composition. Cappo et al. (2004) found that BUVS sampled significantly different tropical reef fish assemblages compared to prawn trawls. In temperate waters Willis et al. (2000) detected spatial variability in relative fish

abundance, comparing BUVS with UVC and angling. Several other studies tested BUVS performance compared to UVC and unbaited underwater video systems (Langlois et al., 2010; Watson et al., 2005). Watson et al. (2007) found that the establishment of a marine reserve caused changes in assemblage composition in a temperate-tropical transition zone. All references above are studies in shallow (< 30 m) waters and do not assess fish assemblage compositions below safe SCUBA diving depths. This study used BUVS to describe benthic fish assemblages in temperate deep-water (> 30 m) rocky reef environments.

### **2.5.1 BUVS design and components**

The BUVS frame was shaped like a truncated pyramid with an oblong base. It consisted of four galvanised steel parts, these were:

- (i) the frame base, which besides forming the base of the frame acted as a redundant safety device. In case of BUVS entanglement, vigorous pulling detached the base from the top. The top part, consisting of the underwater housings and cameras, can be retrieved with the minor loss of the base. 6 kg galvanised steel bars for weighting and balancing the frame can be attached to all four sides of the frame base.
- (ii) the frame top held the camera bar and also provided an attachment point for the rope.
- (iii) the camera bar was designed as an independent unit for ease of camera calibration in a swimming pool environment. Two tubular underwater housings

made from pressure-pipe PVC with detachable plexiglas front dome and fixed rear dome were attached to the bar,  $\sim 75$  cm apart and inwardly converged by  $8^\circ$  for optimised field of view (Harvey and Shortis, 1996).

- (iv) the detachable bait arm was intended to decrease overall unit dimensions and ease of transport. Whilst one end attached to the camera bar, the outward end served as an attachment point for the bait basket and LED array. The array was visible in the video footage of both cameras and the LED blinking sequence provided a reference to synchronise video footage of the left and right camera. Synchronisation reduces photogrammetric measurement error by overcoming motion parallax (Harvey and Shortis, 1996).

A negatively buoyant rope (12 mm diameter) attached to the frame top allowed for easy BUVS retrieval by hauling with assistance of an electrical winch. Two white polystyrene surface floats (250 mm diameter) were attached to the end of the rope to provide flotation and increase visibility from distance. A schematic of the frame and camera housings is provided in Fig. 2.3.

### **Underwater camera housings**

The tubular camera housings, depth rated to 150 m, were made from pressure-pipe PVC and plexiglass domes. The detachable front dome connected to an aluminium frame that served as a base for the video camera. An alignment pin on the front of the PVC tube assured the same dome (camera) position after camera retrieval.

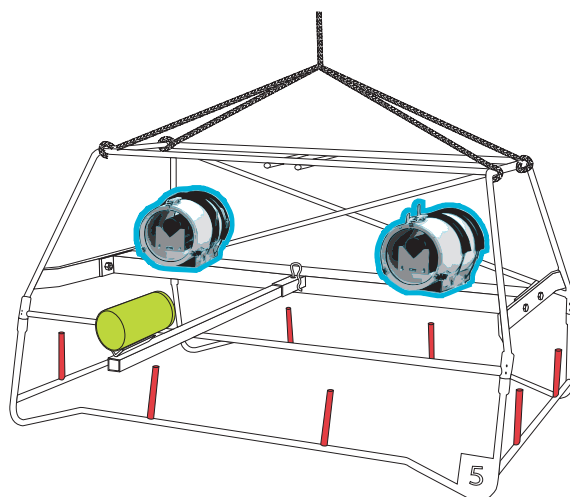


Figure 2.3: Schematic of BUVS unit; LED array (green) on bait arm, pins (red) for weight attachment, cameras and underwater housings (blue outline).

## Video cameras

Six JVC GZ-MS100 PAL (720×576 pixels) off-the-shelf video cameras, two for each of the three frames, were used during this study. A Raynox wide angle conversion lens (conversion factor 0.7) was attached to the cameras to increase the field of view. Using the higher capacity JVC battery pack (BN-VF823U) increased recording time, ~4 hours. Video footage was recorded on 16 GB SDHC memory cards.

### 2.5.2 BUVS camera calibration

Calibrating stereo camera systems ensures precise photogrammetric measurements. Off-the-shelf cameras are rarely metric and therefore deviate from a perfect central projection. This deviation needs to be modelled during the calibration process (for more technical details see Harvey et al. (2003)). Calibrations were conducted after every setup change; movement or removal of camera housings. Differences in

optical properties between seawater and freshwater are negligible with respect to measurement accuracy (Harvey et al., 2003). Hence calibrations were conducted in a public swimming pool due to ease of access. An object of known dimensions (calibration cube) was recorded for later calibration in the video lab. Dimensions of the precision-made calibration cube were 1 m  $\times$  1 m  $\times$  0.5 m (Fig. 2.4). The photogrammetric bundle adjustment package CAL (Seager, 2009c) was used to derive a set of constants specifying the coordinate system of the stereo camera unit (datum). The resultant parameters and internal characteristics of the video cameras such as focal length, principal points, lense distortion, orthogonality and affinity terms as well as the relative orientation of the two cameras to one another were necessary for photogrammetric length estimation of objects using the PhotoMeasure software package (Seager, 2009a).

### 2.5.3 BUVS sampling design

#### Bait

BUVS are baited to attract fish to come close to the cameras. Unbaited underwater video systems record one quarter of the number of individuals recorded by baited systems (Watson et al., 2005). The de facto standard bait used in BUVS research is crushed pilchard *Sardinops* spp. However, Wraith (2007) reports significant differences in relative abundance and species richness recorded using three different bait sources, pilchard, abalone and urchin. Although Wraith (2007) studied a temperate embayment, Jervis Bay, New South Wales, Australia, published BUVS



Figure 2.4: Schematic of calibration cube, every white dot (target) refers to a number in a file that contains their x, y and z coordinates; targets within the five different symbols (each corner and center) were usually sufficient for the CAL software package to automatically detect the remaining targets

results in Tasmanian waters were non-existent at the time of writing. To find the most efficient bait source three different baits were tested, crushed pilchard, crushed salmon and Hook'em Fish Kandy (commercial fish attractant, Hook'em Fishing). Pilchard was the most effective bait –  $MaxN$  for target species was highest, biodiversity (species richness and Shannon index) was greatest, time of first arrival (fish at BUVS station) was shortest and bait plume dispersal period was longest – and was used for all subsequent BUVS deployments. For each deployment 800 g of *Sardinops sagax* was crushed to promote odour dispersal and placed in a plastic craypot bait basket (Quin Marine Pty Ltd) suspended  $\sim 1$  m in front of the two BUVS cameras. The bait basket was re-filled before each deployment. Replicate BUVS locations were separated by at least 200 m to prevent overlapping bait plumes. This would have increased the risk of recording the same individual with two different BUVS units and therefore inflated relative abundance estimates.

### **BUVS deployment**

BUVS deployment duration differs between temperate and tropical locations (Watson et al., 2005; Cappo et al., 2004), which is largely attributed to higher species richness in the latter. Investigations in the tropics require less BUVS deployment time to record the same number of species compared to investigations in temperate regions (Cappo et al., 2004). Watson et al. (2005) state that  $>36$  min of deployment time is necessary to record “the majority of fish species” in temperate regions of Western Australia. To determine to what extent Watson et al. (2005)’s findings are applicable to Tasmanian rocky reefs, the relationship between duration

---

of deployment (soak time) and species richness  $S$  was investigated during a pilot study. The pilot study found that at least 40 min of soak time are required to obtain  $S$  as high as the average species richness. Subsequently, soak time at the bottom was 45 min. BUVS were deployed between 14 May 2009 and 22 August 2010 during daylight hours (8 AM to 6 PM) depending on season using a  $\sim 6$  m boat. Sampling depth ranged from 32 – 81 m. The study area was subdivided into sites based on distinct reef complexes. These reef complexes were chosen using a high-resolution bathymetric map obtained during survey leg one. This study focused on fish assemblages on reef areas with high range values (range: local relief measure, subtracting the minimum elevation from the maximum elevation in a local neighbourhood of 6, 10 and 18 m kernel radius); for further details see Moore et al. (2009). Hence, BUVS were deployed on high relief reef habitats (high range values). From the moment the BUVS unit is dropped to the moment it reaches the seafloor, the unit can drift and may not always land in the same geographical position or habitat. To ascertain that the right habitat was sampled the footage was visually inspected using the visible camera footprint. BUVS deployments in non-targeted habitats were discarded. Sampling locations are depicted in Fig. 4.1. Three replicate samples were taken for each site and each season.

#### **2.5.4 BUVS video annotation**

Video footage was viewed and annotated using the software package EventMeasure (Seager 2009).  $MaxN$ , the maximum number of individuals of a given identified species per video frame was recorded to avoid repeated counting of the same

individual (Cappo et al., 2004).

### **EventMeasure**

The software package EventMeasure (Seager, 2008) was used to record species abundance and diversity as well as fish behaviour by interrogating footage from the left or right video camera. Every species entering the field of view was recorded by right-mouse clicking on the individual and choosing the desired attributes (species name, stage and behaviour). Each of these events was saved to a .emObs file for later fish length measurements in the software package PhotoMeasure.

Additional information, such as time (frame number) when the BUVS frame hit the bottom, habitat type, first arrival of first fish and time when the frame was lifted off the bottom were recorded.  $MaxN$ , the maximum number of species  $x$  in video frame  $y$  for each 45 min deployment, was used throughout this study to indicate fish abundance and derive diversity measures such as Simpson's index ( $D$ ).  $MaxN$  is considered a *relative* abundance measure as opposed to a *absolute* density measure such as number of individuals of species  $x$  per  $m^2$ . Polymorphic species such as the blue-throated wrasse *Notolabrus tetricus*, provided a male and female entered the field of view, allowed for a different relative abundance measure than  $MaxN$ . For example, if a male and female *N. tetricus* entered the field-of-view but not at the same time (video frame  $y$ ), relative abundance for this 45 min deployment was considered 2 rather than 1 ( $MaxN$ ).

## 2.6 Towed video platform

Geoscience Australia developed small ( $30 \times 50$  cm [sic]), shallow-water RayTech towed interlaced video system consisted of two steel side panels connected by several rods and bars, that gave stability as well as attachment points for sensors (Fig. 2.5) (Nichol et al., 2009). A wing on the back of the platform stabilised the ‘flight’ path (pitch, yaw and roll). A stable platform provides a consistent field of view, i.e., a consistent sample area. The umbilical cable served as tether and communications cable to control lights and laser pointers and receive real-time PAL video footage onboard the support vessel. The two 250 W lights could be switched on and off on demand but remained off most of the time due to adequate ambient light conditions and the high sensitivity of the digital video camera. Two laser pointers, 15 cm apart, underneath the lights served as an indication of scale in the video footage. A ultra-short baseline system tracked the precise geo-location of the platform during deployment.

### 2.6.1 Towed video sampling design

Towed video platform sampling occurred from 25 - 27 February 2009 on R/V *Challenger* (Nichol et al., 2009). Video transect length ranged from 200 m to 1.1 km. Transects were conducted in two directions; along depth contours and across depth gradient. Towed video transects were placed to overlap AUV tracks and cover roughly the same areal extent for later comparison. The platform was towed at 0.5 – 1.5 knots approximately 2 m above the seafloor. Platform altitude

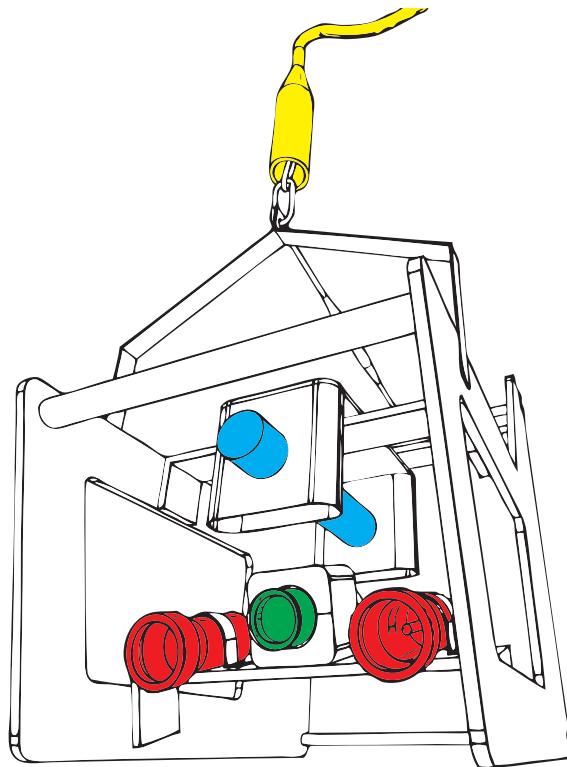


Figure 2.5: Schematic of towed video system; high sensitivity video camera (green), two 250 W lights (red), USBL tracking system (blue) and umbilical (yellow)

was controlled by a winch operator, watching the real-time video footage, onboard the support vessel.

### **2.6.2 Towed video annotation**

Digital video footage with overlaid geographical position was transferred from tape to hard drive and saved as an AVI-file (Audio Video Interleaved). I used the open source software package VARS (Video Annotation and Reference Software (Schlining and Stout, 2006) for viewing and annotation. Mobile invertebrates and vertebrates were identified to species level where possible based on species identification guides (Gomon et al., 2008; Edgar, 1997).

### **VARS**

Several data processing steps were required to extract relative abundance and species richness from the imagery. Video footage taken with the towed video platform was viewed on a large screen and annotated using MBARI's open source software package VARS (Schlining and Stout, 2006). VARS consisted of three parts:

- (i) Knowledgebase
- (ii) Annotation
- (iii) Query

The Knowledgebase consisted of a phylogenetic tree which had to be modified to accommodate Tasmanian (Australian) fish species. For example, in order to add

---

the ocean perch, *Helicolenus percooides* to the Knowledgebase it was also required to add its Family, Order, Class, Phylum and Kingdom. VARS Annotation provided a general user interface to play, pause and stop the digital video file and label individuals when they occurred in the footage. The resulting record stated time and videoframe in which a particular individual occurred. Finally, the resulting VARS Query file enabled the generation of tallies for each species by tow. The hierarchical phylogenetic tree structure within Knowledgebase allowed for querying other levels such as genus or family.



---

## Chapter

# 3

## Image-based continental shelf habitat mapping using novel automated data extraction techniques

*This Chapter has been accepted for publication and will be printed in Continental Shelf Research. The manuscript (unformatted and unedited PDF) is now available online at: <http://dx.doi.org/10.1016/j.csr.2012.06.003>.*

### 3.1 Abstract

We automatically mapped the distribution of temperate continental shelf rocky reef habitats with a high degree of confidence using colour, texture, rugosity and patchiness features extracted from images in conjunction with machine-learning algorithms. This demonstrated the potential of novel automation routines to expedite the complex and time-consuming process of seabed mapping. The random forests ensemble classifier outperformed other tree-based algorithms and also offered some valuable built-in model performance assessment tools. Habitat prediction using random forests performed most accurately when all 26 image-derived predictors were included in the model. This produced an overall habitat prediction accuracy of 84% (with a kappa statistic of 0.793) when compared to nine distinct habitat classes assigned by a human annotator. Predictions for three habitat classes were all within the 95% confidence intervals, indicating close agreement between observed

and predicted habitat classes. Misclassified images were mostly unevenly, partially or insufficiently illuminated and came mostly from rugged terrains and during the autonomous underwater vehicle's obstacle avoidance manoeuvres. The remaining misclassified images were wrongly or inconsistently labelled by the human annotator. This study demonstrates the suitability of autonomous underwater vehicles to effectively sample benthic habitats and the ability of automated data handling techniques to extract and reliably process large volumes of seabed image data. Our methods for image feature extraction and classification are repeatable, cost-effective and well suited to studies that require nonextractive and/or co-located sampling, e.g., in marine reserves and for monitoring the recovery from physical impacts, e.g., from bottom fishing activities. The methods are transferable to other continental shelf areas and to other disciplines such as seabed geology.

## **3.2 Introduction**

Habitat mapping is an essential tool to aid managers in assessing and managing the status of marine ecosystems. Currently mapping of marine habitats is principally based on two data sources, which are acoustic and optical. Both sources are acquired remotely and sampling requires no physical contact with the substrate as opposed to grab samples. Acoustic mapping technologies include single-beam and multi-beam echo sounder (MBES) and side scan sonar (SSS). Most of Tasmania's shallow coastal waters (< 40 m) have been mapped using single-beam echo sounders. Accuracies of up to 3 m can be achieved using differential GPS, however due to the small footprint of the single beam, essentially a point source, acoustic data collection is less efficient

than multi-beam echo sounders. Optical mapping technologies include satellite and aircraft remote sensing, platform-based video camera and sediment profile camera (Rhoads and Germano, 1982). In shallow water ( $< 100$  m), the density of individual MBES soundings is generally several per square metre. In contrast, extractive sediment samples with a footprint usually  $< 0.25$  m<sup>2</sup> are generally placed several hundred metres apart. However, it is commonly the combination of the two (broad and fine-scale) that culminates in habitat maps. The latter discrete fine-scale samples are a reliable and necessary means of groundtruthing remote measurements. Visual techniques, such as digital photography and video, are also considered to work at fine scales ( $\sim 1$  m) and smaller scales. Non-extractive, image-yielding examples include investigations of Arctic habitat-forming epibenthic megabenthos (Piepenburg and Schmid, 1997) and organism-sediment relationships (Rhoads and Germano, 1982). Assis et al. (2007) used a towed video platform to rapidly assess elasmobranch populations within MPAs. A recent review of underwater videometric measurements, especially with respect to the recent introduction of high definition video cameras can be found in Shortis et al. (2007). Autonomous Underwater Vehicles (AUV) are increasingly used as carriers of high-resolution imaging sensors due to their ability to manoeuvre very close to potentially rugged terrain (Williams et al., 2010a), thereby facilitating a constant image footprint. Images taken by an AUV provide two advantages: (1) the continuous photographic record yields intermediate-scale data, thereby bridging the gap between MBES mapping and point sampling and (2) the image itself is an ideal candidate for automated data extraction. Interrogation of digital imagery is necessary to extract qualitative and quantitative

information. This task is usually carried out by a trained annotator. Whilst image capture takes only a fraction of a second, image annotation can take several minutes to tens of minutes depending on the nature and detail of information required. In fact, image interpretation and species identification is extremely time consuming and potentially subjective. Considering the various steps to produce a habitat map, annotating imagery, epitomises the proverbial bottleneck. This study was conducted to expedite the lengthy and time-consuming process of image annotation by means of automation. Other efforts to automate the annotation process include the use of machine-learning algorithms to detect cold-water corals and sponges, as well as coverage enumeration after initial computer system training (Purser et al., 2009). It should be noted though, that this automation requires the computer system to be trained with a training set of images labelled by a human expert. This way, only a subset of the imagery is scored by a human expert and the remainder is scored (classified) by the computer system, usually with associated quantifiable error rate. Purser et al. (2009) report 45 min as the time taken to manually assess per cent coverage for dominant species (sponges and cold-water corals), where each image used 89 subsamples per image. After initial training, it took the computer system 22 s to accomplish the same task. Purser et al. (2009) used image texture features which numerically represent optical and structural attributes of corals and sponges. Whilst Purser et al. (2009) quantify the percentage of seabed covered by two organisms within an image, our study applies the machine-learning algorithm random forests (Breiman, 2001) to automate the process of assigning habitat classes to an entire image of the seafloor. The novelty in our approach is the use of

geo-referenced stereo imagery from AUV mounted digital cameras to generate a centimetre-scale bathymetric reconstruction in the form of a triangulated irregular network. This results in a rugosity value for the overlapping footprint area of each image pair. Usually multiple features are required to describe a habitat comprehensively. We therefore used additional descriptors such as image texture (Local Binary Patterns, LBP), image colour (Hue- Saturation Values, HSV) and patchiness (Patch-Gap summeries, PG) to increase the accuracy of semi-automated habitat prediction. LBP and HSV are well-established methods in industrial machine vision applications (Ojala et al., 2002). In order to reliably employ these methods in an industrial setting, conditions such as lighting are constant and machine tasks are simple, i.e., separating red and green apples. Applying the above-mentioned methods to imagery collected in the field with variable lighting regimes and complex machine tasks is a challenging proposition. Our study explores this challenge by testing the applicability of machine-learning algorithms to automate habitat classification in a practical application, using AUV derived images acquired on Tasmanian deep-water rocky reefs. Existing maps of Tasmania’s inshore marine habitats are based on based on single-beam echo-sounder data and manually annotated video footage for ground-truthing and are restricted to depths  $< 40$  m (Barrett et al., 2001). With the exception of a multibeam sonar mapping trial in this region (Nichol et al., 2009) in which the AUV imagery was acquired as a means of ground-truthing, no other studies in this area exist. The study focused on highly complex rocky reef habitats below 40 m depth, which are difficult to efficiently sample using extractive methods, such as Agassiz trawl or grab sampler. Due to the

geology of Tasmania's south-east coast, our study site exemplifies deep-water rocky reef environments in this area.

The specific aim of this paper is to develop a novel analytical method to automate the process of assigning habitat classes to images of the seafloor, by automatically extracting colour, texture, rugosity and patchiness values from typical field acquired images and therefore curtail image processing time. To assess the success of this process, we evaluate the error rate of misclassifying images and sources of error. Two new processing techniques are developed to extract fine-scale bathymetry from stereo image pairs to calculate a common complexity measure, rugosity and extract fine-scale habitat distributions to calculate multivariate measures of 'patchiness'. We also discuss the relevance of this repeatable and cost-effective method to process the large volumes of image data needed to document the largely unknown fine-scale variability in habitat distributions.

### **3.3 Methods**

#### **3.3.1 Study area**

The study area is situated immediately to the east of O'Hara Bluff, eastern Tasman Peninsula, Tasmania, Australia (Fig 3.1). It forms part of the "Peninsula Mapping Region" (Barrett et al., 2001) which has a dominantly easterly aspect, high vertical cliffs, deepwater reefs (to 100 m depth) and medium to high wave exposure. Geologically, the coastline is composed of dolerite, sedimentary rock and, to a lesser extent, granite (Barrett et al., 2001). This study uses data from 4.6 km of

transects over the deep-water rocky reef of O’Hara Bluff and its offshore extension and transition zones between hard and soft substrate in 34 – 77 m depths. The traverse took just over three hours (vehicle speed = 0.4 m/s).

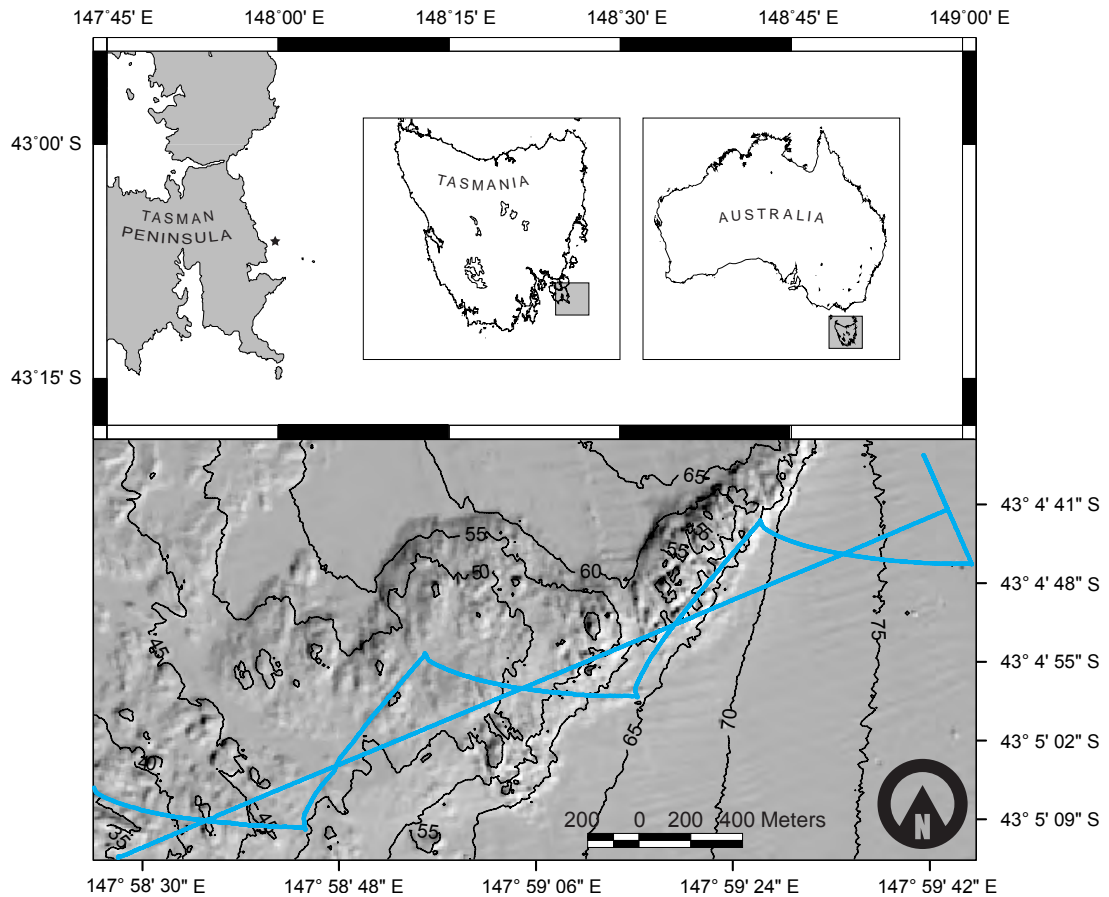


Figure 3.1: Map showing continental shelf study area off O’Hara Bluff in south-eastern Tasmania, Australia. Star in top panel identifies the location of sampling on the hill-shaded seabed relief map in the bottom panel; bathymetric contour lines at 5 m intervals and cyan line represents AUV track.

### 3.3.2 Data acquisition

The Autonomous Underwater Vehicle (AUV) *Sirius*, operated by the Australian Centre for Field Robotics at the University of Sydney, sampled benthic habitats using a pair of downward-looking Pixelfly HiRes (1360 × 1024 pixels) digital

---

cameras. Two strobes synchronously illuminated the field of view. The AUV was able to maintain a virtually constant altitude of 2 m above the seafloor, which equates to an image footprint of  $1.6 \times 1.3$  m. Image acquisition at a one second interval with a speed over ground of  $\sim 0.4$  m/s provided an unbroken photographic record.

*Sirius* is a modified version of the *SeaBED* AUV (Singh et al., 2004b) built by the Woods Hole Oceanographic Institution designed to be passively stable in pitch and roll. Yaw, forward and backward movement is controlled by a pair of aft-facing thrusters. Vertical (depth) movement of the positively buoyant vehicle is accomplished by one vertical thruster. Geographical vehicle positioning on the surface was accomplished using GPS. Navigation underwater is achieved using a Doppler velocity log, inertial measurement unit, ultra-short baseline acoustic positioning system, pressure sensor and a compass. To further reduce positional error introduced by dead-reckoning and sensor inaccuracies, the simultaneous localisation and mapping (SLAM) technique was used to re-navigate the estimated vehicle trajectories (Williams et al., 2008a). Consequently, the intersecting survey pattern (Fig. 3.1 bottom panel) was necessary to maintain high spatial accuracy using SLAM.

### **3.3.3 Automated feature extraction**

Colour, shape and texture features were used to characterise benthic habitats in each image. Stereophotogrammetry was used to construct micro-topography for each stereo image pair to provide a measure of terrain complexity or ‘rugosity’ where the

more complex surfaces had higher rugosity values. The three sets of features used were first and second order statistics of (a) modified hue-saturation-values, (b) local binary patterns, and (c) simple ‘patch-gap’ summaries and rugosity (Table 3.1).

Once a feature is part of the random forests data set, it is referred to as a predictor. The random forest data set consisted of 3586 rows (images) and 26 columns (predictors). We used an extension of the classification and regression tree (CART) concept called ‘random forests’ (Breiman, 2001) to predict habitat classes based on extracted image features. The reason for inconsistent approaches in the literature to accomplish automated classification, such as the use of neural networks (Purser et al., 2009), decision tree classifiers (Rattray et al., 2009), or combinations thereof, is partly due to personal preference and availability of systems that are easily adjusted to one’s task at hand.

#### **3.3.4 Modified hue-saturation values (HSV)**

One of the three basic image features used in pattern recognition is colour. Colour histograms in the Hue Saturation Value (HSV) colour space vary between images, and are thus able to distinguish image content. Min and Cheng (2009) introduced the modified HSV space providing equally distributed building blocks. First and second order statistics of the colour histograms make up five descriptors (HSV 1-5). Underwater imagery may be poorly suited to HSV approaches due to variation in exposure, colour and from varying distance above the seafloor, irregular illumination,

Table 3.1: Overview of extracted image features and brief description used to map habitats on the continental shelf study area off south-eastern Tasmania.

### Modified hue-saturation value

HSV	Hue (H), Saturation (S) and Value (V); cylindrical-coordinate depiction of points in a RGB colour model, where Value is the vertical distance starting at black (bottom centre of cylinder) and ending at white (top centre of cylinder), the radial distance from the centre corresponds to Saturation i.e. tints and shades and Hue is the visible spectrum arranged in a circle (from red to red).
HSV1 (modified)	Standard deviation of $X$ , $S \cos(2\pi H)$
HSV2 (modified)	Standard deviation of $Y$ , $S \sin(2\pi H)$
HSV3	Standard deviation of $V$
HSV4	Mean of $S$
HSV5	Mean of $V$

### Local Binary Pattern (LBP)

LBP	Local Binary Pattern; powerful element for texture classification in computer vision
LBP 1 – 10	Combination of line, spot, edge and other texture filters of eight sampling points covering a radius of one pixel (for examples see Fig 3.2)

### Patch-gap summaries (PG)

maximum continuous patch length  
 number of patches per subsample  
 mean patch length  
 standard deviation of mean patch length  
 variance of mean patch length  
 Patch-gap ratio

### Rugosity

Measure of topographical complexity, usually the ratio between real surface area and the area of its orthogonal planar projection. In a one-dimensional example one takes the ratio of the length of a rope that follows the contour of a reef in a straight line and its linear distance between the endpoints (ignoring profile).

complex terrain and specific substrate reflectivity. The first three factors are connected and their effects were reduced to a minimum by ensuring that the AUV maintained a near-constant height above the seafloor during this study. Specific substrate reflectivity was partially compensated for by bulk-processing the imagery. This HSV approach is well suited to detect signals in the variety, strength and contrasts in colour of benthic biota at the study site, however, HSV descriptors do not formally take account of the ecological affinities of biota with similar colour space.

### 3.3.5 Local binary pattern (LBP)

Since images with the same colour histogram may represent habitats defined by different patterns of spatial distributions, Local Binary Patterns (LBP) was used as a second feature that describes ‘texture’. Machines typically classify textures by comparing an unknown sample with a known training sample. Texture analysis is applied to industrial surface inspection, remote sensing and biomedical imaging but are unable to detect variations in orientation, scale and grey-scale properties (Ojala et al., 2002). LBPs fulfil invariance with respect to grey scale properties and rotation by a joint distribution of grey scale values of a circularly symmetric set of neighbouring pixels in a local neighbourhood (Fig. 3.2 a). Several subsections of the images were sampled using eight sampling points at a radius of one pixel. The sampling points are compared to the centre point. If this grey scale value is greater, the sampling point is assigned 1. If it is smaller, it is assigned 0. This results in one of 36 unique binary patterns (Fig. 3.2 b – f). Uniform LBPs are those that exhibit zero

to exactly two 0/1 transitions. These uniform patterns effectively detect analogues for benthic habitat microstructures such as edges (Fig. 3.2 c), lines (Fig. 3.2 d), spots (Fig. 3.2 e) or pits (Fig. 3.2 f), see Ojala et al. (2002) for more details. The frequency of occurrence of these microstructures is expressed in histograms and form predictors LBP 1-10.

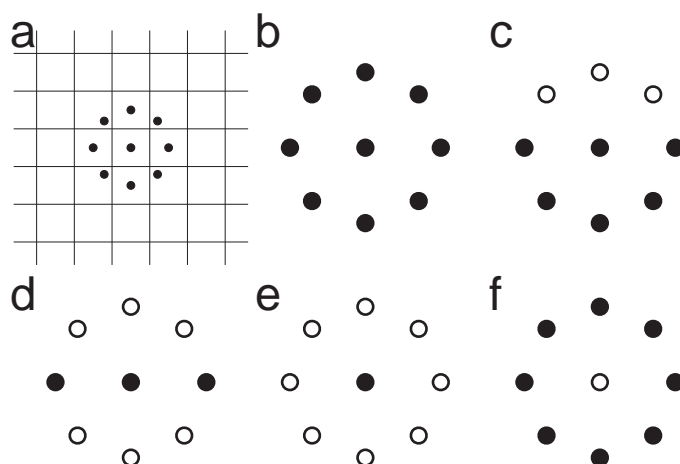


Figure 3.2: Schematic illustrating the concept of Local Binary Patterns (LBP) (a) circularly symmetric neighbour set of 8 points 1 pixel away from centre pixel superimposed on image raster, (b to f) subset of unique rotation invariant binary pattern that can occur using the setup seen in (a) where black and white circles correspond to bit values of 0 and 1 in the 8-bit output of the operator, (b) flat area detector, (c) symmetric edge detector, (d) line detector, (e) peak detector and (f) pit detector. Modified after Ojala et al. (2002).

### 3.3.6 Patch-gap summaries

The novel patch-gap technique attempts to increase prediction accuracy by increasing the number of predictors. The procedure captures additional spatial information on patchiness that includes making contiguous areas representing dominant taxa, e.g., kelp fronds or sponges, and retains information that may

otherwise be lost, e.g., on the distribution of sand patches. The method uses the composition of black (patch) and white (gap) areas in a binary (intensity value 0 (black) and 255 (white)) representation of the original image. The spatial frequency domain of greyscale images from the right camera was transformed using the Adobe Photoshop CS3 high pass filter (HPF) with a radius setting of 10 pixels. HPF enhances the contrast between adjacent pixels by retaining high frequency and reducing low frequency information. HPF is considered to be an edge sharpener in image processing. A threshold intensity value of 128 reduced 256 shades of grey into a binary bitmap (black and white). A routine written in MATLAB was used to extract six features based on subsamples of 10 equally spaced, one pixel high rows per image. These are:

- (i) maximum continuous patch length,
- (ii) number of patches per subsample,
- (iii) mean patch length,
- (iv) standard deviation of mean patch length,
- (v) variance of mean patch length, and
- (vi) patch-gap ratio.

K-means clustering, using the statistical package R (R-Development-Core-Team, 2009) with the number of clusters set to an arbitrary 10, utilised the six patch-gap features and added another 10 predictors to each image.

### 3.3.7 Deriving rugosity

A rugosity measure for the seafloor area covered by each stereo image pair was derived by extracting  $\sim 800$  corresponding image features in each image per pair and to photogrammetrically calculate their position in 3D space. The resulting point cloud, converted to a Delaunay triangulated mesh, is used to calculate the surface area of the seafloor ( $A$ ). The fitted planar surface area ( $A'$ ), using Principal Component Analysis (PCA) on the 3D point cloud, forms the denominator. The resulting ratio ( $A/A'$ ) provides a measure of bathymetric complexity. For an exhaustive description refer to Friedman (2010); Friedman et al. (2012).

The next section describes novel attributes of the process of extracting rugosity from stereo image pairs. Rugosity estimates, based on gridded digital elevation models in a GIS environment, are calculated from the planar surface area by multiplying the number of grid cell in the  $x$ -direction times the number of grid cells in the  $y$ -direction times the surface area of one grid cell. Rugosity was decoupled from slope using PCA to determine the orthogonal projection of the data onto the principle subspace (a lower dimensional linear space) such that the variance of the projected data is maximised.

### 3.3.8 Manual image scoring

Within the survey area, the AUV collected 11,278 overlapping colour images. To achieve independent (non-overlapping) quadrats (images), only every third image was scored. These 3586 images were manually scored and assigned one of the nine

habitat classes (Table 3.2). The habitat classes used in this study can be divided into three primary groups: hard substrate, soft substrate and transitions zones between the former two substrates. Classes of ‘high relief reef’, ‘low relief reef’ and ‘Ecklonia’ comprised the hard substrate group; ‘coarse sand’, ‘sand’, ‘screw shell rubble’ and ‘screw shell rubble/sand’ comprised the soft substrate group; and ‘reef-sand ecotone’ and ‘patch reef’ the remaining transition zone group. ‘Ecklonia’ refers to the dominant macroalga *Ecklonia radiata* and screw shell refers to the invasive mollusc *Maoricolpus roseus*. Example images of each habitat class are shown in Fig. 3.3. Vehicle altitudes  $> 3.5$  m resulted in underexposed images which were excluded from further analysis ( $n = 510$ ).

### 3.3.9 Random forests classifier training and evaluation

We present a method of predictive habitat modelling where relationships between the various automatically extracted image features mentioned above (quantifiable, environmental variables) and human scored habitat classes are investigated using the random forests classifier (Breiman, 2001). Statistical modelling techniques that have been used to predict habitat distribution comprise Classification And Regression Trees (CART, Holmes et al. (2008)) and Quick, Unbiased and Efficient Statistical Trees (QUEST, Rattray et al. (2009)). A collection of recursive rules based on predictors shape the decision tree, i.e., the position of branches and leaves. Random forests is a classification and regression method that derives a classifier by ‘growing’ an ensemble of decision trees and letting them vote for the most popular class. We used the random forests method for two reasons: (1) the random forests

Table 3.2: Habitat class code, habitat class, brief habitat description and frequency of occurrence of each habitat class within AUV transect on the continental shelf study area off south-eastern Tasmania.

Code	Habitat class	Habitat description	Occurrence
RSE	reef-sand eco-tone	interface between hard (reef) and soft (sand) substrate cf patch reef (PR)	6.13%
LRR	low relief reef	hard substrate but low relief (<20 cm excluding benthos)	14.22%
CS	coarse sand	usually shell gravel mixed with sand, however, not screw shells	6.00%
PR	patch reef	patchy hard substrate (reef) covers <50% within soft substrate (sand)	6.27%
S	sand	fine sand with/without sand ripples or waves	2.89%
SSR	screw shell rubble	substrate with >50% covered by screw shells ( <i>Maoricolpus roseus</i> ) cf SSRS	21.25%
SSRS	screw shell rubble/sand	substrate dominated by sand, screw shell cover <50% cf SSR	2.52%
HRR	high relief reef	hard substrate (reef) with high relief >20 cm	33.72%
ECK	<i>Ecklonia radiata</i>	hard substrate covered by kelp ( <i>Ecklonia radiata</i> )	6.75%

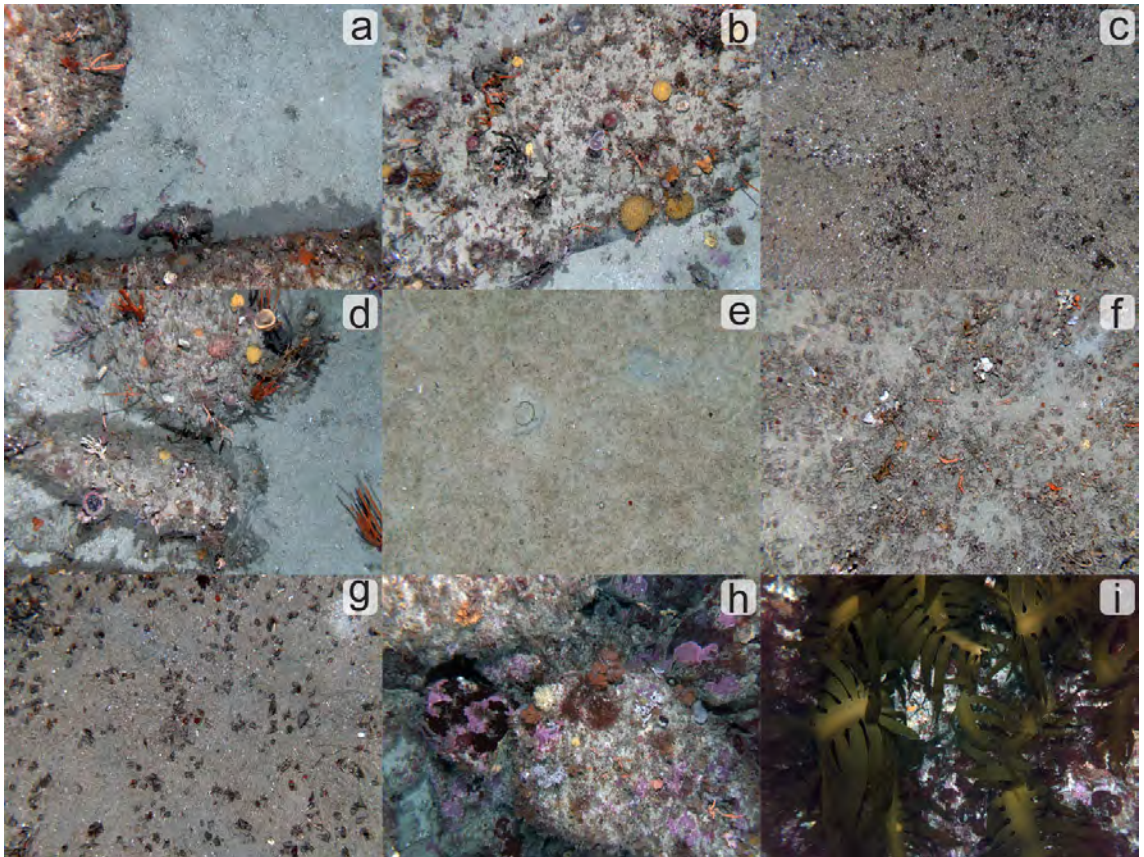


Figure 3.3: Example images for each habitat class identified in the continental shelf study area off Tasmania, south-eastern Australia: (a) reef-sand ecotone, (b) low relief reef, (c) coarse sand, (d) patch reef, (e) sand, (f) screw shell rubble, (g) screw shell rubble/sand, (h) high relief reef, and (i) the alga *Ecklonia radiata*.

approach achieved the highest prediction accuracy, albeit by a small margin, based on comparing prediction accuracy between CART, QUEST and random forests approaches and (2) the random forests approach gives useful internal estimates of classification error, predictor strength, case correlation and variable importance (Breiman, 2001). A subset of 500 randomly sampled images was used to create an ensemble classifier using the randomForest package (Liaw and Wiener, 2002) for R (R-Development-Core-Team, 2009). In addition, the importance of predictors was assessed by extracting variable importance measures produced by random forests and a proximity measure among rows was calculated to identify similarities between habitats as predicted by random forests. Different subsets of predictors were used to investigate the impact of fewer predictor variables on classification error rate, i.e., only the patch-gap summaries predictor set, then adding the HSV predictor set, then adding the local binary pattern predictors set and finally rugosity. The model was run with combinations of the three predictor sets and rugosity culminating in a final model including all 26. Each model run produced an error rate estimate based on bootstrapping. The different random forests models derived from the training data set were then applied to predict habitat classes for the remaining 3086 images. Fleiss' exact and habitat class-wise  $\kappa$  were computed to evaluate prediction accuracy compared to observed habitat classes (Fleiss, 1971). In addition, confusion matrices, a common visualisation tool in the machine learning realm, were used to further clarify model strengths and weaknesses. Each matrix column represents predicted instances and each row represents the actual observed class (habitat). This way it is easy to assess which classes were misclassified, expressed as being on either side

of the diagonal line of numbers (Table 3.3 numbers in bold). The random forests algorithm estimates the importance of a variable (predictor) based on prediction error increase when out-of-bag (randomForest intrinsic prediction error estimation) data for that variable is permuted while the remaining variables are left unchanged. Calculations are carried out tree by tree as the random forest is constructed. The more the estimated error rate increases the more important is a predictor, i.e., leaving an important descriptor out decreases prediction accuracy. We performed a  $\chi^2$  goodness-of-fit test to assess differences between observed and predicted habitat classes. Bootstrapping and the calculation of 95% confidence intervals helped to visualise which habitat classes the random forests model was able to predict within confidence boundaries. The entire vector containing all observed habitat classes was re-shuffled with replacement 25 times. These 25 permuted habitat distributions were used to calculate 95% confidence intervals to visually assess prediction performance for each habitat class. Random forests provides intrinsic proximity values for each case (image), in our case culminating in a square ( $500 \times 500$ ) proximity matrix with value 1 on the diagonal and values between 0 and 1 in the off-diagonal positions. Multi-dimensional scaling (MDS) was used to plot the scaling coordinates contained in the proximity matrix to visualise case (image) similarities. The rationale behind MDS is the representation of samples (images) as points in two-, sometimes three-dimensional space so that distance (proximities) between points corresponds to similarities in the intrinsic random forests proximity matrix. Applying this principle, points in an MDS plot that are close together stand for samples (image classification outcomes using random forests) that are very similar and points far apart stand for

samples that are very different.

Observed and predicted habitat classes were superimposed on bathymetry for visual assessment. All statistical analyses described in this section were performed using the R base package and the MASS package (R-Development-Core-Team, 2009).

## **3.4 Results**

### **3.4.1 Prediction accuracy**

Habitat prediction using random forests performed most accurately when all 26 predictors (Table 3.1) were included in the model (Fig. 3.4). Increasing the number of predictors increased the accuracy of correct habitat classification. Using only the 10 predictors derived from the patch-gap summaries (PG) resulted in habitats being accurately classified 31% of the time. Predictors obtained from HSV achieved a higher correct classification rate of 62%. HSV and LBP predictors in combination made the greatest contribution to overall classification accuracy (68%). Adding PG to the HSV-LBP combination increased classification accuracy by only 1% (69%). The ensemble classifier using all 26 predictors combined (HSV, LBP, PG and rugosity) correctly classified 71% of the images. This is 5% lower than the error rate estimate (24%) from the training set, i.e., 76% correctly classified images, showing that bootstrapping the training data set with only 500 images is overestimating prediction accuracy compared to predictive modelling applied to the remaining 3086 images. Sample sizes for different habitat classes were unequal (Table 3.2). This will have an effect on prediction accuracy if a different set of 500 randomly selected

images is used in the classifier (forest) formation process but is not assessed here. Running the randomForests algorithm several times with the same image subset resulted in small differences in error rate (mean = 21.064, SD = 0.553,  $n = 25$ ).

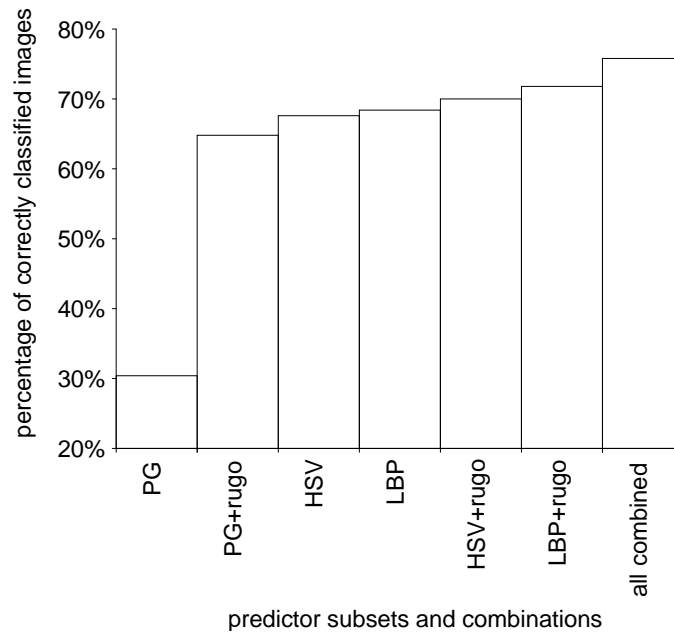


Figure 3.4: Comparison of different predictors to percentage of correctly classified images in continental shelf seabed habitats off Tasmania, south-eastern Australia. Number of images = 3086. PG = patch-gap summaries, HSV = Hue-Saturation Value, LBP = Local Binary Pattern, rugo = rugosity.

### 3.4.2 Predictor importance

In increasing order, local binary pattern 2, hue-saturation value 4 and rugosity were found to be the most important predictors when averaged over all habitats (Fig. 3.5, bottom panel). However, predictor importance by habitat class differed dramatically from the average overall predictor importance (Fig. 3.5, top nine panels). Rugosity was the most important predictor for habitat classes of Ecklonia, patch reef, reef-sand ecotone, screw shell rubble and screw shell rubble/sand. Hue-

---

saturation values, especially HSV1, were the most important predictors for the habitat class of sand. Texture attributes (local binary patterns) dominated high importance values for the habitat class of coarse sand (Fig. 3.5, top panel). For the remaining habitat classes, high relief reef and low relief reef predictor importance was less defined and comprised a mixture of hue-saturation values, local binary patterns, and rugosity. Patch-gap summaries out-competed hue-saturation values with respect to importance for habitat class of ‘low relief reef’.

### 3.4.3 Confusion matrices

Although the patch-gap summaries predictor set appeared to have little importance (Fig. 3.5, open circles), retaining them decreased the classification error for habitat class ‘screw shell rubble/sand’ by 60%. This improvement was based on comparing confusion matrices obtained from running random forests with and without the patch-gap summaries predictor set. The confusion matrix (Table 3.3) revealed which habitat classes had been confused and which had been classified correctly. From the 45 possible unique observed-predicted combinations, 12 combinations were never scored incorrectly, e.g., the habitat class of *Ecklonia* was never mistaken for coarse sand (Table 3.3). To acknowledge prediction error on an image-by-image basis, we used Fleiss’ inter-rater measure  $\kappa$ . This measure of inter-rater agreement compares observed and predicted habitat classification for each image. Pooling all observed instances of a particular habitat class and comparing these to the corresponding pooled predicted habitat class showed that prediction accuracy was highest for ‘screw shell rubble’ (99.5%) and lowest for ‘patch reef’ (77.7%). Other habitat

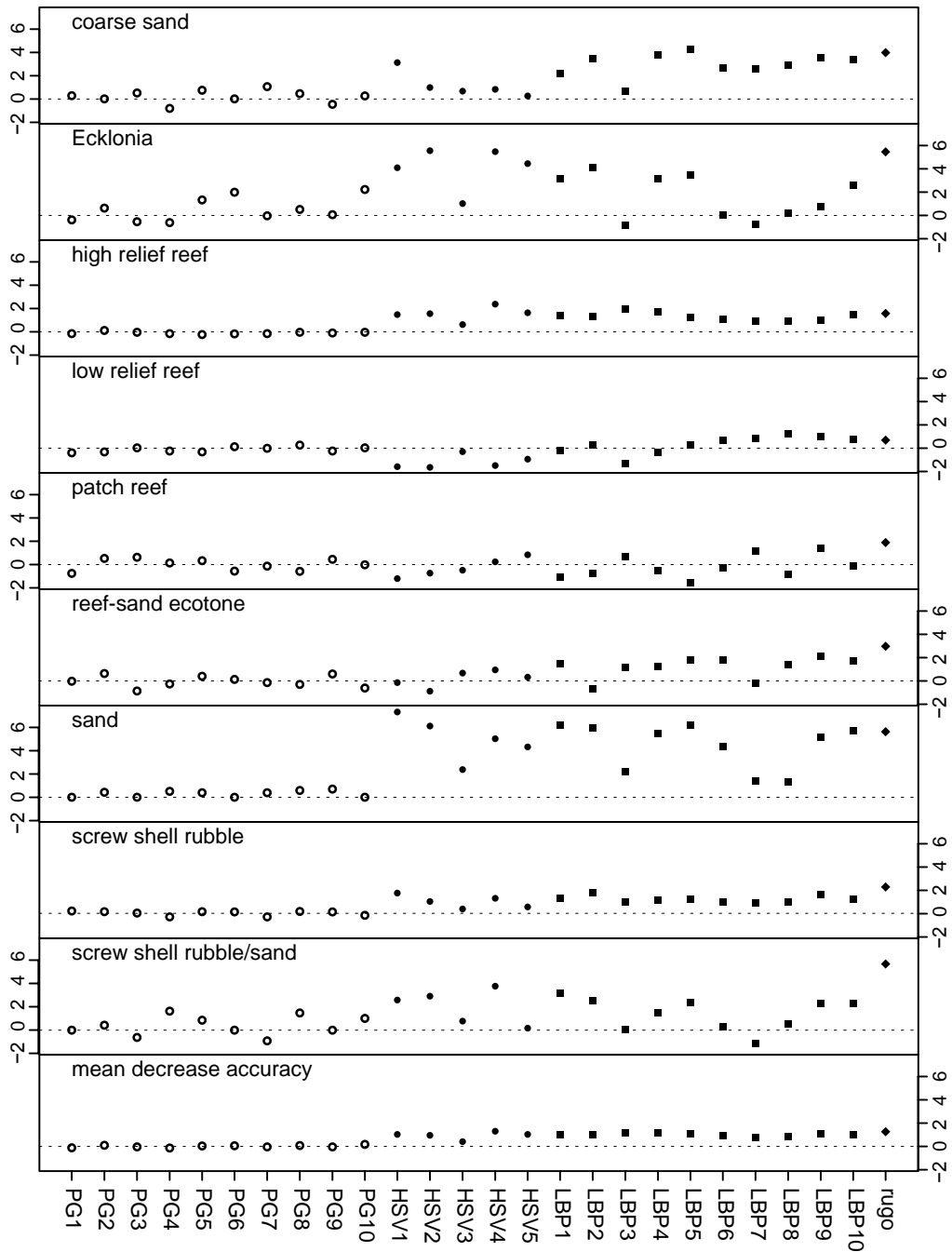


Figure 3.5: Importance of each predictor (abscissa) used to map habitats expressed as mean decrease accuracy, i.e., leaving out rugosity reduces the accuracy by a factor of 0.16. Open circles = PG1-10 = patch-gap summaries, filled circles = HSV1-5 = hue-saturation value, filled squares = LBP1-10 = local binary pattern, filled diamond = rugosity.

---

classes predicted with low percentages of correct classification were sand (79.3%) and *Ecklonia* (80.3%). With respect to Fleiss'  $\kappa$  statistic, screw shell rubble (SSR) scored the highest agreement ( $\kappa = 0.992$ ,  $z = 55.083$ ,  $p = < 0.001$ ), whilst patch reef (PR) scored the lowest agreement ( $\kappa = 0.583$ ,  $z = 32.413$ ,  $p = < 0.001$ ). In fact, both habitat types (reef-sand ecotone and patch reef) containing a mixture of elements of consolidated and unconsolidated habitats scored low ( $\kappa < 0.6$ ). Landis and Koch (1977) assigned terms such as 'moderate' ( $\kappa$  values from 0.41 – 0.60), 'substantial' ( $\kappa$  values from 0.61 – 0.80) and 'almost perfect' ( $\kappa$  values from 0.81 – 1.00) to describe strength of agreement between raters. Their clearly arbitrary divisions are criticised by Gwet (2001). Accordingly, the overall  $\kappa$  statistic = 0.793 ( $z = 88.600$ ,  $p = < 0.001$ ) would warrant the label of 'substantial agreement'. Between-habitat class confusion was highest for high and low relief reef (HRR and LRR, respectively). Seventy-nine per cent of incorrectly classified images that were scored as 'low relief reef' were predicted to be 'high relief reef'.

#### 3.4.4 $\chi^2$ and permutation

A  $\chi^2$  goodness-of-fit test to statistically assess agreement between observed and predicted habitat classes led to the rejection of the null hypothesis at the 1% level. The test confirmed that there are significant differences between observed and predicted habitat classes ( $\chi^2 = 31.7978$ ,  $df = 8$ ,  $p = < 0.001$ ). This can also be seen in a bar-plot of observed and predicted habitat classes with superimposed error bars (Fig 3.6), representing 95% confidence intervals calculated from 25 permuted observed habitat class distributions. Whereas the  $\chi^2$  test gave an absolute statement

Table 3.3: Confusion matrix for habitat classification using a random forest classifier and 26 predictors including Fleiss' category-wise  $\kappa$  (a measure of rater agreement; ranges from 0 – 1, 1 being total agreement). Numbers in bold refer to number of correctly classified images. \* denotes classes without erroneous prediction. CS = coarse sand, ECK = Ecklonia, HRR = high relief reef, LRR = low relief reef, PR = patch reef, RSE = reef-sand ecotone, S = sand, SSR = screw shell rubble, SSRS = screw shell rubble/sand.

observed	predicted									$\kappa$
	CS	ECK	HRR	LRR	PR	RSE	S	SSR	SSRS	
CS	<b>143</b>	0	0	0	12	4	20	0	14	0.77
ECK	0*	<b>53</b>	19	2	2	0	0	0	0	0.77
HRR	0*	8	<b>1051</b>	114	10	36	0	1	0	0.82
LRR	1	0	54	<b>209</b>	14	25	0	0	0	0.59
PR	4	0	2	14	<b>89</b>	19	1	0	0	0.58
RSE	6	0	17	19	32	<b>137</b>	2	0	0	0.60
S	0	0*	0*	0*	4	0	<b>63</b>	0	2	0.80
SSR	2	0*	0	0*	1	0*	1	<b>796</b>	3	0.99
SSRS	18	0*	0*	0*	2	0*	0	2	<b>58</b>	0.73

that predictions and observations do not correspond, the bar-plot (Fig 3.6) elucidates prediction failures and successes for each habitat type. Predictions for habitat classes ‘screw shell rubble’, ‘reef-sand ecotone’, and ‘screw shell rubble/sand’ were all within the 95% confidence intervals, indicating close agreement between observed and predicted habitat classes. At least in one instance, this compares favourably to Fleiss'  $\kappa$  statistic of 0.992 (highest) for ‘screw shell rubble’. However, the remaining six habitat classes of ‘sand’, ‘high relief reef’, ‘low relief reef’, ‘coarse sand’, ‘patch reef’ and ‘Ecklonia’ predictions were all outside the 95% CI boundaries, and demonstrate a somewhat worse prediction performance.

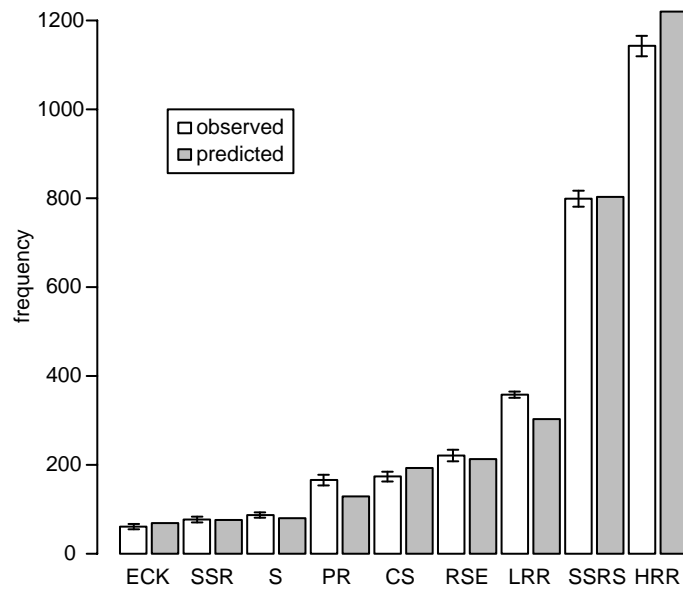


Figure 3.6: Frequency of occurrence of observed and predicted habitat classes on the continental shelf study area off south-eastern Tasmania. Error bars superimposed on white bars represent 95% confidence intervals calculated from 25 permuted observed habitat class distributions. CS = coarse sand, ECK = Ecklonia, HRR = high relief reef, LRR = low relief reef, PR = patch reef, RSE = reef-sand ecotone, S = sand, SSR = screw shell rubble, SSRS = screw shell rubble/sand.

### 3.4.5 Multi-dimensional scaling and proximity

We used multi-dimensional scaling of random Forest’s intrinsic proximity matrix to visualise classification performance. Fig. 3.7 showed one clearly defined cluster on the left hand side of the graph (purple \*) representing ‘screw shell rubble’. This well-defined cluster also corresponded well with Fleiss’  $\kappa$  statistic of 0.992, i.e., virtually no misclassification for this habitat class. The cluster of light-green + representing ‘high relief reef’ and forming an arm on the right hand side of the graph owed its conspicuous appearance to the fact that this particular habitat dominated the habitat distribution ( $\sim 30\%$  of all instances, Table 3.3). Although reasonably well defined in the upper reaches of the arm (light-green +), the lower reaches coincided with (in decreasing order) instances of ‘low relief reef’ (green  $\times$ ), ‘Ecklonia’ (orange  $\triangle$ ), and ‘reef-sand ecotone’ (blue  $\blacktriangledown$ ). This relatively well defined cluster (‘high relief reef’, light-green +) also corresponded well with the relatively high  $\kappa$  statistic of 0.821 for this habitat class (Table 3.3) but was largely due to the dominance within the habitat distribution ( $\sim 30\%$ , Table 2). The fact that clustering in the MDS plot can be explained by the habitat-wise  $\kappa$  statistic (Table 3.3) and habitat frequency of occurrence (Table 3.2) is exemplified in the third cluster ‘coarse sand’ (red  $\circ$ ) in the bottom right of Fig 3.7. Again, the lower reaches of the stubby ‘coarse sand’ arm were well defined but the upper reaches coincided with the ‘confusion zone’ where misclassification became most apparent. Although the stubby ‘coarse sand’ arm and the long ‘high relief reef’ arm were similar in appearance, their respective  $\kappa$  statistics were quite different (0.765 and 0.821, respectively). Again, the lower  $\kappa$

---

statistic (0.765) for habitat class ‘coarse sand’  $cf \kappa = 0.821$  ‘high relief reef’ was due to its relatively small frequency of occurrence (coarse sand = 6%, Table 2). The ‘confusion zone’ in Fig. 3.4 (bottom right corner) gave a good indication of which habitat classes have been misclassified represented by different symbols, representing different habitat classes, appearing close together. Conversely, the MDS plot also showed which habitat classes have been classified correctly represented by identical symbols appearing close together with relatively few ‘impurities’, i.e., other symbols appearing in a given cluster. One of the unusual features of the MDS plot (Fig. 3.4) is the depiction of three ‘arms’. This is due to the way the proximity matrix within random forests is created. The random forests approach runs all cases (images) of the training set down the unpruned tree. If two cases (images) end in the same terminal node of a tree their proximity is increased by one. Finally, all proximities are divided by twice the number of trees grown (Breiman, 2002). This increase in proximity by  $1/2n_{trees}$ , results in the generation of ‘arms’.

### 3.4.6 Habitat mapping

Scored and predicted habitat classes along the AUV track are presented in Fig. 3.8. Screw shells (*Maoricolpus roseus*) dominated the substrate at  $> 72$  m depth and kelp (*Ecklonia radiata*) dominated in depths  $< 40$  m. Between 40 and 72 m depth, the remaining habitat classes were present, although dominated by high and low relief reef. Overall, the predicted habitat map was very similar to the observed habitat map, except for a  $\sim 150$  m stretch of coarse sand, incorrectly predicted as screw shell rubble/sand (top right corner, Fig. 3.8). Superficially the observed (top panel)

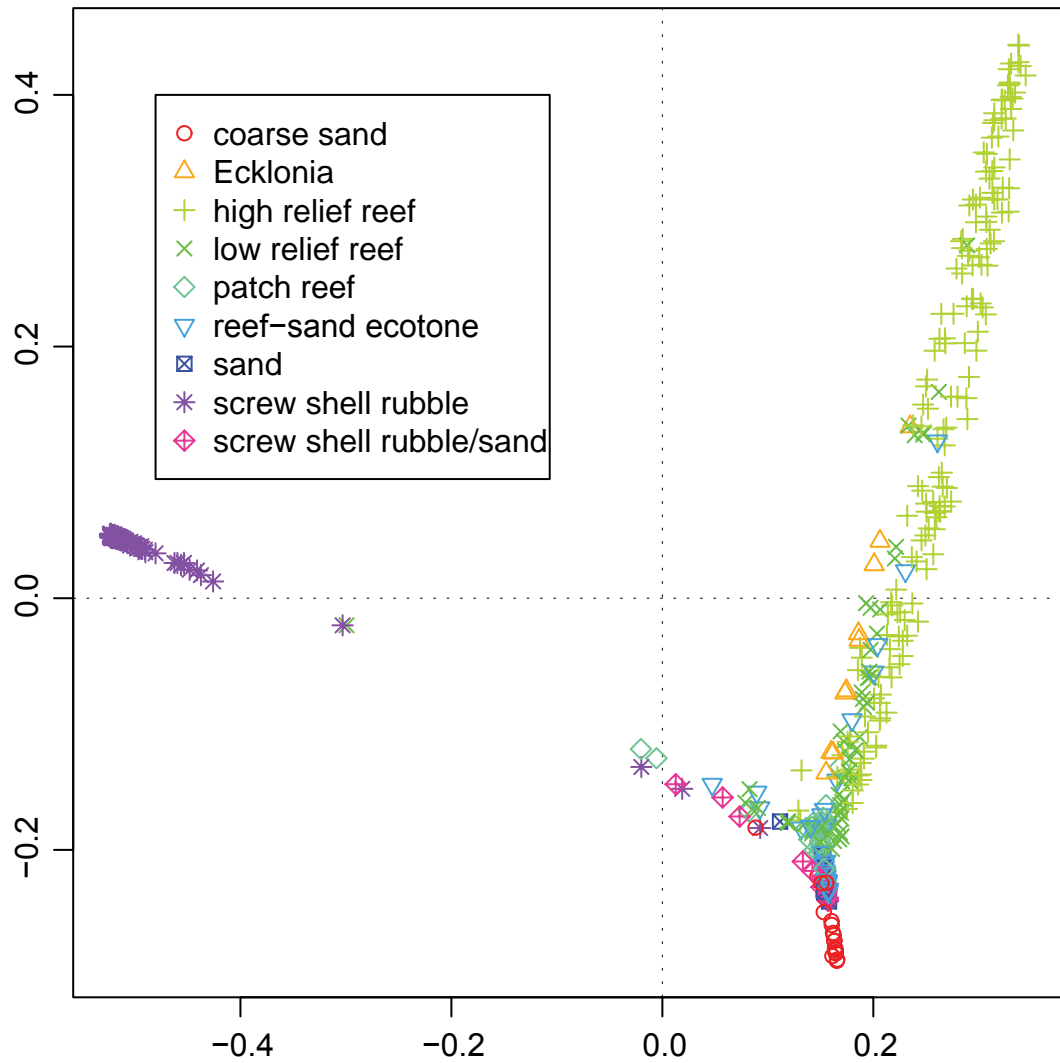


Figure 3.7: Multi-dimensional scaling plot of the proximity matrix produced by random forests for habitat classes on the continental shelf study area off south-eastern Tasmania. Each habitat is colour-coded and represented by a unique symbol; refer to legend,  $n = 500$ .

and predicted (middle panel) looked identical; only after closer inspection was the missing stretch of ‘coarse sand’ apparent as well as minor deviations in the highly diverse shallows (< 50 m water depth).

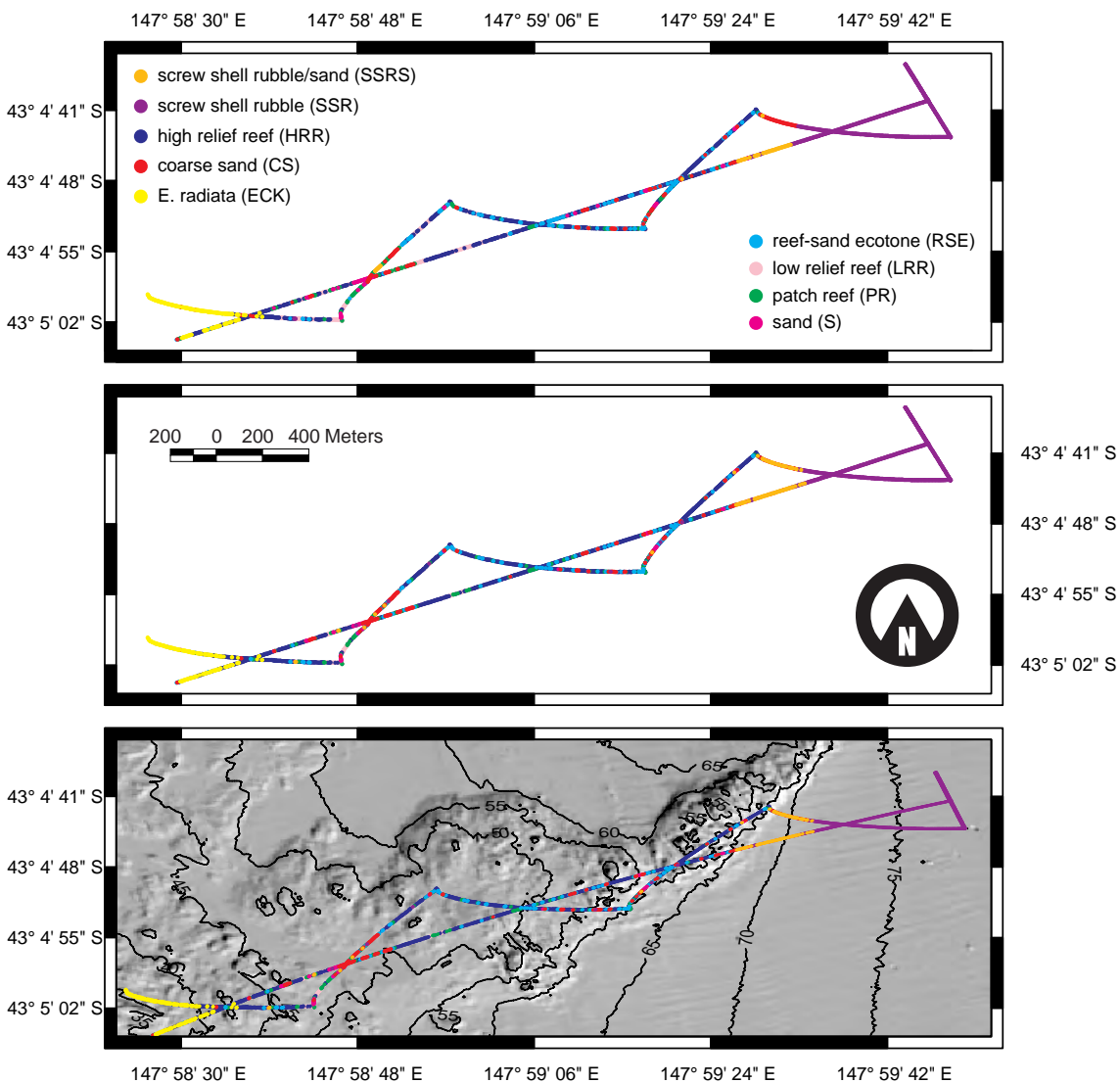


Figure 3.8: Colour-coded observed (top panel) and predicted (middle panel) habitat classes along AUV track. See legend for details. Bottom panel represents colour-coded predicted habitat classes superimposed onto 5-m contoured shaded relief bathymetry.

### 3.5 Discussion

The composition of benthic habitats along a 4.6 km AUV track at the O’Hara Bluff site was predicted, with a generally high degree of confidence, using 26 automatically extracted image features in conjunction with the random forests ensemble classifier. With the exception of the rugosity feature, which requires stereo-imagery, all feature extraction techniques presented in this study can be applied to any kind of imagery data and to other (non-biological) disciplines, e.g., to classify sediment morphology in geological studies. Using random forests to classify images according to habitat type based on image features proved to be successful and is considerably more cost-effective than traditional techniques, such as manually assigning habitat classes. Cost-effectiveness is particularly important because we found that the full predictor dataset achieved the most accurate ensemble classifier. Large datasets may rapidly exceed the capacity of non-automated methods, for example, our 4.6 km single-site dataset comprised 3586 images each with 26 predictors. This finding is consistent with the view of Breiman (2002) who stated that “newer methods in machine learning thrive on variables — the more the better. There is no need for variable selection, ...”.

To understand the reasons that led to habitat misclassification, wrongly classified images were reviewed manually. The majority of misclassified images was partly- or underexposed, which reduced the information obtained by the feature extraction routines. The remaining images were wrongly or inconsistently labelled by the human annotator. Reasons for images being partly- or underexposed were two-

---

fold: (i) uneven illumination and (ii) substrate reflectivity. Uneven, partial or insufficient illumination occurred mostly over extremely rugged terrain and during obstacle avoidance manoeuvres over highly complex reef environment with vertical drops of several metres. Different reflectivity and absorption properties of different substrates, e.g., sand, shell rubble, macroalgae, sponges, etc. also caused under/over-exposure. Whereas sand has a relatively high reflectivity and images of this habitat class might be slightly over-exposed, thick macroalgal cover has a low reflectivity resulting in slightly under-exposed images. Although this was a minor effect, it was evident in the imagery. With respect to the poorly performing patch-gap summaries (PG) as a predictor, it is conceivable that adjusting the threshold value, used in converting grey-scale images to black and white images based on the overall brightness of the image, could improve PG predictor performance. The current method used a constant threshold value of 128. Wrong or inconsistent labelling of imagery by the human annotator occurred primarily for three reasons. First, the threshold that distinguished habitat classes ‘screw shell rubble’ and ‘screw shell rubble/sand’ was defined as  $> 50\%$  and  $< 50\%$  screw shell cover, respectively. Without actually measuring the area, this estimate could be out by up to 20% (personal communication, Mark Green, CSIRO) and will differ between different observers. The aforementioned principle also applies to the habitat class ‘Ecklonia’, which was scored when *Ecklonia radiata* cover exceeded 50% of the image. Second, camera orientation affects perception of sloping surfaces and appeared to account for the high misclassification rate of ‘low relief reef’ as ‘high relief reef’ and *vice versa*. Inconsistent labelling by the human annotator will confuse the random forests model.

The rule distinguishing ‘high’ and ‘low’ relief reef was  $> 20$  cm or  $< 20$  cm elevation change, respectively. In some situations this might be a difficult annotation decision and is prone to error with a downward-looking field of view. Thirdly, distinguishing between the habitat classes ‘patch reef’ and ‘reef-sand ecotone’ might in some cases require knowledge of neighbouring images to come to a conclusive decision, that is, whether a small isolated reef is ‘patch reef’ or the beginning of a larger reef and therefore ‘reef-sand ecotone’. Although this knowledge is available to a human annotator, random forests is oblivious of this knowledge since it classifies habitats on a case by case (image by image) basis.

Jensen (2004) advocates the use of a hybrid neural network – classification tree system, to reduce classification error. We cannot use our data to validate this proposal but were able to demonstrate that there are differences in prediction accuracy between different tree-based classification methods — CART, QUEST and random forests. Although Pal and Mather (2003) report QUEST to outperform CART using terrestrial remotely sensed imagery, our study results show the opposite; CART outperformed QUEST. Notably, random forests outperformed both CART and QUEST and also offered some valuable built-in assessment tools to evaluate model performance. The first tool offers insights into the ‘variable (predictor) importance’ and can be useful in the exclusion of predictors that contribute little or nothing to prediction accuracy. Using this feature, the patch-gap summaries proved to be of little importance for overall accuracy, but were essential to increase specific habitat classification accuracy for ‘screw shell rubble/sand’. However, an overall increase in accuracy will also be reflected in habitat specific prediction accuracy.

The discrepancy between estimated error rate of the bootstrapped training data set and prediction error rate could be remedied by ‘growing’ more trees, thereby giving random forests a better chance to learn. However, in some instances the number of trees ‘grown’ does not warrant a lower estimated error rate due to the nature of the data. In our case, increasing the number of trees did not change the error rate estimation. In some cases, increasing the number of images in the training data set, which at the same time will magnify human work load, can help decrease the estimated error rate. However, since this paper is presenting methods to decrease human work load, a balance must be struck between work load and accuracy.

Prediction accuracy is related to the number of habitat classes. Reducing our habitat classes to two, i.e., rock and sand, would have resulted in virtually 100% prediction accuracy (Friedman, 2010). Lucieer and Pederson (2008) found similar improvements in accuracy by reducing the number of classes from 3 to 2 (72% vs 81%). It should be noted though, that misclassifications are usually random. For example, assuming a 100 m stretch of homogenous habitat, a minimum of 5 images out of  $\sim 80$  images would have been misclassified at a significance level of 5%. These 5 images would have been placed randomly along the 100 m stretch and would not have changed the overall impression of the habitat composition. As with many other predictions in statistical modelling, it is good standard practice to provide an error estimate for every predicted value. The entire method, image feature extraction and classification, described in this paper could be easily extended to full coverage acoustic data sets, e.g., gridded bathymetry and geo-referenced visual ground-truthing data such as digital stills and video. Our predicted habitat map

provides a snapshot of the habitat composition that is bound to change over time. In its current form, it already provides evidence of the extent of the invasive New Zealand screw shell *Maoricolpus roseus* (Allmon et al., 1994). The use of the AUV in conjunction with the new methods described in this study is not restricted to Tasmanian deep-water rocky reefs. Other highly complex and vulnerable habitats such as coral reefs can be monitored to assess storm damage to corals or the extent of coral bleaching events. Not only do images provide a permanent record that can be reviewed or analysed at a later date, their collection is non-extractive, leaving habitats unchanged. In contrast to extractive sampling methods, such as dredging, our non-invasive geo-referenced imagery-yielding technique allows us to re-visit the same sampling area in the future. Thus, image-based methods supported by cost-effective methods of habitat mapping with known estimates of uncertainty, will underpin frameworks for monitoring programs to assess environmental change and management performance. Their applications will include determining the direct impact of bottom fishing methods and subsequent changes — particularly the changes that occur when previously disturbed areas are protected within marine reserves. With regard to habitat mapping, every subsequent, congruent survey could use the initial random forests model, thereby eliminating the need for human image annotation. In this context, we acknowledge the need for an uncertainty measure to account for prediction inaccuracies; here it is incorporated (rather coarsely) in the permuted habitat distributions. Future advancements in image content recognition or more sophisticated information extraction methods than those presented in this paper might yield better habitat maps than is currently possible.

It is also conceivable that combining co-located acoustic backscatter data and AUV imagery surpasses the accuracy of the map presented in this study. These parameters could then be used to predict habitats outside the sampled area using MBES data, e.g., Rattray et al. (2009). Currently acoustic backscatter analysis can distinguish hard and soft substrate with high degrees of confidence but would be insufficient as the sole source to distinguish 9 habitat classes as in this study. Backscatter data would be another predictor in the random forest algorithm and the algorithm decides whether the backscatter data are a strong predictor for certain habitat classes.

It should be stated that most of the above mentioned advantages are closely linked to the design of the actual AUV itself. Geo-referenced imagery, a virtually-constant height-above-seafloor calibrated stereo camera system, altimeters and depth sensors are all required to implement the techniques described here. In conclusion, the AUV served as an excellent, stable and mature platform in this study to autonomously survey benthic habitats. While this AUV is relatively large in size, (Singh et al., 2004b) report successful AUV deployment from a 42' (12.8 m) vessel equipped with an A-frame during their investigation of coral reef habitats in Puerto Rico, indicating the high utility of AUV platforms for habitat mapping in many different environments.

---

## Chapter

# 4

## Beyond diver's depth: evaluating stereo baited underwater video systems as a tool to monitor deep-water temperate reef fish assemblages on the continental shelf

### 4.1 Abstract

Diver based underwater visual census, a commonly used method to study reef fish assemblage composition, i.e., species richness, individual species abundance and size structure, is unsuitable below safe SCUBA diving depths. Here, baited underwater video systems (BUVS) are used as an alternative to assess reef fish assemblage composition on temperate deep-water rocky reefs. BUVS recorded 48 species and the most abundant families were Labridae and Monacanthidae. Assemblage composition was linked to habitat complexity measures (e.g., slope, fractal dimension and aspect) but not linked to oceanographic data (e.g., salinity, chlorophyll *a* and optical backscatter). Significant differences in individual species abundances between onshore and offshore assemblages were found for *Latris lineata*, *Notolabrus tetricus*, *Pseudolabrus psittaculus* and *Pseudophycis bachus*. Mean *L. lineata* length was 190 mm larger compared to line-fishing data. A new relative abundance estimate, based on a tally of individuals, differentiated by photogrammetrical length measurements, proved to be inferior to the current de facto standard *MaxN* but was informative

when combined with *MaxN*. *MaxN* is defined as the maximum count of species  $x$  in video frame  $y$  during each BUVS deployment. A novel statistical approach to conduct power analysis on count data, for which the common assumption of normality does not apply is presented. This method, using *MaxN*, detected differences in abundance of  $> 50\%$  between two sites for *Nemadactylus macropterus* and *N. tetricus*. Results confirm that, in deeper water, BUVS can provide the same information as underwater visual census in the shallows.

## 4.2 Introduction

This chapter is based on the premise that, in deep-water, Baited Underwater Video Systems (BUVS) can provide the same information as Underwater Visual Census (UVC) in the shallows. Information gained from UVC include:

- presence of reef fish assemblages
- abundance of individual reef fish species
- reef fish size structure

This chapter will demonstrate how the above-mentioned information can be obtained using BUVS in temperate deep-water continental shelf reef environments below safe SCUBA diving depths ( $> 30$  m).

Underwater visual census is frequently used to assess composition, abundance and size structure of reef fish assemblages in shallow depths ( $< 30$  m). UVC is

particularly well suited to monitor Marine Protected Areas (MPAs) due to its non-intrusive nature (Barrett et al., 2007). Globally, MPAs and other discretely defined management areas are seldom restricted to safe SCUBA diving depths. For example, the south-east Commonwealth Marine Reserve Network covers 226,458 km<sup>2</sup> and is entirely below safe SCUBA diving depths. In order to assess composition, abundance and size structure of reef fish assemblages below these depths (> 30 m), remote sampling platforms, such as BUVS, need to be employed. This study investigates whether deep-water BUVS can provide the same information that UVC offers in shallow water.

Management objectives after establishing a MPA are manifold. In general, MPAs aim at long-term ecological viability of marine systems, maintaining ecological processes and systems, and protecting biological diversity at all levels (DPIWE, 2000). Traditionally, three levels of diversity are recognised; genetic, species and ecosystem diversity. An example, at the species assemblage level, would be differences in fish assemblage composition between protected and unprotected marine areas using BUVS in a tropical-temperate transition zone Watson et al. (2007). A management regime is usually put in place after dramatic changes in a system have occurred. In the Tasmanian context, Ling et al. (2009) found that large Spiny lobsters *Jasus edwardsii* increase kelp bed resilience through predation on the invading long-spined sea urchin *Centrostephanus rodgersii*. Hence, protecting large individuals of *J. edwardsii* from fishing reduces the risk of a catastrophic shift to widespread sea urchin barrens (Ling et al., 2009). Kelp forests are an

important habitat for a variety of reef fish such as the blue-throated wrasse and banded morwong and its decline would be reflected in changing reef fish assemblage compositions assessed using BUVS. Indeed, abundance and individual size of *J. edwardsii* and other species have increased in Tasmanian MPAs (Barrett et al., 2007). In fact, Barrett et al. (2007) observed an increase in the abundance of large fish (> 30 cm) and a doubling of species richness (biodiversity) following 10 years of protection through the establishment of an MPA on the east coast of Tasmania. All examples above are currently monitored using non-extractive sampling tools. This study examines the usefulness of BUVS in monitoring key species and biodiversity below safe SCUBA diving depths. It also demonstrates the capability of stereo BUVS to reliably measure fish length (measurement error < 1%, Harvey et al. (2003)) and to potentially overcome one shortcoming of *MaxN*, underestimation of relative fish abundance. *MaxN* is the de facto standard relative abundance measure using BUVS; it is defined as the maximum number of individuals of species  $x$  in video frame  $y$ .

### **Habitat complexity measures**

Presence and absence of specific habitats limit the distribution of species. Affinities to certain habitat components are so strong that reliable predictive models can be developed for several fish species. For example, Chatfield et al. (2010) combined benthic habitat features such as substratum, water depth, macroalgal presence/absence and sessile invertebrates presence/absence to explain and predict the structure of demersal fish distributions in shallow waters of the Recherche

Archipelago, southern Western Australia. Habitat complexity measures quantify physical habitat attributes such as roughness, slope, aspect and geomorphology. Habitat complexity measures derived from Digital Elevation Models (DEM) have been successfully used in creating habitat suitability indices and maps for five demersal fish taxa in Discovery Bay, south-east Australia (Monk et al., 2010), four demersal fish species in waters of the Cape Howe MNP located on the easternmost point of the Victorian coastline in southeastern Australia (Moore et al., 2009) and the European lobster (Galparsoro et al., 2009). Strong predictors are reef complexity (Moore et al., 2009). The DEM of the study area of this project was derived from multibeam sonar data (Nichol et al., 2009). Several habitat complexity measures were computed for all BUVS sampling locations to quantify relationships with reef fish assemblages.

### **Species accumulation curve**

*Detection error* is one potential source of error when estimating biological diversity (Yoccoz et al., 2001) and refers to the fact that most sampling methods cannot detect all individual animals and/or all individual species in a given survey area. An empirical Species Accumulation Curve (SAC, Magurran (2004)) was created in this study to identify detection probabilities for fish species richness using BUVS on deep-water rocky reefs. Sufficient sampling to detect all detectable species is achieved when an empirical SAC intersects the Michaelis-Menten model of the same data (Magurran, 2004) or an asymptote is reached. Cappo et al. (2004) showed that the BUVS SAC was consistently below the prawn trawl SAC, that both curves could

be fitted using logarithmic functions and both curves did not reach an asymptote, i.e., insufficient sampling occurred to estimate total species richness. The Michaelis-Menten model generates an asymptotic curve, based on the negative exponential model, which predicts the increase in species richness for additional sampling effort (Magurran, 2004). This chapter describes the extent that BUVS are able to capture the ichthyofaunal composition in deep-water temperate rocky reefs.

#### **4.2.1 Individual species abundances of reef fish assemblages**

Whereas some conservation management objectives aim at stopping the decline of biodiversity, other objectives aim at maintaining or increasing the abundance of certain species that are either endangered or exploited. Abundance, or population size, is an important consideration from a management perspective if there is a positive relationship between population fitness (ability to both survive and reproduce) and population size or density. This relationship is known as the Allee effect (Allee, 1931; Courchamp et al., 2008). For a simplistic example, consider a population of species  $x$  that reproduces by internal fertilisation. This population decreases in size below a certain threshold, at which sexual encounter is insufficient to offset natural and fishing mortality. This will inevitably result in the cessation of key ecological processes. Determining changes in abundance is a common objective of conservation management. Hence, being able to differentiate between different sites (protected and unprotected) or between different points in time (before and after a management regime was put in place) will assess whether a certain management strategy was successful or a failure. Barrett et al. (2007) found that *Latridopsis*

*forsteri* and large fish (> 300 mm) increased after ten years of protection. However, Babcock et al. (2010) found that initial direct effects on target species are detectable after more than 5 years. Hence, abundances of the five most numerous fish species in the BUVS data set were analysed to test whether two environmentally distinct areas, inshore and offshore sites, differed in assemblage composition.

Interestingly, line fishing data show a sharp decline in the Blue-throated wrasse *Notolabrus tetricus* catches in depths > 60 m (Neville Barrett, unpublished data). I investigated whether the same sharp decline could be observed using BUVS.

#### 4.2.2 Size structure of two commercial species

The performance of new sampling tools such as BUVS needs to be compared to existing sampling methods to assess their usefulness and efficacy. The performance of BUVS was assessed by comparing BUVS-collected and existing extractive size-frequency data for two commercially important fish species, *Notolabrus tetricus* and the Striped trumpeter *Latris lineata*. These species were further investigated with respect to their size-frequency distributions. The existing data referred to earlier was obtained by extractive sampling methods, line fishing (Sean Tracey, IMAS) and trapping and gill netting (Barrett, 1995). Line fishing data and BUVS data were collected in the same 30 seconds fishing block, a common spatial unit of fisheries assessments in Tasmania (Lyle and Hodgson, 2001) during the same month.

### 4.2.3 Improving estimates of relative abundance

One of the three major challenges in using BUVS to estimate relative abundance listed by Cappo et al. (2003) is: “separating repeated visits of the same fish from new arrivals within video tapes to get a better *MaxN*”. *MaxN*, the de-facto standard measuring unit for BUVS investigations has advantages as well as disadvantages. It was originally designed to avoid inflated abundance estimates by considering each fish visit of species  $x$  as a visit from a different individual. *MaxN* records the maximum number of individuals of species  $x$  visible in video frame  $y$ . This ensures that the same individual visiting multiple times is only accounted for once. Consequently, one of the limitations of *MaxN* is that it underestimates true abundance, i.e., several solitary visits by more than one individual of species  $x$  scores  $MaxN = 1$ . In the absence of any distinguishing features to tell individuals apart, this is a reliable approach. However, photogrammetric measurements using stereo video footage allow the identification of individual fish by their length. Length measurements were therefore taken for *L. lineata* and *N. tetricus*. The sum of unique fish lengths is equivalent to a relative abundance estimate. This study describes whether this new relative abundance estimate performs better than *MaxN*.

### 4.2.4 Power analysis

The probability of rejecting the null hypothesis,  $H_0$  when it is false, is known as the power of a test, e.g.,  $t$ -test or ANOVA (Crawley, 2007). Power analysis can be used to calculate the sample size (number of replicates) necessary to detect

a specified difference in the mean, i.e., using a two-sample  $t$ -test. The practical example below illustrates the need and utility of power analysis using BUVS data. Cappo et al. (2003) state that contrary to expectations, not only carnivorous and scavenging functional fish groups are attracted to the bait plume, but herbivorous and corallivorous groups are also frequently recorded using BUVS. The majority of these species do not feed on the bait but are attracted to the commotion associated with BUVS deployments. To what extent can fish, that are not attracted to bait, be repeatedly and consistently recorded using BUVS depends on the species in question. For example, in this study, the zoobenthivorous Banded morwong *Cheilodactylus spectabilis*, primarily feeding on benthic amphipods and brittle stars Russell (1983), was rarely recorded by BUVS. For over three quarters of the survey time, *C. spectabilis* was not present in the video footage. Although indicative, whether this probability of encounter is low should be tested rigorously using power analysis. I investigated the effectiveness of BUVS to monitor five commercially important fish species, *Cheilodactylus spectabilis*, *Cheilodactylus macropterus*, *Latris lineata*, *Latridopsis forsteri* and *Nemadactylus tetricus*. Whereas *C. spectabilis* and *N. tetricus* are desired for the life fish export market, *L. lineata*, *L. forsteri* and *C. spectabilis* are sold gutted and filleted. Species destined for the life fish export market are caught in shallow depths to avoid over-inflation of the swim bladder and resulting mortality if retrieved from deeper depths. However, these species are not restricted to depths  $< 30$  m. Fisheries data are therefore unreliable, biased and unsuitable to monitor population dynamics. Suppose that an exhaustive pilot study was conducted to establish a reliable benchmark with respect

to abundance of species  $x$ . Two management questions arise: (1) what is the number of replicates necessary to detect, for example, a 50% difference in abundance between years, habitat types or management regimes and (2) what difference of abundance can be detected with a given sampling effort. Traditionally, statistical power analysis is used to detect differences in the response variable between two samples, for example, abundance of species  $x$  in survey 1 and survey 2. Currently, these power analysis tests are confined to data that are normally distributed. Point count data and *MaxN*, the de-facto standard using BUVS, even after transformation, usually violate assumptions of normality. This is particularly true for low abundances and zero counts. This chapter covers methods of how to conduct power analysis, despite non-normality, based on Seavy et al. (2005) and presents results using the proposed methods.

### 4.3 Material and Methods

For further information on the study area, BUVS design and deployment and general video annotation techniques, the reader is kindly referred to chapter 2. Figure 4.1 provides a map of the study site and BUVS deployments.

Whilst visual census methods usually require the observer to move along a predetermined track and count species of interest, BUVS are stationary and it is the species of interest that approach the field of view (FOV) of the camera (bait basket). The record of a sighting of a species by an annotator is from here forth referred to as a visit. *MaxN* and relative abundance are used interchangeably throughout this

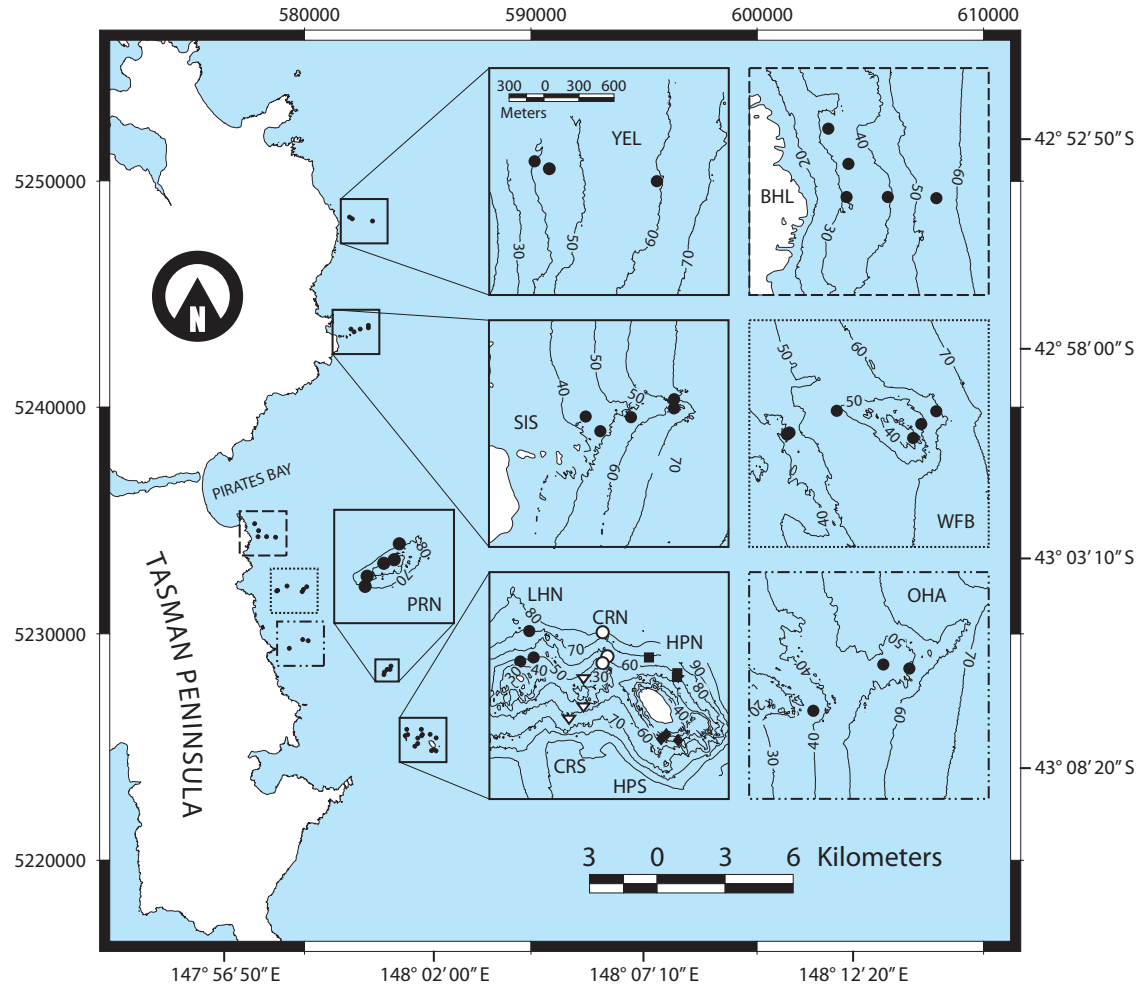


Figure 4.1: Location of BUVS deployments. Different types of dashed borders refer to different sites in overview map. Inshore sites: SIS = Sisters, BHL = Blowhole, WFB = Waterfall Bay, OHA = O'Hara Bluff. Offshore sites: PRN = Patchreef North, Bottom left inset: triangles = CRS (Chevron Rk South), open circles = CRN (Chevron Rk), squares = HPN (Hippolyte Rk North), diamonds = HPS (Hippolyte Rk South). Scale bar in YEL (High Yellow Bluff) applies to all insets. Filled circles and symbols mentioned above refer to individual BUVS deployment locations. Bathymetric contours are in 10 m intervals. Projected coordinates UTM 55G (WGS84).

---

chapter. Total number of individuals refers to the sum of *MaxN* for each species for each deployment or site.

### 4.3.1 Composition of reef fish assemblages

Multivariate analyses were performed using the software package PRIMER v6 (Clarke and Gorley, 2006). Biological data were fourth-root transformed after removal of singleton species (species that occurred only once during the entire study) and BUVS deployments with less than three individual sightings, thus giving less weight to abundant species and to reduce skewness, deviation from normality, found in the species abundance distribution (Clarke and Gorley, 2006). In addition, non-parametric multidimensional scaling (nMDS) of the Bray-Curtis similarity matrix of the fourth-root transformed species abundance data was performed to visualise distinct assemblages and their distribution in two-dimensional space.

To test the *a priori* hypothesis, that fish assemblage composition is related to distance from shore, a canonical analysis of principal coordinates (CAP, Anderson and Willis (2003)) was conducted. CAP is related to canonical correspondence analysis and performs a constrained ordination based on the Bray-Curtis dissimilarity measure (Anderson and Willis, 2003). BUVS data were split into an inshore and offshore component. Sites that are submerged extensions of rocky outcrops along the main coastline are considered inshore sites (see Fig. 4.1). Conversely, offshore sites are disconnected from mainland rocky outcrops by expanses of soft sediment (see Fig. 4.1). Distance from shore, inshore or offshore, was considered a proxy for environmental variables such as seabed exposure to shear

stress produced by waves, wind, tides and ocean currents (Bax, 2011). CAP was also used to examine correlations between individual species and distance from shore (canonical axis 1) (Anderson and Willis, 2003). A correlation value  $|r| > 0.3$  (Anderson et al., 2008) was considered sufficiently high to indicate significant relationships between species and distance from shore. In order to eliminate depth as a confounding factor, BUVS deployments were conducted over the same depth range (38 – 67 m) between inshore and offshore reefs.

### **Habitat complexity measures**

Ship-borne multibeam sonar data were collected prior to this study using the research vessel *Challenger* (Nichol et al., 2009). The gridded multibeam sonar data were of a resolution of  $2 \times 2$  m. Habitat complexity measures such as fractal dimension, plan curvature, profile curvature, slope and aspect were computed from the gridded multibeam sonar data from the study area using the freely available software package LandSerf version 2.3 ([www.landserf.org](http://www.landserf.org)). Habitat complexity measures of several scales,  $3 \times 3$  ( $36 \text{ m}^2$ ),  $5 \times 5$  ( $100 \text{ m}^2$ ) and  $9 \times 9$  ( $324 \text{ m}^2$ ) pixel array, were examined and related to reef fish composition. Since all habitat complexity measures were derived from the gridded bathymetric data, they were not independent and were treated as paired samples (i.e., measurements were taken from the same location). To formally test for associations between paired samples (e.g., depth and slope, fractal dimension and aspect, etc), Kendall's rank correlation coefficient  $\tau$  was computed to assess dependencies between habitat complexity measures. The BEST procedure in PRIMER v6 was used to find habitat complexity

measures that explain species composition based on the Bray-Curtis similarity matrix. Habitat complexity measures were normalised before analysis as suggested by Clarke and Gorley (2006). Statistical significance of the BEST procedure results were tested using the global BEST match permutation routine (999 permutations). Table 4.1 gives a short definition of the habitat complexity measures used in this study.

Table 4.1: Habitat complexity measures derived from DEM with definition and references

Measure	Definition	Reference
Bathymetry	Elevation relative to Australian Height Datum (AHD)	Jenness (2004)
Slope	Average change in elevation based on a $3 \times 3$ pixel array in degrees	Wilson et al. (2007)
Aspect	Azimuthal bearing of steepest slope ( $0 - 360^\circ$ )	Wilson et al. (2007)
Profile curvature	Measure of concavity/convexity parallel to the slope (cross-section)	Dikau (1988)
Plan curvature	Measure of concavity/convexity perpendicular to the slope (contour lines)	Dikau (1988)
Fractal dimension	Ratio of detail in fractal pattern and scale at which it is measured: index of complexity	Mandelbrot (1967)

### Species accumulation curve

A species accumulation curve (SAC), cumulative number of species recorded as a function of sampling effort (Magurran, 2004), was created to estimate the species richness, that BUVS can detect in the study area. Once empirical SAC and Michaelis-Menten model curve intersect, total species richness can be estimated

using estimators such as Chao 1 (Chao, 1984) or ACE (Chazdon et al., 1998). Six species richness estimators were calculated using the software package EstimateS, version 8 (Colwell, 2006), setting the number of randomisations to 100.

#### 4.3.2 Individual species abundances of reef fish assemblages

Permutational multivariate analysis of variance (PERMANOVA) was used to test for differences between inshore and offshore locations and between sites based on the fourth-root transformed abundance data of the five most numerous fish species (see Table 4.3). The multi-factor design included two factors, distance from shoreline with two levels (inshore and offshore) and sites with ten levels (inshore: WFB=Waterfall Bay, BHL=Blowhole, SIS=Sisters, YEL=High Yellow Bluff, OHA=O'Hara; offshore: PRN=Patch Reef North, CHRK=Chevron Rock, HIP=Hippolyte Rock North, LHS=Hippolyte Rock South, LHIP=Little Hippolyte Rock). The distance measure chosen was the Bray-Curtis dissimilarity. The individual abundances of the same five species were investigated to test whether abundance in inshore and offshore sites were different using negative binomial Generalised Linear Models (GLMs) as described below.

Two commercially important species were also selected for further analysis. The abundance of *Latris lineata* (Striped trumpeter) and *Notolabrus tetricus* (Blue-throated wrasse) was investigated to test whether abundances in inshore and offshore sites were different. The method used for the two commercially important species *L. lineata* and *N. tetricus* was identical to the method used to test for difference between inshore and offshore sites for the five most abundant species. *MaxN* counts

for all species individually were tested for significantly different means for inshore and offshore sites using negative binomial GLMs in the statistical programming software R (R-Development-Core-Team, 2009). Negative binomial GLMs were used due to non-normality and overdispersion in the *MaxN* count data.

The relationship between the frequency of occurrence of *N. tetricus* and depth was investigated using a binary GLM to model presence/absence as outlined in Zuur et al. (2009). My results were compared to UVC results stated in Shepherd and Clarkson (2001).

### 4.3.3 Size structure of two commercial species

*Latris lineata* and *Notolabrus tetricus* were selected to investigate their size structure using photogrammetric length estimates. Size structure data for both species were also compared to data obtained by extractive sampling methods, e.g., line fishing, trapping, gill netting and spear-fishing.

#### Photogrammetric length estimation

Photogrammetric fork length estimation of each *Latris lineata* and *N. tetricus* visit was conducted with the software package Photomeasure (Seager, 2009c), which is designed to analyse stereo BUVS footage. The criteria for length measurements were (1) tail orientation of fish should be  $< 60^\circ$  from optical axis, (2) take the mean of five consecutive video frame measurements per individual, and (3) avoid measurements where fish are excessively bent (Harvey et al., 2003). It was attempted to take

length measurements of all individuals at video frame  $x_{MaxN}$  (i.e., the video frame, for each 45 min deployment, where  $MaxN$  occurred). However, for reasons outlined in Harvey et al. (2003), estimating fork lengths of all individuals in video frame  $x_{MaxN}$  was not always possible. In these instances the method outlined in the next section (Improving estimates of relative abundance) was adopted.

Some fisheries assessments use biomass (weight) in addition, or as an alternative, to size frequency distributions. To accommodate this preference, *Latris lineata* length was converted into biomass using the equation below.

$$W = 2 \times 10^{-5} \times L^3$$

where  $L$  = fork length in cm and  $W$  = weight in kg (Tracey and Lyle, 2005)

Records from UVC and line fishing in depths  $< 100$  m indicate that *N. tetricus* is the most abundant wrasse (Labridae) in Tasmanian waters (Edgar and Barrett, 1997). However, conversion from length to weight for *N. tetricus* was omitted due to the lack of a published length-weight relationship. Due to the fact that male and female individuals of *N. tetricus* can be easily told apart by the external stripe pattern, analyses were also conducted separated by gender.

#### 4.3.4 Improving estimates of relative abundance

$MaxN$  underestimates true abundance (Cappo et al., 2004), so two novel methods are proposed here to overcome this limitation. Both methods aimed to identify individual fish and generate a list of individuals recorded during the deployment.

The first method used gender-specific markings in *N. tetricus* and the second used photogrammetrically-measured body lengths for both commercial fish species. The details of both methods are outlined below.

### **Method 1**

Strictly speaking,  $MaxN$  for a particular species equals 1 even when one female and one male individual of this species were sighted, i.e, in this case  $n = 2$ . Because the male and the female individual were not in the same video frame  $MaxN$  equals 1. In the case of *N. tetricus* improved abundance estimates were obtained by generating separate values of  $MaxN$  for male and female fish visiting the station which are combined to make a single abundance estimate for the deployment.

### **Method 2**

Length measurements of one individual fish in five consecutive video frames resulted in a mean length measurement. This approach was adopted to account for tail flex and muscle contractions which affect the total fish length, i.e., less than 1% (Harvey et al., 2003). I measured all individuals of the species *Latris lineata* and *Notolabrus tetricus*. Every individual entering the field of view was given an identifier and repeatedly measured using five consecutive video frames. This was done for the entire video footage (45 min, 67,500 video frames). Scoring the entire footage and measuring every visiting individual bears the risk of measuring the same individual several times and therefore overestimating total abundance – the

reason *MaxN* was devised. Therefore, boxplots of all measurement sets for each 45 min deployment were inspected. Measurement sets with overlapping whiskers (boxplot) were considered to be the same individual. In addition, Student's *t*-test was used to test whether the means for each possible combination of five consecutive photogrammetric length measurements were different at the 5% level. A *p*-value  $< 0.05$  was taken as proof that these two measurement sets are different and therefore comprise two individual fishes. The number of individual fish obtained by this method was denoted with *N*. Note the differences between *MaxN* and *N* (number of individuals based on unique length estimates) in Table 4.5, 4.6.

#### 4.3.5 Power analysis

In this study abundance pattern were simulated and compared. For each comparison two abundance pattern, labelled survey 1 and survey 2, were simulated, using different numbers of replicates and different effect sizes (25%, 50% and 75% change in relative abundance). I used power analysis to calculate the sample size (number of replicates) necessary to detect a 25%, 50%, 75% change in abundance with power = 80%. Standard assumptions of  $\alpha = 0.05$  (significance level) and  $\beta = 0.2$  (probability of accepting the null hypothesis when it is false) gives power = 80% (Crawley, 2007). Readily available statistical software packages (SPSS, SAS JMP, R) that offer tests to determine statistical power require the data to be normally distributed (Thomas, 1997). However, many abundance estimates in ecology comprise of count data, which often do not follow the normal distribution (Seavy et al., 2005). *MaxN* data are rarely normally distributed and the use of traditional tests to determine statistical

---

power is inappropriate. For non-normal data three alternatives exist to compare two abundance estimates (i) non-parametric tests (Kruskal-Wallis, Mann-Whitney U), (ii) data transformation ( $\sqrt{x}$ ,  $\log(x)$ ,  $\log(x + 1)$ ) and (iii) generalised linear models with appropriate link function (Crawley, 2007). This study used GLMs to test for differences in two randomly generated (simulated) abundance estimates (survey 1 and survey 2) drawn from a theoretical probability distribution. The probability distribution was fitted to empirical *MaxN* data for each species. Empirical and fitted values were compared using  $\chi^2$  tests. A  $\chi^2$  test result with  $p < 0.05$  was considered indicative of a close fit between empirical data and probability distribution. Two likely probability distributions that would fit *MaxN* data are Poisson and negative binomial. If these probability distributions could not be fitted ( $\chi^2$  test  $p > 0.05$ ), bootstrapping, resampling with replacement, the empirical *MaxN* data were used to simulate two abundance estimates. The Poisson distribution assumes that the variance is equal to the mean and can be described by one parameter  $\mu$  (mean), whereas the negative binomial distribution is more appropriate for overdispersed data (where sample variance exceeds the sample mean) and requires an additional parameter  $k$  (dispersion or aggregation parameter). The dispersion parameter  $k$  was estimated using maximum likelihood (Crawley, 2007). Hypothetical data for survey 1 and survey 2 were generated with different numbers of replicates; 18 – 102 in increments of 3 with different mean abundances (25%, 50%, 75% higher/lower than survey 1). The generated data were compared using GLMs with either Poisson or negative binomial link function and survey as a factor. The null hypothesis, abundance of species  $x$  between survey 1 and survey 2 is not significantly different,

was rejected when  $p < 0.05$  for the survey parameter. Simulations for each sample size (number of replicates) were repeated 100 times. Hence, statistical power is the percentage of cases where  $p < 0.05$ . All simulations and analyses were performed in R (R-Development-Core-Team, 2009).

## 4.4 Results

Edgar (1997) gives the depths range of *Cheilodactylus spectabilis* as 3 – 50 m. During this study the same species was recorded in depths up to 67 m (sampling depth ranged from 32 – 81 m). The discrepancy is largely attributable to the fact that depth ranges were mostly based on visual SCUBA diver assessments. A similar observation was made with respect to *Latridopsis forsteri* where the maximum depth was given as 60 m (Edgar, 1997). This study recorded *Latridopsis forsteri* in depths as deep as 67 m. Both instances indicate that both species have been sampled at least to their maximum referenced depth.

### 4.4.1 Composition of reef fish assemblages

A total of 48 species belonging to 30 families were recorded during BUVS deployments (Table 6.1 chapter 6). The most species-rich families were Labridae (wrasses) and Monacanthidae (leatherjackets) with six species each. Labridae (100% of samples), Cheilodactylidae (96%) and Monacanthidae (84%) occurred most frequently.

Individual species, that characterise the inshore and offshore assemblages identified

---

using CAP (all CAP  $|r| < 0.3$ ) were: *J. edwardsii*, *L. lineata* and *P. psittaculus* (more abundant offshore than inshore) and conversely *A. vittiger*, *E. mosaicus*, *M. australis*, *M. scaber*, *N. tetricus*, *P. laticlavus*, *P. melbournensis* and *T. degeni* (more abundant inshore than offshore).

Non-parametric multi-dimensional scaling of the Bray-Curtis similarity matrix applied to the fourth-root transformed data showed two clusters, inshore and offshore BUVS deployments (Fig. 4.2).

### Habitat complexity measures

Using habitat complexity measurements to explain fish assemblage composition based on the Bray-Curtis similarity matrix, excluding depth, resulted in a weak but significant relationship (BIOENV Global Test Sample statistic  $\rho = 0.18$ , significance level of sample statistic: 0.2%, number of permutations: 999). The strongest single variable explaining assemblage composition was slope ( $\rho = 0.18$ ) (Fig. 4.3). Offshore sites consistently scored steeper slopes than inshore site. Kendall's  $\tau$  coefficient, testing for associations between depth and slope, was  $\tau = 0.118$  and not significant at the 5% level. The result excludes the possibility that the significant result (slope,  $\rho = 0.18$ ) was an artefact of depth — slope values were derived from depth using a nearest-neighbour approach. Although, strictly speaking, not a descriptor of habitat complexity, depth was included in a second BEST analysis to explain assemblage composition. Including depth as an environmental factor resulted in a stronger, significant relationship (BIOENV Global Test Sample statistic  $\rho = 0.347$ , significance level of sample statistic: 0.1%, number of permutations:



Figure 4.2: Two-dimensional representation of nMDS scaling of the Bray-Curtis similarity matrix applied to the fourth-root transformed data, open triangles represent offshore deployments and filled triangles represent inshore deployments

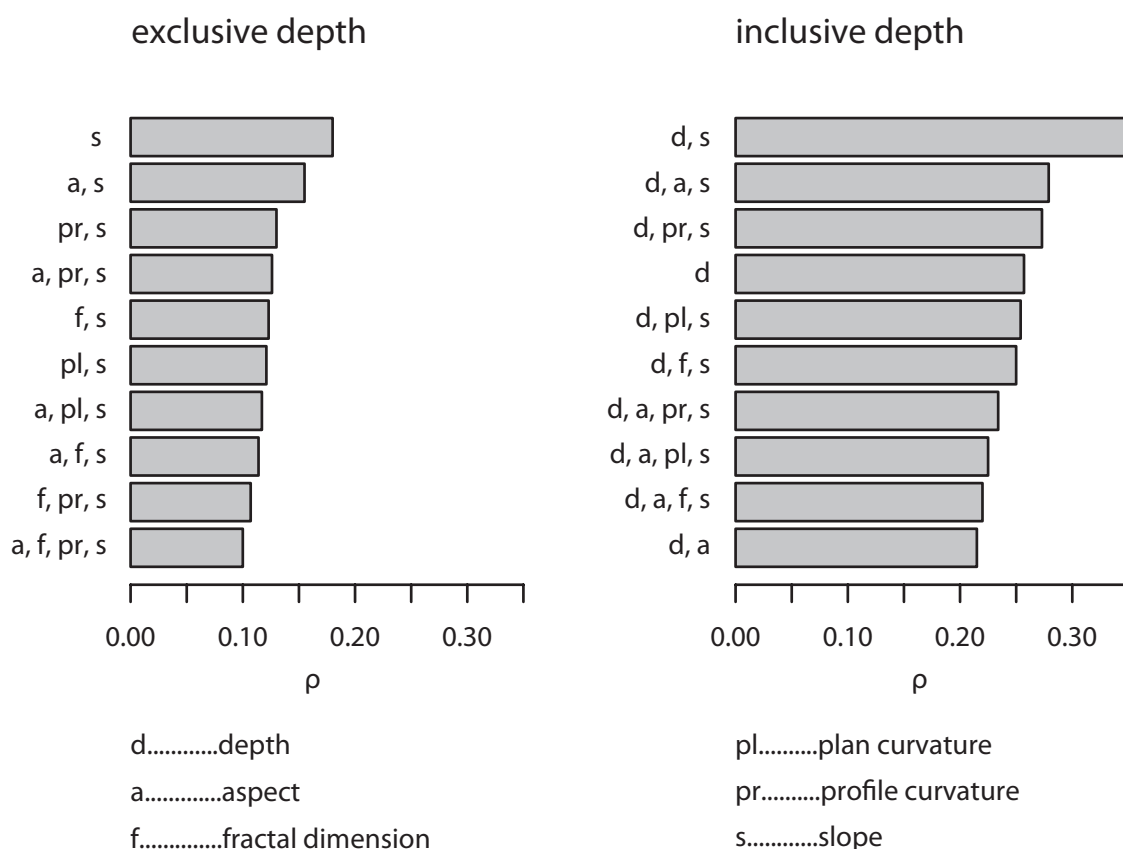


Figure 4.3: Spearman's ranked correlation coefficient ( $\rho$ ) for single and combined habitat complexity measures and fish assemblage composition. Left barplot is exclusive of depth, whereas the right barplot is inclusive of depth as a factor. Letters next to bars are explained in the legend.

999). This time, the strongest single variable explaining assemblage composition was depth ( $\rho = 0.257$ ) (Fig. 4.3). Except for slope ( $\rho = 0.18$ ), the remaining habitat complexity measures contributed little to explain assemblage composition (see Fig. 4.3).

### Species accumulation curve

The intersecting observed species accumulation and Michaelis-Menten model curves (Fig. 4.4, bottom left panel) attest that sampling effort was sufficient to capture

virtually the entire detectable species assemblage. This intersection can be considered a stopping rule with respect to sampling effort (Magurran, 2004). Both curves crossed at 87 deployments ( $n = 96$ ). Total species richness estimates using five different parametric and non-parametric methods were higher by 3 – 10 species (Table 4.2) compared to the empirical species richness value of 48.

Table 4.2: Total species richness estimates (standard deviation) using five different estimators. Empirical species richness = 48.

estimator		estimated species richness $S$ (SD)
Chao 2	non-parametric	52 (3.86)
ICE	non-parametric	54 (0.01)
Jackknife 1	parametric	56 (2.69)
Jackknife 2	parametric	58 (1.26)
Bootstrap	parametric	52 (0.34)

#### 4.4.2 Individual species abundances of reef fish assemblages

A list of the five most abundant species and their total  $MaxN$  count recorded during 96 BUVS deployments is presented in Table 4.3.

Table 4.3: Species and common names and total  $MaxN$  count of the five most numerous fish species in the BUVS data set

species	common name	count
<i>Caesioperca lepidoptera</i>	Butterfly perch	1236
<i>Trachurus declivis</i>	Common Jack mackerel	1059
<i>Pseudolabrus psittaculus</i>	Rosy wrasse	669
<i>Nemadactylus macropterus</i>	Jackass morwong	479
<i>Pseudophycis bachus</i>	Red cod	179

The PERMANOVA results showed that abundance of the five most numerous fish species were not significantly different between inshore and offshore sites ( $F = 1.5552$ ,  $df = 1$ ,  $p_{perm} = 0.2208$ ,  $p_{MC} = 0.2272$ ) and between sites ( $F = 1.0577$ ,

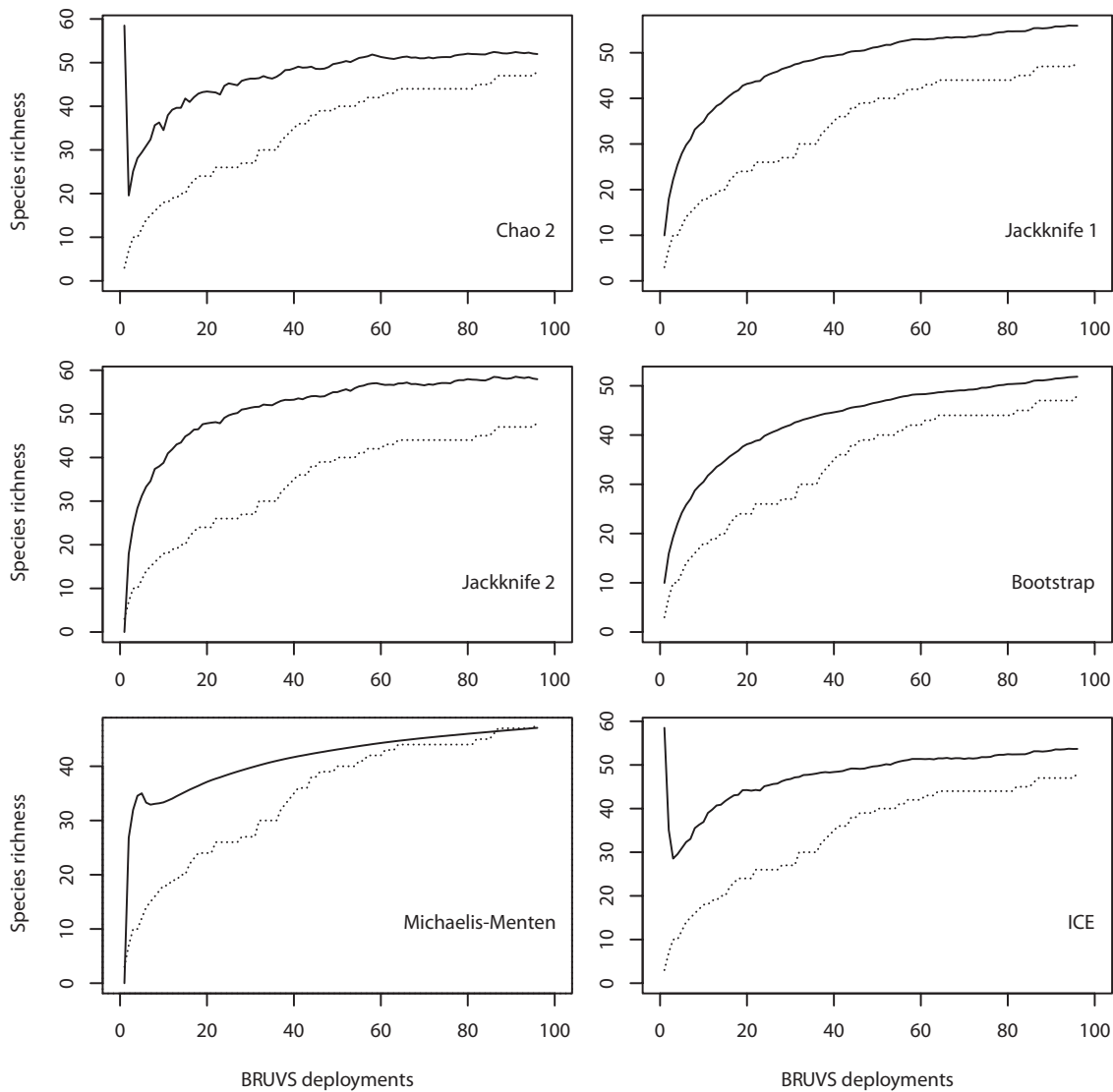


Figure 4.4: Performance of six species richness estimators compared to observed species accumulation curve (dotted). Note all observed curves are identical but differently scaled to accommodate estimates. BRUVS deployments:  $n = 96$ .

$df = 8$ ,  $p_{perm} = 0.4013$ ,  $p_{MC} = 0.3966$ ). However, GLM results, testing whether each species individually shows differences in abundance between inshore and offshore sites, excluding factor site, showed significant differences for two species. Whereas, *T. declivis*, *C. lepidoptera* and *N. macropterus* showed no differences in abundance between inshore and offshore sites, *P. psittaculus* and *P. bachus* did (Table 4.4). Both species were more abundant in offshore sites compared to inshore sites. With respect to the two commercially important fish species; *L. lineata* abundance in offshore sites was significantly higher than in inshore sites (Table 4.4, Fig. 4.5), in contrast, *N. tetricus* abundance was significantly higher in inshore sites than in offshore sites 4.4.

#### 4.4.3 Size structure of two commercial species obtained by photogrammetric length estimation

##### Striped trumpeter

BUVS recorded 71 individuals of *Latris lineata*. Out of 96 BUVS deployments at least one individual (i.e.,  $MaxN = 1$ ) of *L. lineata* was recorded 28 times. Sixty-four per cent of *L. lineata* visits recorded during BUVS deployments were suitable for photogrammetric length measurements. Forty-seven photogrammetric length estimates of *L. lineata* could be obtained using video footage from 96 BUVS deployments. Individual trumpeter ranged in size from 300 mm to 760 mm (Fig. 4.5). The two maxima in Fig. 4.5 indicate two cohorts. The length difference between cohorts is consistent with findings by Tracey (2007).

Table 4.4: Negative binomial GLM results comparing fish abundances between inshore and offshore sites. Distance from shoreline is a two level factor (inshore, offshore). \* denotes the dispersion parameter for each model. CI denotes Confidence Interval.

species		Estimate	95% CI (Estimate)	<i>p</i> value
<i>L. lineata</i>	intercept	-1.5581	-2.5892, -0.7901	< 0.01
	distance from shoreline	1.9721	1.0898, 3.0650	< 0.01
	dispersion	* 2.422		
<i>N. tetricus</i>	intercept	0.5213	0.3202, 0.7098	< 0.01
	distance from shoreline	-2.1054	-2.8862, -1.4652	< 0.01
	dispersion	* 0.946		
<i>T. declivis</i>	intercept	2.4717	1.9798, 2.8942	< 0.01
	distance from shoreline	-0.1846	-0.9752, 0.5531	0.63
	dispersion	* 36.31		
<i>P. psittaculus</i>	intercept	1.7621	1.5833, 1.9308	< 0.01
	distance from shoreline	0.3944	0.1496, 0.6394	< 0.01
	dispersion	* 2.604		
<i>C. lepidoptera</i>	intercept	2.5193	2.2037, 2.8050	< 0.01
	distance from shoreline	0.0861	-0.3799, 0.5419	0.71
	dispersion	* 16.579		
<i>N. macropterus</i>	intercept	1.6707	1.3662, 1.9470	< 0.01
	distance from shoreline	-0.1638	-0.6542, 0.3063	0.50
	dispersion	* 6.620		
<i>P. bachus</i>	intercept	0.3758	0.0749, 0.6491	< 0.01
	distance from shoreline	0.5250	0.1344, 0.9192	< 0.01
	dispersion	* 1.773		

*L. lineata* line fishing catch data from the same sampling area (Fishing Block 6H3, fishing blocks of 30 minutes of longitude and latitude are a common spatial assessment unit used in Tasmanian fisheries research) during the same time of BUVS sampling (August, October and November 2010) indicate that BUVS are more efficient in recording this species. Fourteen days of BUVS sampling (96 deployments) recorded a total of 72 *L. lineata* individuals, whereas 5 days of line fishing resulted in 82 individual fish. However, a formal analysis using mean observations per day per unit time (MOPUT, Assis et al. (2007)) revealed that mean MOPUT for BUVS is 21 times higher than mean MOPUT for line fishing, 0.744 (SD = 0.645,  $n = 8$ ) and 0.035 (SD = 0.018,  $n = 5$ ), respectively but variability for BUVS MOPUT is high. A Wilcoxon rank sum test showed that MOPAT for BUVS are significantly different from MOPAT for line fishing ( $W = 1$ ,  $p$ -value = 0.003). Mean observations per day for line fishing data were calculated by dividing the total amount of hook drops per day by the number of striped trumpeter caught that day. Likewise, BUVS mean observations per day was calculated by taking the mean of striped trumpeter *MaxN* for each BUVS drop per day. Line fishing data were collected by 2–3 anglers using 3 hooks per line. The length-frequency distribution of *L. lineata* obtained using BUVS and line fishing was also very different. Mean length for line fishing data was 190 mm less compared to BUVS ( $\mu_{BUVS} = 481$  mm,  $\mu_{line} = 291$  mm). There were obvious differences between both sampling methods. BUVS recorded larger individuals (range: 310 – 756 mm,  $n = 49$ ), whereas line fishing selected for smaller individuals (range: 187 – 447 mm,  $n = 82$ ).

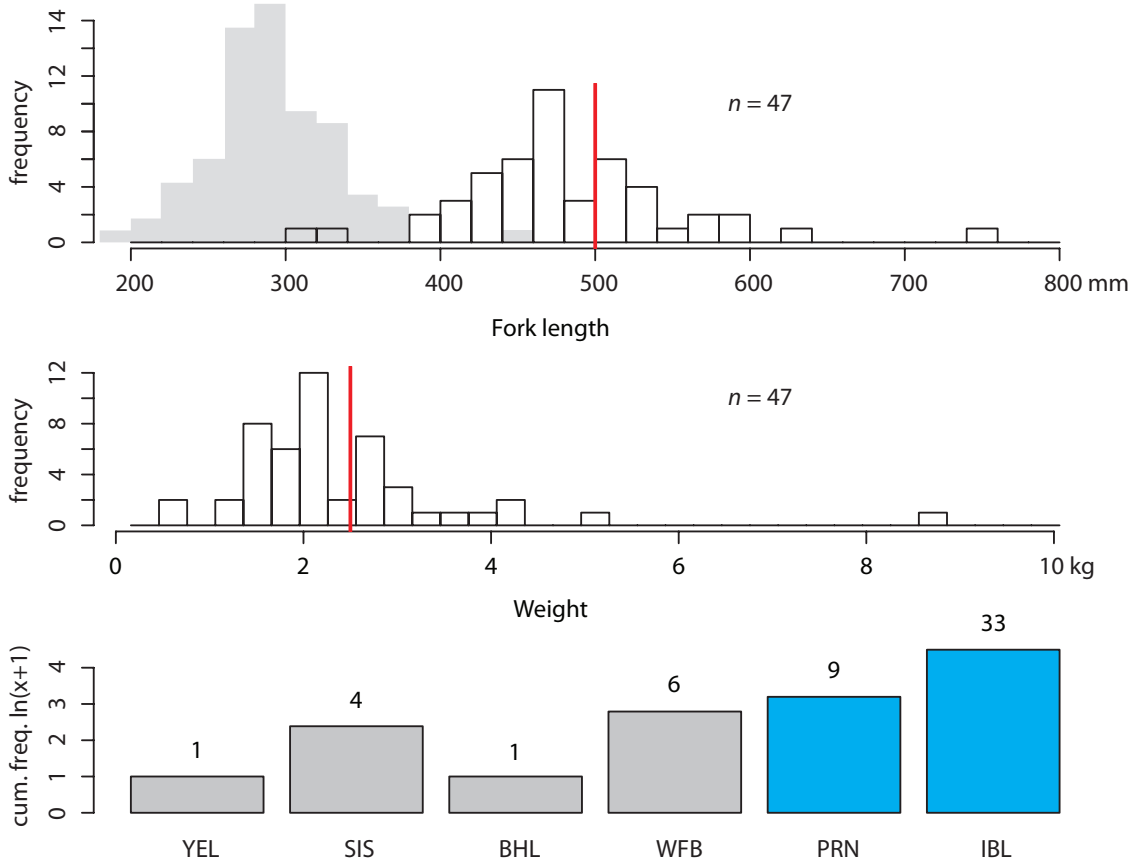


Figure 4.5: Photogrammetrically estimated length and calculated weight frequency distribution, and pooled *MaxN* location of striped trumpeter (*Latris lineata*) sampled from May 2009 to August 2010. Top: length-frequency distribution (20 mm size classes), red line indicates minimum catch size limit (500 mm) in 2010, gray bars represent line fishing data for comparison. Middle: calculated weight-frequency distribution (0.3 kg weight classes), red line indicates weight at minimum size limit. Bottom:  $\ln(x + 1)$  transformed cumulative *MaxN* by insets in Figure 4.1, YEL = High Yellow Bluff, SIS = Sisters, BHL = Blowhole, WFB = Waterfall Bay, PRN = Patch Reef North, IBL = pooled sites close to Hippolyte Rk, numbers above bars are untransformed counts. Gray bars = inshore sites, cyan = offshore sites.

### Blue-throated wrasse

BUVS recorded 104 individuals of *Notolabrus tetricus* (63 females and 41 males). Out of 96 BUVS deployments at least one individual (i.e.,  $MaxN = 1$ ) of *N. tetricus* was recorded 54 times. Sixty-three per cent of *N. tetricus* visits recorded during BUVS deployments were suitable for photogrammetric length measurements. Thirty photogrammetric length estimates for males and 15 length estimates for females for *N. tetricus* could be obtained using video footage from 96 BUVS deployments. Female *N. tetricus* ranged in size from 220 mm to 420 mm, whereas males ranged from 300 mm to 540 mm. The overlap in size range between this hermaphroditic species was 300 mm and 420 mm (Fig. 4.6).

Edgar (1997) gives 500 mm as the maximum recorded length for *N. tetricus*. In contrast, photogrammetric length measurements of using BUVS footage recorded a maximum size of 540 mm. Other obvious differences between another study by Barrett (1995) were the lack of juvenile and small individuals (<220 mm) in the BUVS footage and the lack of larger males (>400 mm) in Barrett (1995) who used different mesh size gill nets, traps, spearing and handlining. In addition, the overlap of males and females in this study (300 mm – 420 mm) contrasts with findings by Barrett (1995) where transitions (from female to male) occurred between 270 and 320 mm.

A GLM with quasi-binomial link function, to adjust for overdispersion, revealed significantly different probabilities of *N. tetricus* occurrence with depth (GLM  $b = -0.1179$ ,  $SE = 0.0203$ ,  $p < 0.001$ ).

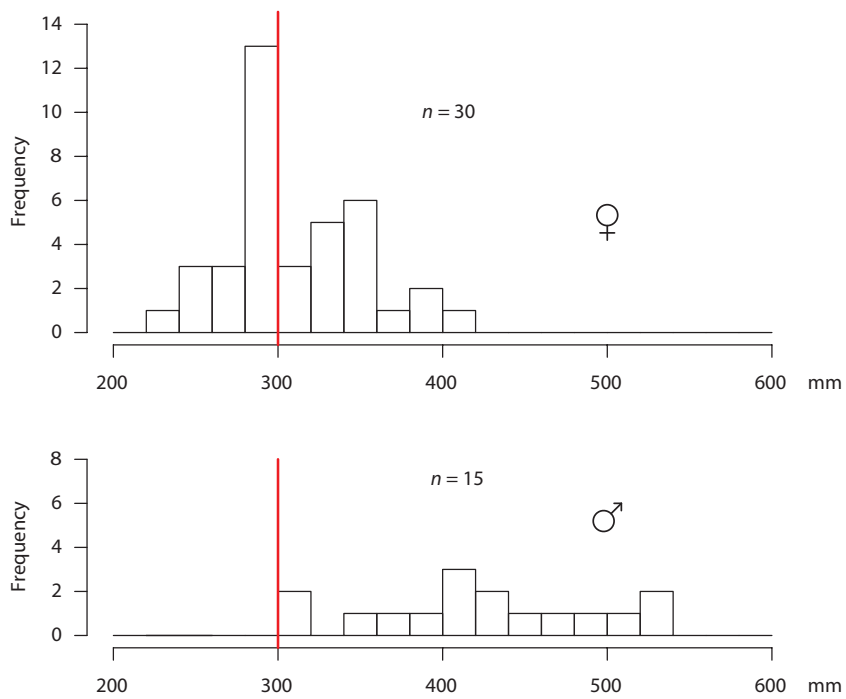


Figure 4.6: Photogrammetrically estimated length frequency distribution of blue-throated wrasse (*Notolabrus tetricus*) sampled from May 2009 to August 2010. Length-frequency distribution of females (top) and males (bottom) in 20 mm size classes, red lines indicate minimum catch size limit (300 mm) for all wrasses in Tasmania.

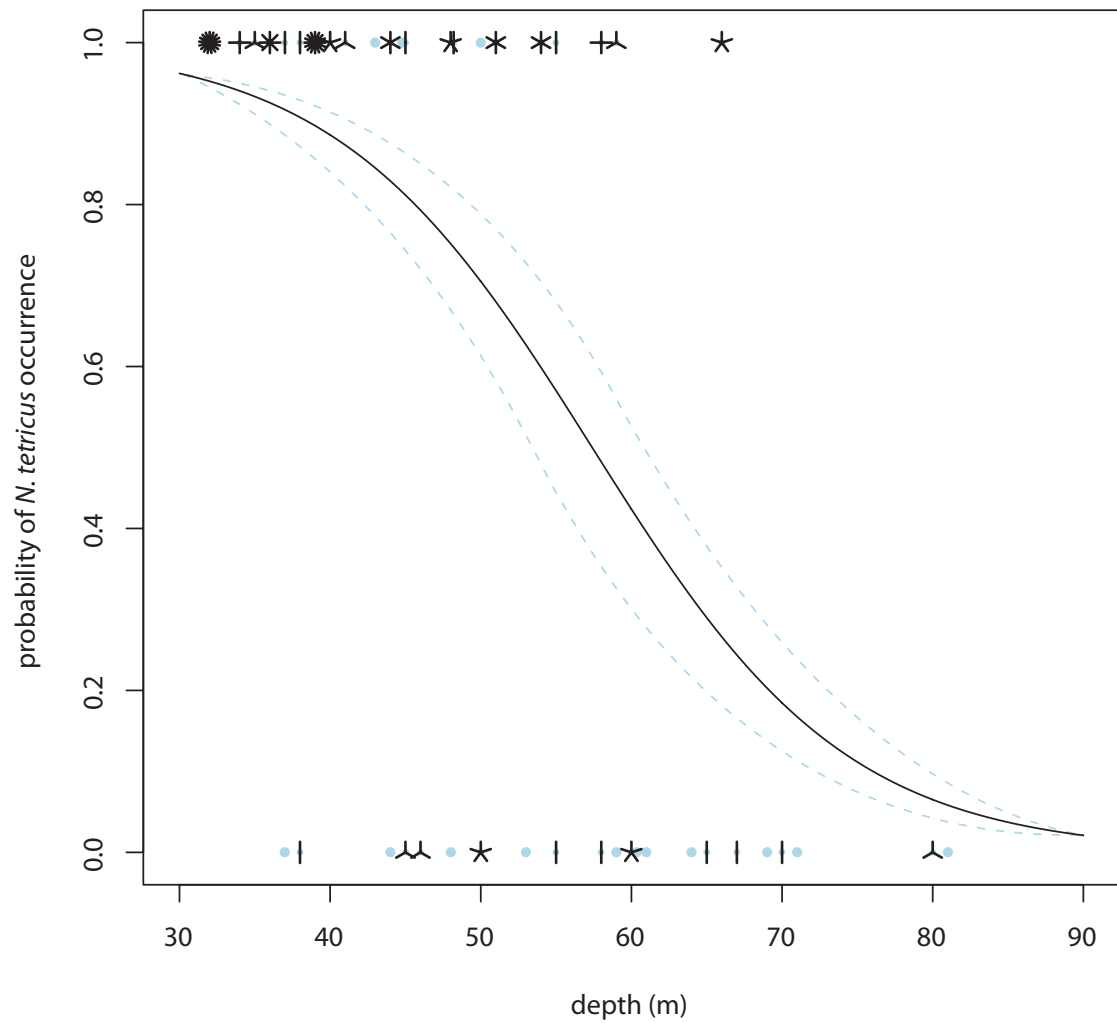


Figure 4.7: GLM predicted probabilities of *N. tetricus* occurrence with depth. Broken lines represent 95% confidence interval and “sunflowers \*” represent presence/absence data. Number of sunflower petals represent number of *N. tetricus* presence/absence for this particular depth.

#### 4.4.4 Improving estimates of relative abundance

##### Striped trumpeter

Underestimating true abundance is a known caveat of  $MaxN$ . Using  $N$ , the sum of individuals, differentiated by an individual's length, instead of  $MaxN$  showed no difference with respect to total relative abundance (Table 4.5). Both total relative abundance estimates,  $MaxN$  and  $N$ , were 47. However, there were differences between  $MaxN$  and  $N$  within individual deployments. In general, relative abundance estimates using  $N$  were greater where  $MaxN$  was small and *vice versa*. Combining,  $N$  and  $MaxN$  increased total abundance by six individuals (53). This figure was obtained by adding the larger abundance estimate, either  $N$  or  $MaxN$ , found for each BUVS deployment. A lower  $N$  value, compared to  $MaxN$  for a particular deployment, was due to the inability to stereophotogrammetrically obtain as many length measurements as the  $MaxN$  value. The video frame where  $MaxN$  was highest for *L. lineata* ( $MaxN = 9$ ) did not provide clear views of nine individual snout and tail pairs; a prerequisite to measure fish length using photogrammetry.

##### Blue-throated wrasse

$N$  yielded 59 (57%) less individuals of *N. tetricus* than  $MaxN$ . Table 4.6 gives  $MaxN$  and  $N$  (number of individual *N. tetricus* determined by length). Females and males combined resulted in a relative abundance estimates of  $MaxN = 104$  and  $N = 45$ . The proportion of females over males for both relative abundance estimates was

Table 4.5: Comparison of *L. lineata*  $MaxN$  and  $N$  for BUVS deployments by site, replicate and date.

Site	replicate	Date	$MaxN$	$N$
Blowhole	1	19/06/2009	1	4
Chevron Rk	1	12/03/2010	1	2
	1	22/08/2010	1	2
	2	15/10/2009	1	1
Chevron Rk South	3	12/03/2010	9	7
Hippolyte Rk	1	22/08/2010	2	3
	3	22/08/2010	2	2
Little Hippolyte Rk	3	11/03/2010	1	1
Hippolyte Rk South	1	16/12/2009	5	3
	2	16/12/2009	2	2
	2	22/08/2010	3	3
	3	16/12/2009	4	4
Patch Reef North	1	15/12/2009	2	2
	2	11/03/2010	2	2
	2	29/01/2010	3	2
Sisters	3	11/03/2010	3	2
Waterfall Bay	2	29/01/2010	3	3
	2	30/07/2010	2	2
Total			47	47

---

$F/M_{MaxN} = 1.6$ ,  $F/M_N = 2.0$ . Combining the two relative abundance estimates resulted in 108 individuals, i.e., 4 additional female individuals.

#### 4.4.5 Power analysis

*MaxN* data of five commercially important fish species were subjected to power analysis. Fitted probability distributions and distribution parameters for *MaxN* data for species *N. tetricus*, *L. lineata* and *N. macropterus* are presented in Table 4.7.

*MaxN* data for *L. lineata* fitted a negative binomial distribution with parameters,  $\mu = 0.740$  and  $k = 0.274$  ( $\chi^2$ ,  $df = 2$ ,  $p = 0.538$ ), see Fig. 4.8. Statistical power to detect differences in *L. lineata* abundance was below the conventional 80%. The results showed that BUVS are not suited to monitor changes in *L. lineata* abundance. As for *L. lineata*, power analysis also showed that BUVS are not suited to monitor changes in *C. spectabilis* and *Latridopsis forsteri* (results omitted). The inability of the power analysis to detect changes in abundance is based on the low detection rate of these three species using BUVS.

*MaxN* data for *N. tetricus* fitted a Poisson distribution with parameter,  $\mu = 0.75$  ( $\chi^2$ ,  $df = 1$ ,  $p = 0.258$ ), see Fig. 4.8. Using BUVS as a sampling tool to monitor *N. tetricus* abundance is feasible to a certain extent as can be seen in Fig. 4.8; statistical power to detect 50% and 75% difference in *N. tetricus* abundance was above the conventional 80%.

*MaxN* data for *N. macropterus* fitted neither a Poisson nor a negative binomial distribution due to the extreme positive skew ( $\gamma_1 = 2.78$ ). Hence, the bootstrap

Table 4.6: Comparison of *N. tetricus* *MaxN* and *N* by gender for BUVS deployments. F = female, M = male, F + M = females and males combined

Site	replicate	Date	<i>MaxN</i>			<i>N</i>			
			F	M	F+M	F	M	F+M	
Blowhole	2	17/12/2009	1	1	2	0	0	0	
	3	17/12/2009	1	1	2	1	0	1	
	1	12/03/2010	2	1	3	0	0	0	
	1	19/06/2009	2	1	3	0	0	0	
	1	30/07/2010	2	1	3	1	1	2	
	1	14/05/2009	1	0	1	0	0	0	
	2	12/03/2010	1	1	2	1	1	2	
	2	16/10/2009	1	1	2	0	0	0	
	2	19/06/2009	1	1	2	0	0	0	
	2	30/07/2010	1	0	1	1	0	1	
	1	17/12/2009	1	1	2	1	0	1	
	Chevron Rk	1	11/03/2010	1	1	2	1	1	2
		1	15/10/2009	1	0	1	0	0	0
		1	22/08/2010	1	1	2	0	1	1
High Yellow Bluff	1	14/10/2009	2	1	3	0	0	0	
Little Hippolyte Rk	3	11/03/2010	0	1	1	0	0	0	
Hippolyte Rk South	1	16/12/2009	1	1	2	1	0	1	
O'Hara Bluff	1	16/12/2009	2	1	3	0	0	0	
	1	12/03/2010	1	1	2	0	1	1	
	1	16/10/2009	1	1	2	0	1	1	
	1	29/01/2010	1	1	2	3	1	4	
	1	30/07/2010	1	1	2	0	0	0	
	2	12/03/2010	1	1	2	0	0	0	
	2	16/10/2009	1	0	1	0	0	0	
	2	29/01/2010	1	1	2	1	0	1	
	2	30/07/2010	1	1	2	0	0	0	
	3	12/03/2010	1	1	2	1	1	2	
	3	29/01/2010	1	0	1	1	0	1	
	3	30/07/2010	2	1	3	2	1	3	
	Sisters	1	9/07/2010	1	1	2	1	0	1
		2	9/07/2010	2	1	3	1	1	2
2		11/03/2010	1	0	1	1	0	1	
2		29/01/2010	2	0	2	1	0	1	
3		11/03/2010	0	1	1	0	0	0	
3		9/07/2010	1	1	2	1	1	2	
3		29/01/2010	2	1	3	1	1	2	
Waterfall Bay	1	12/03/2010	1	1	2	0	1	1	
	1	16/10/2009	1	0	1	0	0	0	
	2	12/03/2010	1	0	1	0	0	0	
	1	19/06/2009	1	1	2	0	0	0	
	1	29/01/2010	1	0	1	1	0	1	
	1	30/07/2010	2	0	2	1	0	1	
	2	19/06/2009	1	1	2	0	0	0	
	2	30/07/2010	1	0	1	1	0	1	
	3	19/06/2009	1	1	2	0	0	0	
	3	29/01/2010	1	1	2	0	0	0	
	High Yellow Bluff	1	9/07/2010	2	1	3	0	0	0
		1	11/03/2010	2	1	3	1	0	1
		1	29/01/2010	1	1	2	2	1	3
		2	11/03/2010	1	1	2	0	0	0
2		29/01/2010	1	1	2	2	1	3	
3		9/07/2010	1	0	1	0	0	0	
3		11/03/2010	1	0	1	1	0	1	
3	29/01/2010	1	1	2	0	0	0		
Total			64	40	104	30	15	45	

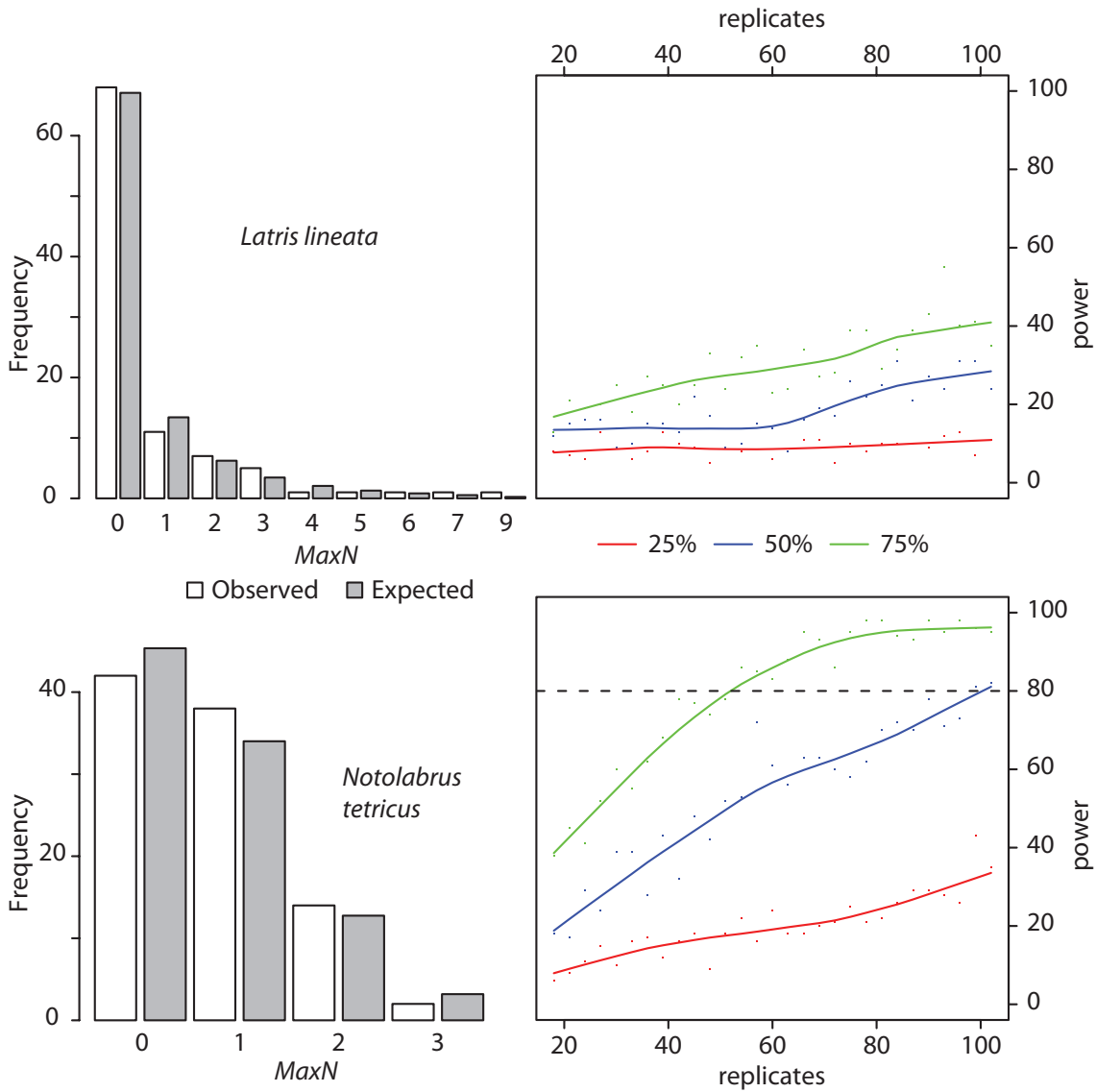


Figure 4.8: Barplots illustrating the fit of raw and generated abundance ( $MaxN$ ) distributions for *L. lineata* top and *N. tetricus* bottom. Line plots display the relationship between statistical power and number of replicates per sample when comparing mean abundance differences of 25% (red), 50% (blue) and 75% (green). Lines are smoothed curves (lowess, non-parametric), data points are colour-coded small dots.

Table 4.7: Distribution and parameters  $\mu$  and  $k$  used in the power analysis for the three species. Mean is based on raw data, dispersion parameter  $k$  was estimated using maximum likelihood.

species	mean abundance	distribution	dispersion parameter ( $k$ )
<i>N. tetricus</i>	0.75	Poisson	NA
<i>L. lineata</i>	0.74	negative binomial	0.28
<i>N. macropterus</i>	4.99	NA	NA

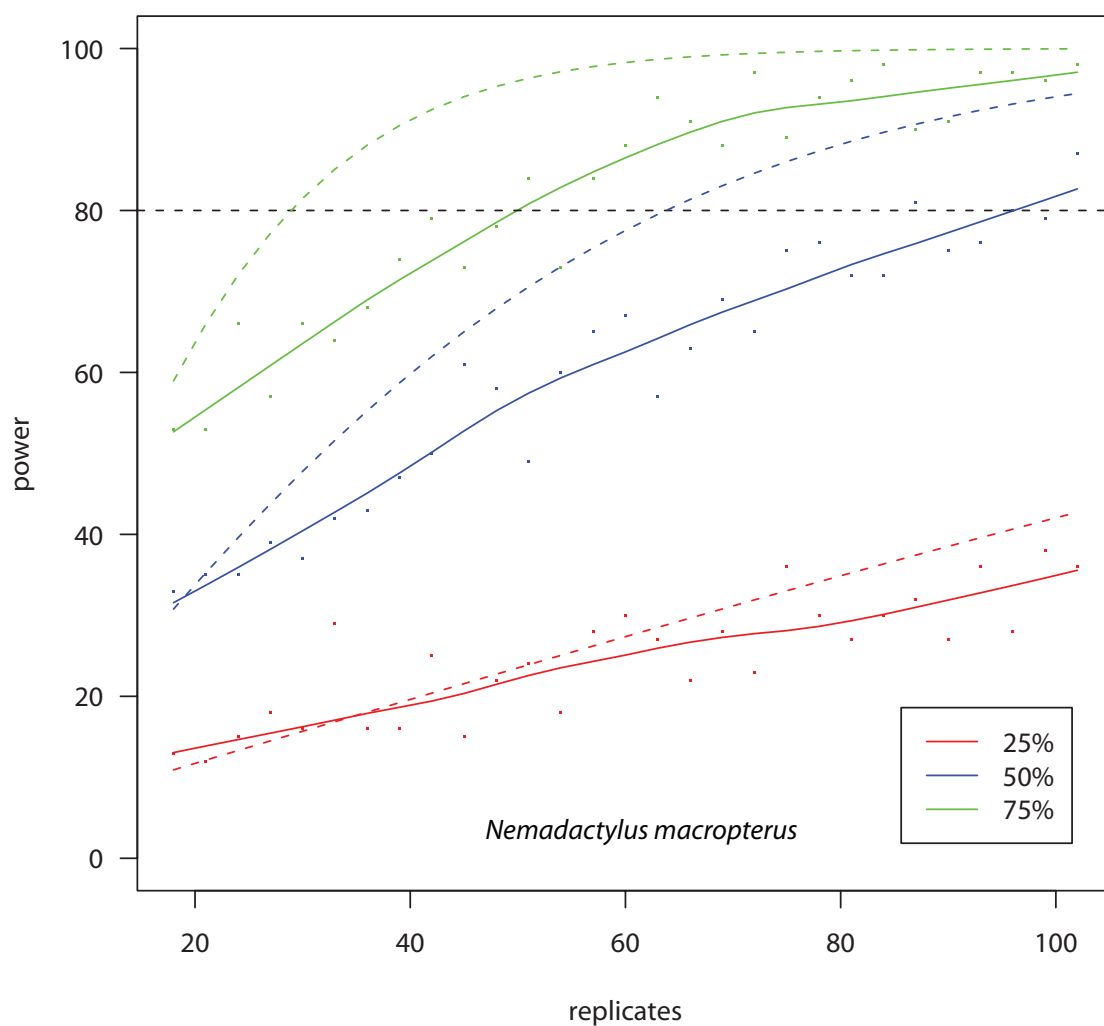


Figure 4.9: Change in statistical power with increasing number of replicates for abundance differences of 25%, 50% and 75% for *N. macropterus*. Lines are smoothed curves (lowess, non-parametric), data points are colour-coded small dots. Dashed lines represent estimates based on traditional power analysis assuming normality on  $\log(x + 1)$  transformed data.

---

method was used to conduct power analysis. As for *N. tetricus*, using BUVS as a sampling tool to monitor *N. macropterus* abundance is feasible; statistical power to detect a 50% and 75% difference in *N. macropterus* abundance is above the conventional 80% (Fig. 4.9). In addition,  $\log(x + 1)$  transformed *MaxN* data were treated as if the normality assumption is true and subjected to power analysis based on the *t*-distribution. Power was overestimated using the transformed data, i.e., fewer replicates, compared to bootstrapped data, were necessary to achieve the same level of power (Fig. 4.9, dashed lines). Assuming normality in the *MaxN* data and using power analysis based on the *t*-distribution required roughly 40% less replicates to achieve power levels of 80%.

## 4.5 Discussion

This chapter has shown that, in deep water, BUVS can provide the same information as UVC in the shallows. The following sections will discuss various aspects of using BUVS to monitor mobile assemblages in deep-water temperate rocky reefs.

### 4.5.1 Composition of reef fish assemblages

Canonical analysis of principal coordinates identified *Jasus edwardsii* as a species that characterises the offshore reef assemblage. Although *J. edwardsii* was present in inshore sites, abundance was different by a factor of 4. The low abundance in inshore sites is not surprising; the study area is a major commercial fishing ground for *J. edwardsii*. Fishermen prefer *J. edwardsii* from shallower depths

(< 30 m). This is due to a positive relationship between depth and discolouration (“redness”). Paler coloured individuals are discounted as a live product to Asian markets (Chandrapavan et al., 2009).

### **Habitat complexity data**

Habitat complexity measures, such as fractal dimension, aspect, slope, plan curvature and profile curvature explained fish assemblage composition. This weak but significant relationship was largely attributed to the complexity measure slope. Moore et al. (2009) found that slope was one of the eight predictors that predicted the presence of *Platycephalus caeruleopunctatus* well, however, the relative contribution was only 3.1% (range 3.1 to 24.3). Galparsoro et al. (2009) also found that slope was a significant predictor with respect to the presence of the European lobster (*Homarus gammarus*). Steep slopes were found to be associated with seafloor depressions at rocky reef-sand ecotones. Although this study aimed to place BUVS on rocky reefs some BUVS landed on rocky reef close to the same ecotone. It is therefore feasible, that the same reason stated by Galparsoro et al. (2009), steep seafloor depressions at ecotones, applies to this study. The habitat heterogeneity (complexity) hypothesis (Simpson, 1949; MacArthur and Wilson, 1967) claims that a greater variety of habitats provides more niches for species to exploit and inhabit, i.e., a greater species diversity. Highly complex rocky reefs with high rugosity values, steep slopes, large overhangs and deep channels not only affect the demersal ichthyofaunal diversity but also algal assemblage structure. Toohey (2007) found that 80% of algal assemblage composition under *Ecklonia radiata* canopies could

be explained by topographic complexity. Similarly, Alexander et al. (2009)) found that macroinvertebrate species richness and abundance could be explained by reef complexity measures such as rugosity substratum composition and refuge metrics. Since the BEST routine in PRIMER v6 lacks the diagnostics to disentangle which species related to which habitat complexity measure; further interpretations of the BEST results are highly speculative. It is conceivable that using Ecological-Niche Factor Analysis (ENFA) conducted by Galparsoro et al. (2009) is superior to the BEST procedure. ENFA calculates the standard deviation of environmental data values where an individual of the species in question was recorded. A low standard deviation value indicates that the species of interest prefers this particular aspect of the environment.

### **Species accumulation curve**

The empirical species accumulation curve and the Michaelis-Menten model intersected at 87 deployments showing that the sampling effort was sufficiently large to capture the species richness in this study area. In contrast, Cappo et al. (2004) found that the BUVS sampling conducted was not sufficient to predict total species richness based on the asymptote of the SAC. Hence, with a sufficient amount of replicates, BUVS can be confidently adopted to monitor fish assemblages in temperate deep-water reefs with respect to ichthyofaunal biodiversity.

#### 4.5.2 Individual species abundances of reef fish assemblages

Analysing *MaxN* records from inshore and offshore sites using GLMs revealed significant differences for species *L. lineata*, *P. psittaculus*, *P. bachus* and *N. tetricus*. This result is of particular importance in the context of Marine Protected Areas (MPAs). The performance of management regimes, such as the establishment of an MPA is usually based on comparing a protected site with an unprotected site. Watson et al. (2007) found that after 10 years of protection targeted and non-targeted reef fish species inside and outside MPAs differed largely. Most importantly, removal of targeted fish species can indirectly alter trophic structure of reef fish assemblages. Based on management objectives the monitoring sampling tool has to be sensitive to detect changes and to be efficient as not to strain resources. The Comprehensive, Adequate, and Representative principle implies that MPAs should include several habitats to protect a large number of species and different life stages and cover the entire depth spectrum of a given species. Curley et al. (2002) suggest that MPAs in New South Wales should be larger than 2 - 6 km or multiple MPAs located as to include all available habitats. Given the breadth of these management objectives and the obligation to annually monitor large and diverse areas it is pertinent to have an efficient and sensitive sampling tool. The results in this chapter have shown that BUVS can detect changes in abundances of several important species and do this in an efficient manner, e.g., BUVS can be deployed in a variety of habitat types including complex rocky reefs, BUVS can be easily deployed by small vessels with few personnel, are sensitive to detect changes in

species richness and abundance inside and outside MPAs, are relatively inexpensive, provide photogrammetric length and volume estimation (stereo BUVS) and are non-extractive and can therefore be used in MPAs where extractive sampling methods are undesirable. However, some shortcomings of BUVS are their propensity to exclude sedentary, cryptic, demersal species such as flatfishes, apogonids, synodontids, triglids and callionymids (Cappo et al., 2004), lack a defined sampling area (provide only relative abundance) and can bias assemblage composition towards predatory and scavenging species.

#### **4.5.3 Size structure of two commercial species obtained by photogrammetric length estimation**

This study successfully used stereo BUVS to photogrammetrically measure fish length of two commercially important fish species. These length measurements culminated in species and gender specific length-frequency data. Whereas trained divers estimate the length of individual fish, stereo BUVS use a calibrated system to measure length with quantifiable accuracy and precision. Harvey et al. (2003) report photogrammetric measurement error to be less than 1%. Blue-throated wrasse data collected using BUVS in deep-water rocky reefs and UVC or extractive sampling techniques in the shallows are very similar. This can be taken as evidence to support the suitability of BUVS to sample this particular species in deeper depths. The maximum depth recorded for *N. tetricus* visits was 66 m. The sharpest decline in probability of *N. tetricus* occurrence started at 50 m depth (Fig. 4.7). In contrast, over the depth range covered by Shepherd et al. (2010), using UVC, there was

no significant increase in abundance of *N. tetricus* males with depth. Although, GLM results suggest that at 80 m depth the probability of *N. tetricus* occurrence approaches zero, this species is known to exist down to 160 m (Edgar, 1997), however, Lyle and Jordan (1999) report that catch by depth strata data analysis indicates that *N. tetricus* catches below 40 m are virtually zero. The majority of *N. tetricus* habitat is beyond safe diver's depths. However similar, comparative results were not identical. One reason could be that Barrett (1995) used extractive sampling methods and also targeted shallower depth (maximum depth = 20 m). There was also a time difference of 20 years between sampling. Further reasons as to why Barrett (1995)'s and this study's results differ are indicated in Shepherd et al. (2010), who found a positive relationship between average female length and distance offshore and exposure index. Barrett (1995) sampled in locations less exposed and further inshore compared to this study. Despite the comparatively small sample size ( $n=45$ ) of *N. tetricus* photogrammetric length estimates, the results are comparable to other studies on this species (Shepherd et al., 2010; Barrett, 1995). The highest female-to-male ratio (F:M) recorded was 3:1 and much lower than reported by Shepherd et al. (2010) (10:1 to 20:1) using UVC in South Australia. Barrett (1995) reported the same female-to-male ratios in Tasmanian waters. Since Shepherd et al. (2010)'s and Barrett (1995)'s findings are consistent, despite their relatively large geographic separation (Tasmania *cf* South Australia), I assumed generality with respect to the F:M ratio. Applying Shepherd et al. (2010)'s F:M ratio to the BUVS data, i.e., multiplying each male visit by 10 or 20 to obtain true abundance, BUVS underestimate *N. tetricus* abundance by 192 – 423%, a factor of 2 – 4. Although, it

---

is conceivable that F:M ratios are different below safe SCUBA diving depths, BUVS records do not indicate changes in F:M ratio with depth. However, BUVS records of F:M ratios range only from 1:1 to 3:1 and should therefore be used with caution when investigating sex ratio–depth relationships. Another reason why the F:M ratio in this study was significantly different from Shepherd et al. (2010)’s findings could be that the BUVS footprint does not cover the entire *N. tetricus* home range. Shepherd et al. (2010) state that the home range of *N. tetricus* is 1000 – 2000 m<sup>2</sup>, whereas the BUVS footprint is about 150 m<sup>2</sup>. This footprint would be sufficient for a species that is attracted to the bait and feeds on the bait, however this is not the case for *N. tetricus*. The Blue-throated wrasse was never recorded to feed on the bait regardless of gender.

With respect to *L. lineata*, two important findings were reported. Firstly, BUVS are not very efficient at capturing *L. lineata* and secondly, BUVS recorded significantly different size spectra. Wrongly assuming identical performance of both, extractive and non-extractive sampling methods can have serious consequences from a management perspective. The *L. lineata* population around Tasmania “has been almost eliminated from the shallow water during the past half-century” (Edgar, 1997). This is consistent with more recent sources: “catches fell by over 30% in 2004/2005 to the lowest level since the mid-1980s” (Ziegler et al., 2006) and “fishing mortality is slightly higher than natural mortality and, in the absence of further strong recruitment, a decline in the stock size is likely if fishing pressure is not reduced.” (Tracey and Lyle, 2005). Tasmanian authorities have responded with increasing the minimum size limit in 2004 and the introduction of a 250 kg trip limit

Ziegler et al. (2006). Setting the size limit based on either one of the methods results in either too low or too high a size limit. The results also exemplify, that several sampling tools are necessary to obtain a balanced picture of the size distribution of a population. BUVS facilitate a potential quantitative non-extractive sampling tool for some species from a fisheries management perspective. However, which species are suitable for BUVS sampling needs to be carefully evaluated.

#### 4.5.4 Improving estimates of relative abundance

One big advantage of line transects using UVC is the ability to calculate the detection probability of an individual during census (Buckland et al., 2001). This detection probability results in more accurate density estimates when extrapolating species abundance over areas that were not sampled, i.e., outside line transects. The reasons why  $MaxN$  underestimates true abundance are manifold and species specific. In this study individual photogrammetric length measurements of two commercial fish species were taken. These measurements served as an aid to differentiate individuals by size. The sum of individuals,  $N$  was then compared to the corresponding  $MaxN$  value. A larger value of  $N$  compared to  $MaxN$  would give further evidence that the latter underestimates true abundance using the same sampling technique but also provide a better method to obtain relative abundance using BUVS. In contrast, a larger  $MaxN$  value would corroborate the current de facto standard status of  $MaxN$  using BUVS. Depending on the species of interest, similar  $N$  values compared to  $MaxN$  are likely related to species-specific dietary preferences. *L. lineata*, a species that was frequently observed to feed on the bait,

---

was equally often recorded regardless of method ( $N$  or  $MaxN$ ). Improving  $MaxN$  was based on the premise that individuals can be differentiated using size and/or obvious markings. It is conceivable that stripe patterns of striped trumpeter *L. lineata* differ between individuals, similar to the spot pattern in whale sharks *Rhincodon typus* (Arzoumanian et al., 2005) or the grey nurse shark (Van Tienhoven et al., 2007). However, to my knowledge, no investigations have been published that compare stripe patterns in *L. lineata*. The author noted one large individual that had a strikingly different stripe pattern compared to the majority of *L. lineata* observed. Given that the individual was unusually large, the stripe pattern could also relate to age. In contrast, *N. tetricus*, a species that was never observed to feed on the bait, was far less frequently recorded using  $N$ . The discrepancy between  $N$  and  $MaxN$  is likely due to high enhanced  $MaxN$  scores caused by combining females and males, despite the fact that both were not recorded in the same videoframe,  $x_{MaxN}$ . It should be noted that in *N. tetricus* only one morphological male is typically present in a given territory (see Table 4.6). This constant could be used to derive a total abundance estimate based on published female-to-male ratios. Photogrammetric precision deteriorates with distance from the bait bag (Shortis et al., 2009). Hence, species that come close to the bait bag can be measured more precisely. Differentiating individual fishes by their body length is based on precise photogrammetric measurements and fails when the variability of repeat (replicate) measurements is high and observed fishes have similar sizes. Fig. 4.5 (top) suggest a reasonably close fit to the bell-shaped distribution curve. This means that the majority of fishes have similar length and the ability to differentiate them

accordingly decreases with decreasing measurement precision, i.e., the standard deviation becomes larger.

Although one limitation of  $MaxN$ , underestimation of true abundance, could be improved as shown in this study the issue of unknown sampling volume remains unresolved. Despite the fact that photogrammetric length measurements give 3D coordinates of every fish recorded and, combined, this information defines a discrete volume, this volume is (1) species specific and (2) does not account for bait plume dispersal. Harvey et al. (2007) found that some fish species are not attracted to bait but are still recorded while passing by and that bait attracts more predatory and scavenging fish species without decreasing herbivorous and omnivorous fish species abundance. Although BUVS data are biased towards predatory and scavenging fish species bait provides greater similarity between replicate samples and therefore better statistical power compared to unbaited underwater video stations. Different species of fish have different abilities to detect prey using their sense of smell. Species with an acute sense of smell can detect the bait plume over a greater distance than species with a less acute sense of smell. It follows, that the more acute the sense of smell of a given species the larger the volume BUVS sample. Bait plume dispersal is mainly governed by tidal current strength. Current meters can be attached to the BUVS frame and record currents strength and direction to model bait plume dispersal. However, currently there are no specific models available that can accurately model bait plume dispersal in habitats with highly complex topography, such as rocky reefs. Even if bait plume dispersal in highly complex reef environments could be accurately modelled, species specific abilities to detect the

---

bait plume have to be established by experiment. Hence, currently the volume of the bait plume is not identical to the field of view.

Only in combining  $N$  and  $MaxN$ , did the total relative abundance value increase. However, since this increase was small (4% and 11%, *N. tetricus* and *L. lineata*, respectively) and the effort to derive  $N$  in addition to  $MaxN$  was large, both methods combined should only be used for key target species. It should be noted that, in order to derive  $N$  and  $MaxN$  the annotator has to score the entire video footage. After scoring the footage  $MaxN$  is immediately available, however, obtaining  $N$  requires three more steps. Photogrammetrically measuring fish length is the most time-consuming step. However, most researchers using stereo BUVS do measure fish length, e.g., Watson et al. (2009, 2010); Harvey et al. (2001, 2002, 2003); Cappelletti et al. (2006); Willis et al. (2003). Applications varied from biomass assessments inside and outside MPAs (Willis et al., 2003) and targeted and non-targeted fish species (Watson et al., 2009), comparisons between length fish estimates by divers and BUVS (Harvey et al., 2002) and accuracy and precision assessments of stereo BUVS length estimation used on tuna ranches (Harvey et al., 2003). In these cases, the two remaining steps to derive  $N$  are trivial and easily conducted, thereby providing valuable information about relative fish abundance. It is unlikely that, in the near future, the process of photogrammetrically measuring fish length can be automated. However, recent developments in pattern recognition, machine learning and artificial intelligence have delivered some promising results and MacLeod et al. (2010) urge taxonomists to collaborate with specialists from the above fields to achieve more accuracy and less drudgery.

#### 4.5.5 Power analysis

Power analysis on *N. tetricus* abundance recorded by BUVS was conducted to see how many replicates are necessary to detect a 25%, 50% and 75% change in abundance between two samples. With the current sampling effort ( $n = 96$ ) a change in abundance of  $> 50\%$  could be detected, which is consistent with findings by Edgar and Barrett (1997) using 104 UVC samples, i.e.,  $4 \times 500\text{m}^2$ . However, Edgar and Barrett (1997) used a different power analysis method method (“the power of each analysis was assessed by adding a fixed log value to 1993 data obtained at reserve sites. The size of this value was gradually increased by iteration until the  $F$ -test of the interaction term in the associated ANOVA indicated that the null hypothesis should be rejected at a probability level of 0.05.”) and were only able to detect changes with 50% power (Most statisticians work with  $\alpha = 0.05$  and  $\beta = 0.2$  and power of 0.8 ( $1 - \beta$ ) or 80% (Crawley, 2007)). Detection error is defined as the probability that a species is not recorded using a certain sampling tool. If a certain sampling tool is not able to effectively sample the target species, it should not be used in a management context where resources are finite. This study showed that three out of five species are not adequately detected using BUVS. Concurrently, it provided a method (power analysis) to quantify detection error for species recorded using BUVS. It is commonly criticised that the species composition of BUVS records is biased towards piscivorous and scavenging species due to the bait used during deployment (Willis et al., 2000; Watson et al., 2005). However, records in this study show that BUVS can detect the zoobenthivorous *N. tetricus* which is not attracted

to the bait (Shepherd and Clarkson, 2001). The overestimation of power by using  $\log(x+1)$  transformed  $MaxN$  data in conjunction with standard power analysis tools emphasises the importance of using the right statistical tools, suitable for the data at hand.

## 4.6 Conclusion

BUVS are effective in assessing reef fish assemblage attributes for some species that are attracted to bait, to the BUVS unit and activities of other fish feeding on the bait, such as size composition and relative abundance below safe SCUBA diving depths. Whereas, comparative studies between different habitats or management regimes are feasible with respect to photogrammetrically measured fish length and species richness, comparative studies based on the relative abundance measure  $MaxN$  are futile, except for a few species (*N. tetricus* and *N. macropterus*).

## Chapter

# 5

## Assessing size, abundance and habitat preferences of the ocean perch *Helicolenus percooides* using a AUV-borne stereo camera system

*This Chapter has been accepted for publication and will be printed in Fisheries Research. doi:10.1016/j.fishres.2012.06.011*

### 5.1 Abstract

Traditional fishery resource assessment methods using trawl gear are unable to sample rocky substratum and are prone to underestimating the biomass of species having partial or strong association with rocky reefs. This study successfully used an Autonomous Underwater Vehicle (AUV) and image-yielding methods to estimate size, abundance and habitat preference of an abundant and commercially important ‘rockfish’ – the ocean perch (*Helicolenus percooides*) – in rocky habitats on the continental shelf off Tasmania, SE Australia. More than half (53%) of the ocean perch observed were photogrammetrically measured with known accuracy using a stereo camera system yielding length-frequency distributions. Observations of juvenile and adult *H. percooides* across a depth gradient showed that adults preferred rocky substrates over soft substrates, whereas juveniles preferred soft substrate over hard substrate. We found a positive relationship between

rockfish abundance and increasing depth in most habitat types. These results demonstrate the utility of image-based methods for determining size composition and habitat preferences of some reef-associated species. However, there is scope to improve image-based methods using length estimation procedures that enable higher proportions of individuals to be measured (compared to the proportion achieved in this study) and by incorporating automated image annotation to decrease image analysis times, particularly when examining species/habitat relationships. The importance of analytical procedures that account for autocorrelation in non-independent image data on habitats and associated species is discussed. We conclude that rapidly maturing image-based observational methods have potential utility in complementing fishery stock assessments of some reef-associated species. Image-based methods are also well-suited to simultaneously provide additional quantitative measures of benthic habitats, invertebrate fauna and fishery environments.

## **5.2 Introduction**

Many commercially important fishes and other species with high conservation significance are associated with rocky reef habitat that is difficult to survey using conventional net-based methods. Non-extractive photographic methods are able to survey rocky reef habitats and have the potential to assess size, abundance and habitat preferences of associated fishes. Manned submersibles (Yoklavich et al., 2000, 2007), remotely operated vehicles (ROV) (Brodeur, 2001; Johnson et al., 2003), an autonomous underwater vehicle (AUV) (Tolimieri et al., 2008) and towed camera platforms (Lauth et al., 2007; Williams et al., 2010c) have been used

for abundance assessments and to investigate species-habitat associations. Each platform brings particular strengths to rocky reef surveys. The manned submersible *Delta* was instrumental in a fishery-independent assessment of the overfished Cowcod (*Sebastes levis*) in depth from 75 – 300 m (Yoklavich et al., 2000). *Delta*'s greatest strength is its ability to take two personnel onboard, a pilot and a fisheries scientist or other relevant specialist. Several viewports and various cameras allow observations from different angles (Yoklavich et al., 2000). The establishment of Cowcod Conservation Areas off the Californian coast aimed at protecting cowcod from commercial and recreational fishing, thereby excluding extractive sampling methods as a monitoring tool (Yoklavich et al., 2000). Being non-extractive, *Delta* provided valuable insights into habitat-specific rockfish distribution. This included highly complex reef habitats where traditional sampling gear is ineffective.

AUVs follow a pre-programmed track (mission) and therefore require no on-board personnel during sampling. Another strength is the AUV's ability to manoeuvre at centimetre accuracy over very complex terrain (Williams et al., 2008b) - an important feature for monitoring purposes. They combine many of the strengths of imagery-yielding sampling platforms, e.g., being non-extractive samplers with extensive depth rating and large size range. Tolimieri et al. (2008) were the first to test an AUV to investigate abundance and habitat-specific distribution of Rosethorn Rockfish *Sebastes helvomaculatus* off the coast of Oregon, USA. This commercially important, species had not been previously surveyed because it lives on rocky reef in depths from 100 to 300 m.

Species-specific habitat preferences can be readily identified from *in situ*

photography and quantified when the image footprint enables precise and accurate size and abundance estimates to be made. This is straightforward when the camera is parallel to a flat seabed and image footprint is a simple function of camera altitude and when fish are also parallel to the plane of the photograph. While this condition may be met by highly dorsoventrally flattened species such as flatfish or scallops (Harris and Stokesbury, 2006), it is rarely the case in highly complex rocky reef environments. Stereophotogrammetry, using calibrated stereo camera systems (Williams et al., 2010c) is free from this constraint and therefore offers many advantages over single camera systems. The AUV platform, with ability to hover at fixed distance from the seabed, deploying a downward-looking digital camera, appears to be an ideal platform for testing such applications.

In this study we use the stereo-vision AUV *Sirius* to assess size, abundance and habitat preference of the ocean perch *Helicolenus percooides* in temperate waters of the south-eastern Tasman Peninsula, Tasmania, Australia. The aim of this study is to demonstrate the potential for stereo-photography on a stable AUV platform to contribute quantitative data on size, abundance and habitat preference to assessing population structure of deep-water reef-associated fishes. We discuss the potential sources of error in the observational and analytical methods and the advantages of an assessment method that is both non-extractive and feasible on any seabed habitat type.

## 5.3 Material and Methods

### 5.3.1 Field Sampling

*Helicolenus percooides* (Richardson & Solander (1842), Family: Sebastidae (Gomon et al., 2008)) is a bottom-dwelling teleost distributed across the Southwest Pacific (Australia and New Zealand, 26°S – 55°S) and is commercially important in much of this range. It occurs on coastal rocky reefs to deeper open sandy bottom (Gomon et al., 2008) in depths ranging from 80 – 350 m (Rowling et al., 2010) with maximum length of 40 cm (Gomon et al., 2008). This study was conducted in adjacent waters of the south-eastern part of the Tasman Peninsula, Tasmania, Australia and covers  $\sim 200 \text{ km}^2$  (Fig. 5.1) in 25 – 95 m water depth. The maximum depth sampled (95 m) was also the deepest depth to which rocky reefs extended. Although, *H. percooides* frequent depths below the maximum depth in this study; there was no opportunity to sample beyond the rocky reef edge. We therefore restrict our results to the depths sampled.

During daylight hours (8 AM – 6 PM) high resolution, geo-referenced imagery of the target species and benthic habitats was acquired using the Autonomous Underwater Vehicle (AUV) *Sirius*, operated by the Australian Centre for Field Robotics at the University of Sydney. Sampling during daylight hours was necessary to eliminate possible diel behavioural effects of fish abundance or habitat use. A multibeam sonar survey was conducted prior to AUV deployment to delineate the extent of deep-water reef systems and enable depth stratified sampling during AUV missions.

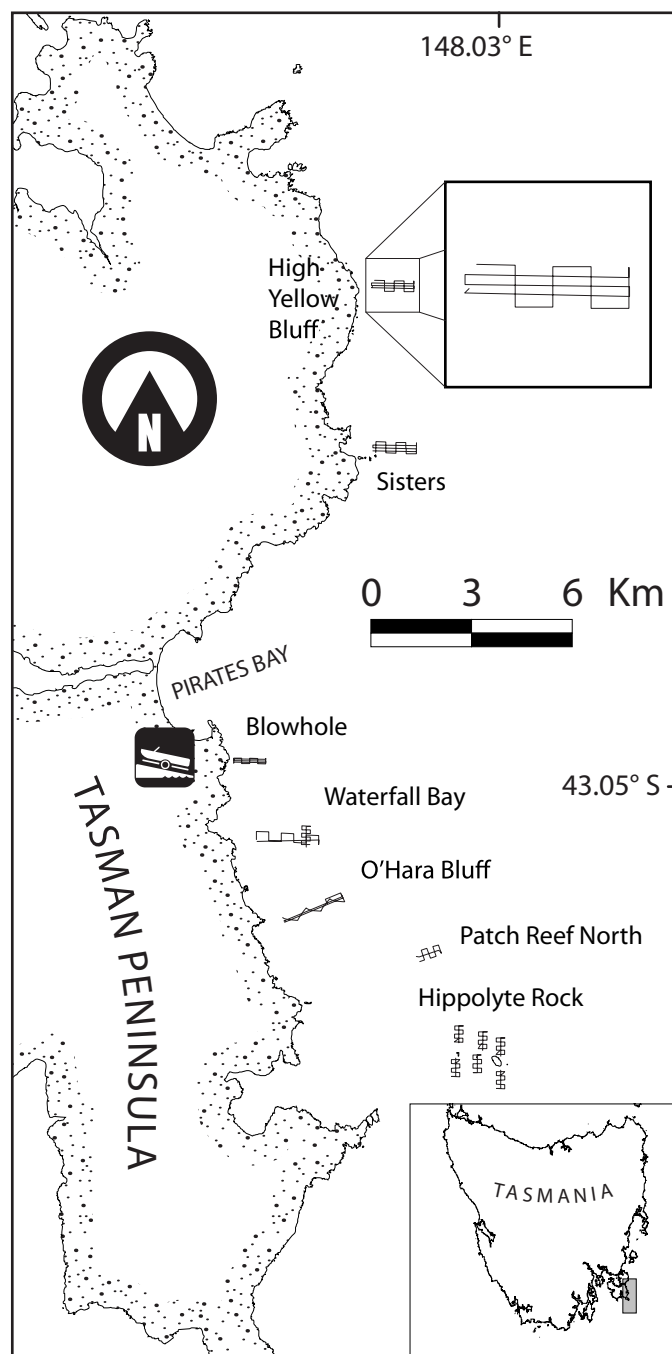


Figure 5.1: Location of 14 AUV dive tracks in adjacent waters of the south-eastern part of the Tasman Peninsula, Tasmania, Australia. Inset (top right) illustrates intersecting survey (transect) pattern. Note location of jetty in Pirates Bay.

Multibeam sonar survey data were gathered using a 200 kHz Kongsberg EM-3002 echo sounder from the 20 m research vessel *Challenger*. Individual AUV dives were then randomly placed on prominent deep-water reefs within the study area (Fig. 5.1) targeting rocky reef and transition zones between reef and adjacent sandy areas. Geographical vehicle positioning on the surface was accomplished using GPS. Navigation underwater was achieved using a Doppler velocity log, inertial measurement unit and ultra-short base-line acoustic positioning system, pressure sensor and a compass. To further reduce positional error introduced by dead-reckoning and sensor drift, the simultaneous localisation and mapping (SLAM) technique was used to renavigate the estimated vehicle trajectories (Williams et al., 2008b). Consequently, the intersecting survey pattern (Fig. 5.1 inset) was necessary to maintain high spatial accuracy using SLAM.

### 5.3.2 Data acquisition and processing

The AUV's ability to hover facilitated a virtually constant altitude of 2 m above the seafloor which equates to an image footprint of  $1.6 \times 1.3$  m ( $\sim 2$  m<sup>2</sup>). The relatively slow 'flying' speed of the AUV is  $\sim 0.4$  m/s. Average image area was 2.04 m<sup>2</sup> ( $\pm 0.09$  SD). A pair of downward-looking Pixelfly HiRes (1360  $\times$  1024 pixels) digital cameras took images every second. The relatively narrow camera separation of 78 mm accommodated the stereo camera system within a streamlined AUV hull, keeping overall vehicle drag to a minimum. Two strobes, one situated at the front and the other at the back of the AUV, synchronously illuminated the field of view. Within the survey area, the AUV collected 126,723 overlapping stereo

---

image pairs. To achieve independent (non-overlapping) quadrats (images) only every fourth image was annotated. Vehicle altitudes  $> 3.5$  m resulted in underexposed images which were excluded from analysis ( $n = 501$ ). These remaining 32,008 images were consistently assigned to one of 11 habitat classes by a single annotator. The very infrequently recorded habitat classes “caulerpa” and “pebble/tuft” were excluded as they occurred only at one site. Both habitats were also devoid of *H. percoides*. The remaining habitat classes were; reef-sand ecotone (RSE), high and low relief reef (HRR, LRR), patch reef (PR), sand (S), coarse sand (CS), screw shell rubble (SSR) and screw shell rubble/sand (SSRS). One habitat class dominated by the large macroalga *Ecklonia radiata* could not be confidently sampled and was also excluded from analysis. The dominant habitat was scored in cases of transition between two types.

The camera system was calibrated by taking 371 stereo image pairs of a chequerboard (calibration grid, Fig. 5.2) with 32 black squares of known dimensions in a seawater tank at an approximate distance of 2 m. The calibration software ‘Cal’ (Seager, 2009a), was used to establish an optional stereo constraint specifically for calibrating stereo camera systems (Seager, 2009a). Within each image pair 82 unique points on the chequerboard were manually assigned to relate to a pixel position in the image. This was done for 25 image pairs. Based on this information the software could solve for all parameters necessary to measure fish length.

The shortest distance between two points (snout and tail) is a straight line. However, *H. percoides* was frequently recorded resting in an excessively curled/bent

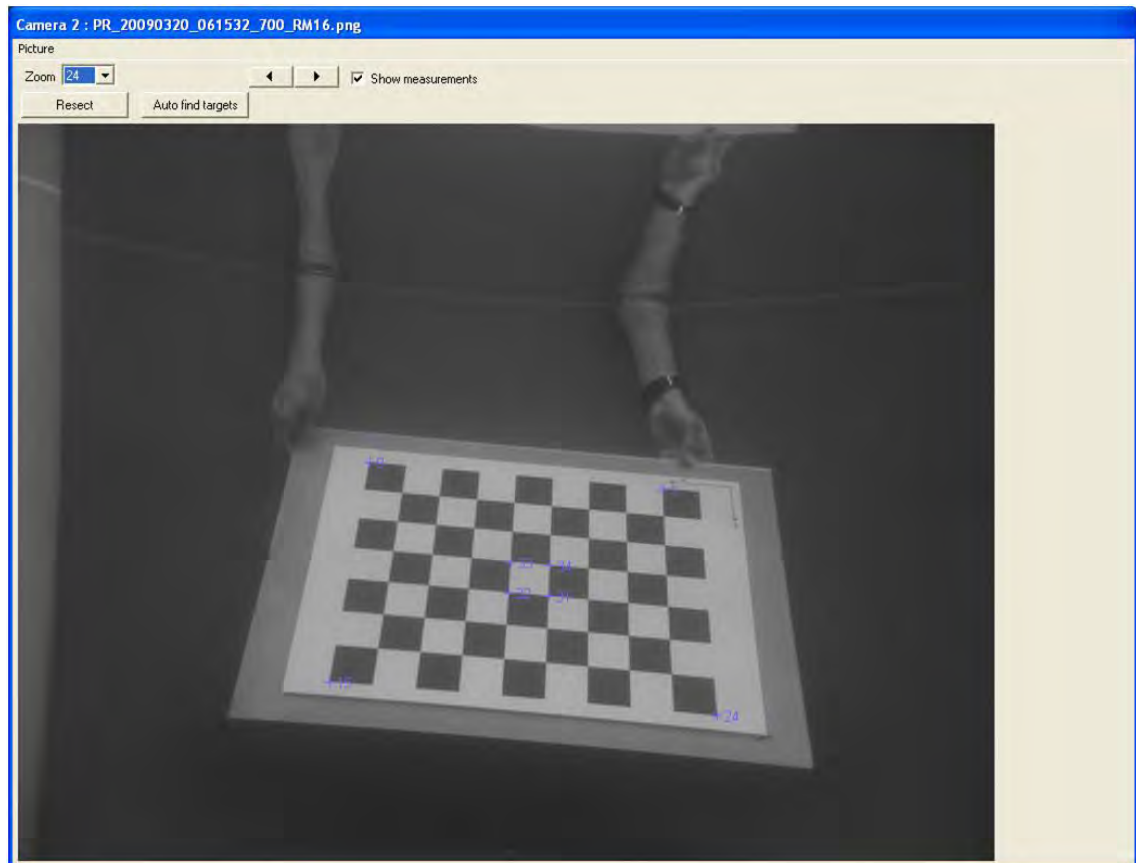


Figure 5.2: Left image of calibration grid (chequerboard) in seawater tank loaded into the software package Cal. Numbers refer to individual measurement points to derive camera parameters.

---

position. Taking length measurements without accounting for this curvature is a misrepresentation of the true fish size. Excessively curled/bent fish sightings were excluded from length measurements. Fish length was measured in 937 of 1766 stereo image pairs in the software package PhotoMeasure (Seager, 2009b). Total length (tip of snout to tip of caudal fin) was measured by manually determining either end of the fish in the left image; automated image matching was used to find the matching point in the right image (Fig. 5.3). When automated image matching failed, positions (snout or tail) were manually chosen. To assess photogrammetric measurement error, a second subset of images, independent of the 25 image pairs used for calibration, was taken to derive 60 random measurements of the chequerboard ranging from 53 – 482 mm. Measurements were taken across all orientations, i.e., horizontal, vertical and diagonal using the software package PhotoMeasure. In addition, we used the built-in image measurement precision setting, set to the software default of 1 pixel (at a camera altitude of 2 m above seafloor, 1 pixel equals 1.17 mm). This setting influences the precision of parameters estimated with the bundle adjustment (Seager, 2009a). The precision estimate is also dependent on camera resolution (rows and columns of sensor array) and camera parameters such as focal length, camera base separation and orthogonality. Images with measurement precision values  $> 40$  mm were excluded. Length measurements were converted to biomass per  $2 \text{ m}^2$  (image footprint) using the published length-weight relationship in (Schofield and Livingston, 1996) where weight (g) =  $a$  (length) <sup>$b$</sup>  (weight in g, total length in cm), which applies to both male and female fish.



Figure 5.3: Screenshot of left and right image loaded into PhotoMeasure. Images are zoomed in by a factor of 4. The red line across the fish is its linear length estimate.

### 5.3.3 Statistical analysis

#### Spatial autocorrelation

Determining habitat-occurrence relationships needs to account for spatial autocorrelation (SAC) in occurrence (abundance), habitat (environmental) or both. The geographic distribution of individuals can be spatially auto-correlated due to movement restrictions, social organisation or aggregative reactions to signals from other individuals of the species. Environmental variables are usually also spatially auto-correlated and are discussed at length in Legendre (1993). To assess the extent to which SAC was evident in our data, we applied an auto-correlation function (ACF) to multiple linear subsections of all AUV transects (dives). The ACF indicates at what lag (distance) SAC disappears. We assumed that observations further apart than the lag (distance) indicated by the ACF were spatially not

correlated. For each dive we generated several lag (distance) values one for each linear subsection. We took the largest lag (distance) as a threshold to rule out SAC. Distances between observations (presence of fishes per image) were calculated using geographical easting and northing and the Pythagorean theorem. This approach was only taken for binomial (presence/absence) analysis. To visualise the extent of spatial auto-correlation we used correlograms (Bjørnstad and Falck, 2001), which depict spatial dependencies between locations at different lag distances using Moran's  $I$ . Two relationships were investigated (A) location (spatial x, y coordinates) of *H. percoides* presence-absence and (B) location and extent of habitat classes.

### **Linear mixed-effects models (LMEs)**

We investigated relationships between continuous variables (fish length and weight) and environmental variables (depth and habitat) using linear mixed effects models (LMEs) in R, package nlme (Pinheiro et al., 2009). The Maximum Likelihood (ML) method was preferred over the default Restricted Maximum Likelihood (REML) method as we intended to compare models with different fixed effects structures. LMEs allow for the observational units (image) to be clustered, e.g., observations by dive. Random effects across dives were assumed to vary. Another advantage of LMEs is their ability to incorporate several random effects that are spatially nested, i.e., habitat classes within dives within sites. LMEs were chosen since they can handle pseudoreplication. In our case, images fall in the category of spatial pseudoreplication where several measurements (length) were made from the same

vicinity (dive). Pseudoreplication violates one of the fundamental assumptions in statistical analysis; independence of errors. Conditions within each habitat class will affect all length measurements within this particular habitat class and therefore violate the independence of errors assumption. The best (minimal adequate) model was chosen by backward selection, where explanatory variables were deleted one at a time from the full (saturated) model. The model was

$$FL_i = \alpha + \beta \times depth_i \times habitat_i + a_i + \epsilon_i$$

log-transformed fish length ( $FL$ ) and weight were modelled as an intercept ( $\alpha$ ) plus the linear interaction between depth and habitat class effect, a random intercept ( $a$ ) and an error term  $\epsilon$ . Index  $i$  refers to an image, where a length measurement was taken. Fixed effects, depth and habitat class, influence the mean of  $y$  (fish length and weight), whereas random effects influence only the variance of  $y$ . The reduced model was compared to the full model utilising  $F$ -likelihood ratio tests. Restricted Maximum Likelihood (REML) was used to compare models with different random effects structures and Maximum Likelihood (ML) was used for models where the fixed effects structure differed. Fish lengths and weights were log-transformed before analysis. Sightings without length measurement were excluded from analysis.

### **Generalised linear mixed-effects models (GLMMs)**

Binary response variables, i.e., presence/absence of *H. percooides* were analysed using GLMM to investigate relationships between species occurrence and habitats. We

---

used the R package lme4 (Bates and Mächler, 2010), as it provides AIC (Akaike Information Criterion) for model selection. AIC is a measure of the fit of a model (Crawley, 2007) and for each model is calculated as:

$$AIC = -2(\log -likelihood) + 2(p + 1)$$

where  $p$  is the number of parameters in the model (1 is added for estimating the variance). The lower the AIC number the better the fit of a model. As with LMEs we arrived at the ‘best’ model by backward selection. The model was:

$$\text{logit}(p_i) = \alpha + \beta \times \text{depth}_i + a_i + \epsilon_i$$

for each habitat class individually the probability ( $p$ ) of *H. percoides* presence in image<sub>*i*</sub> is modelled as an intercept ( $\alpha$ ) plus the linear depth effect, a random intercept ( $a$ ) and an error term  $\epsilon$ . The depleted model was compared to the full model using ANOVA. A non-significant result warranted model simplification, i.e., deletion of explanatory variables. After initial analysis using all habitat classes and dives in one data set we decided to model *H. percoides* presence/absence for each habitat class separately. This would allow for easier presentation of our results. The binary response variable was presence or absence of *H. percoides* in image  $i$ . We investigated the probability of *H. percoides* occurrence per image by depth for each habitat separately. Site, dive and habitat class were incorporated into the model as random effects.

### Habitat preference index

To address habitat preferences of *H. percooides* we used a log likelihood ratio test of goodness of fit (Tolimieri et al., 2008) recommended by Sokal and Rohlf (1995). This method is similar to Pearson's  $\chi^2$  test, however, the test statistic is the deviance from a log-linear model. We tabulated observed counts by habitat and calculated expected counts assuming no habitat preference by adjusting for frequency of occurrence for each habitat. For illustrative purposes we created a preference index (observed proportions minus expected proportions).

### Juveniles and adults

Finally, we investigated the proportion of juvenile and adult individuals by habitat, depth, dive and site. Due to our inability to determine the sex of fishes we used an average value based on numbers reported by (Park, 1993): males mature at 10 – 13 cm TL (approx. 2 – 5 years of age) females mature at 9 – 17 cm TL (2 – 6 years of age). Individuals >12.25 cm (24.7 g) were considered adult fish. Our decision to take an average is based on a sex ratio close or equal to 1 and seems to prevail in other live bearing non-targeted species of the Sebastidae family but there are several reasons why the sex ratio can deviate from 1, e.g., fishing pressure (Harvey et al., 2006). A classification tree model using binary recursive partitioning was also used to investigate habitat preferences of juvenile and adult fish. Here, individual length measurements ( $n_{length} = 937$ ) were split along the coordinate axis of the categorical explanatory variable habitat class ( $n_{habitat} = 8$ ) so that the split

maximally distinguishes the response variable (length) between the two branches (Breiman et al., 1984).

## 5.4 Results

### 5.4.1 Measurement precision

Measurement error (error = actual length – photogrammetrically estimated length) was assessed using images of the calibration grid (chequerboard). Repeated measures showed that the maximum measurement error was 9.7 mm and minimum error was 0.04 mm; 63% of all measurements were within  $\pm 1$  mm of the actual length (Fig. 5.4). This range of error is a relatively small proportion of the total lengths of individual fish, e.g., typically  $< 1\%$ . Because the proportional error is greatest for smaller individuals, data for juvenile fish is likely to be less reliable than for larger fish. In fact, average measurement error was highest for short distances, although the negative linear relationship between log-transformed measurement error and distance measured was non-significant (GLM,  $t = 0.991$ ,  $df = 59$ ,  $p = 0.326$ ).

### 5.4.2 Habitat association and spatial autocorrelation

Because spatial autocorrelation (SAC) was evident in *H. percoides* occurrence, as well as habitat distribution along transects (Fig. 5.5), we created correlograms for each of the 14 dives prior to assessing habitat associations to obtain estimates of distances at which SAC was no longer evident. Spatial dependence is measured by Moran's  $I$  and the distance estimate coincides with the left-most spline intersect

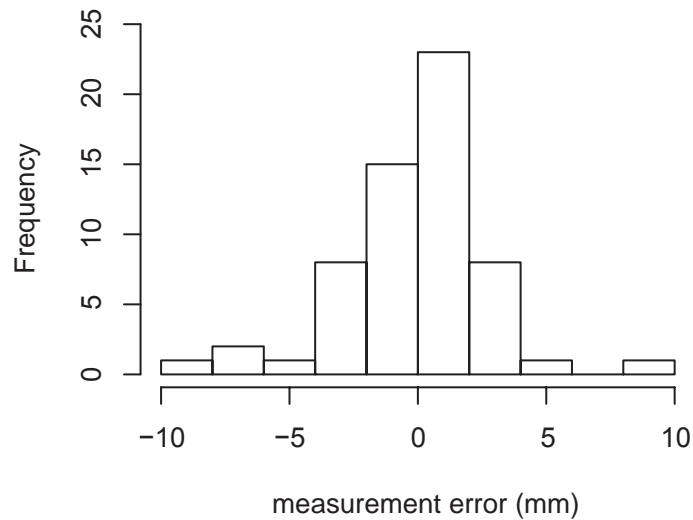


Figure 5.4: Histogram of measurement error in mm based on measurements of the calibration grid (chequerboard), deviation from actual length ( $n = 60$ ).

of the x-axis. SAC was evident in dive06 up until 96.2 m for presence/absence of *H. percoides* per image and up until 168.3 m for habitat classes. Distance estimates at which SAC is no longer evident using correlograms were in general higher than those obtained using the autocorrelation function (ACF). The mean distance estimate for all 14 dives with respect to *H. percoides* presence/absence was 29.23 m (SD 20.99 m). SAC with respect to habitat classes along transects had a mean value of 75.45 m (SD 42.36 m).

#### 5.4.3 Fish occurrence, length and biomass

*H. percoides* density was highest (5 individuals per 100 m<sup>2</sup>) at dive08 (Patch Reef North) which is a comparatively small, isolated (surrounded by soft substrate), deep (60 – 85 m) offshore rocky reef outcrop and lowest (<1 individual per 100 m<sup>2</sup>) at dive15 (Blowhole) which is a shallow (23 – 58 m), low relief reef site closest to

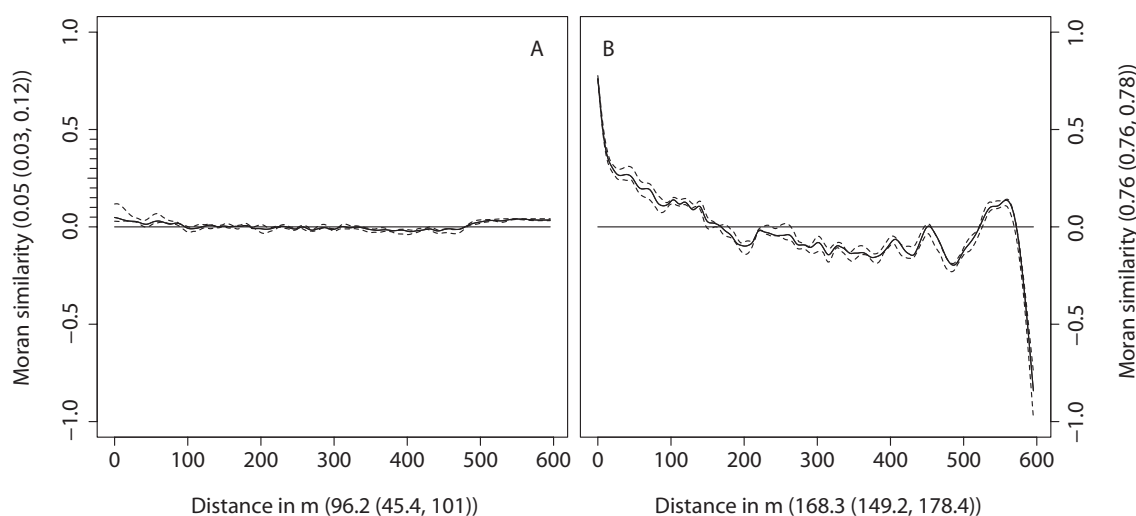


Figure 5.5: Example (dive06) spline-smoothed correlograms with 95% point-wise bootstrap confidence intervals (CI) dashed lines, expressed as Moran similarity (Moran's  $I$ ) against distance for (A) *H. Percooides* presence-absence and (B) habitat occurrence. Numbers on abscissa refer to: (spline intercept with x-axis (lower CI, upper CI)) and ordinate: (spline intercept with y-axis (lower CI, upper CI)).

the Pirates Bay jetty. Numbers of individuals by habitat are presented in Fig. 5.6. In general, fish density appeared to be higher in offshore sites than inshore sites. Sites that are a submerged extension of a mainland cliff are considered inshore i.e. Blowhole, Sisters, High Yellow Bluff and O'Hara (Fig. 5.1). Sites that are "detached" from mainland cliffs are considered offshore, i.e., Hippolyte Rock and Patch Reef North (Fig. 5.1).

Generalised Linear Mixed-Effects Models (GLMMs) were used to predict the probability of occurrence per image by depth. Each habitat class was modelled separately; however, all dives were included. The results of log-linear relationships between presence/absence and depth for each habitat class are presented in Figure 5.7. All models were significant at the 5% level. Generally, there was

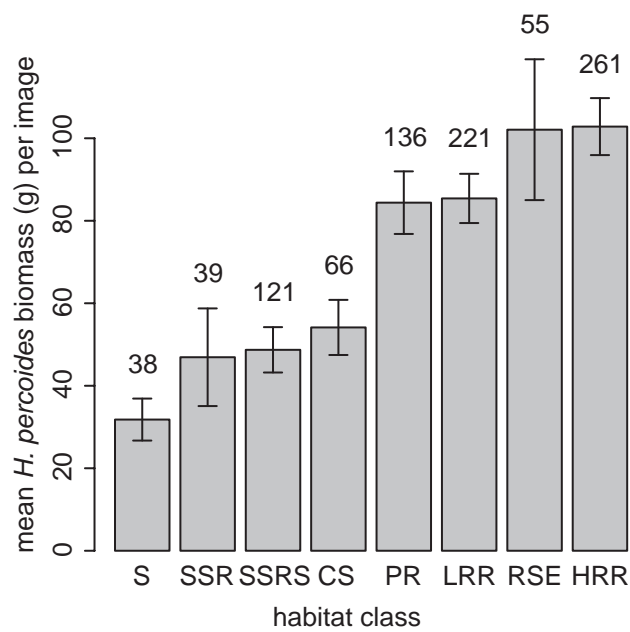


Figure 5.6: Mean biomass in gram of *H. percooides* by habitat per image ( $\sim 2 \text{ m}^2$ ) pooled from all dives. S = sand, SSR = screw shell rubble, SSRS = screw shell rubble/sand, CS = coarse sand, PR = patchy reef. Error bars represent one standard error of the mean. Numbers above bars represent sample size ( $n_{total} = 937$ ).

---

a positive relationship between *H. percooides* probability of occurrence and depth, except for habitat classes ‘screw shell rubble’ and ‘screw shell rubble/sand’ where it was weakly negative. The variability between dives was also highest for the latter two habitat classes. Only ‘screw shell rubble’ and ‘screw shell rubble/sand’ had a significantly different slope than the remaining habitat classes (assessed using one model that included all habitat classes). Probability of occurrence predictions outside the depth range of the shallowest and deepest sightings should be regarded with caution as indicated by the upper and lower confidence intervals (CI). A linear model could be inappropriate for predictions outside the sampled depth range. Habitat class ‘high relief reef’ exhibited a remarkably low variability between dives *cf* ‘screw shell rubble/sand’.

Out of 1766 individual *H. percooides* sightings 937 (53%) fish could be measured. The remainder (47%) was either excessively curved, partly obscured by benthos or substrate or only partly within field of view. Histograms of length and weight showed the majority of fish were between 125 mm and 175 mm long and the length frequency distribution was skewed to the left (skewness = 0.851); 250 fish (36%) were classified juvenile and 687 fish (64%) adult (Figure 5.8).

The total number of sightings per habitat from the total 1766 individual fish observed are shown in Fig. 5.6. Mean biomass between habitat classes pooled over all dives was significantly different (Table 5.1), it was highest for hard substrate habitats (patch reef, high and low relief reef and reef-sand ecotone) and lowest for soft substrate habitats (sand, coarse sand, screw shell rubble and screw shell

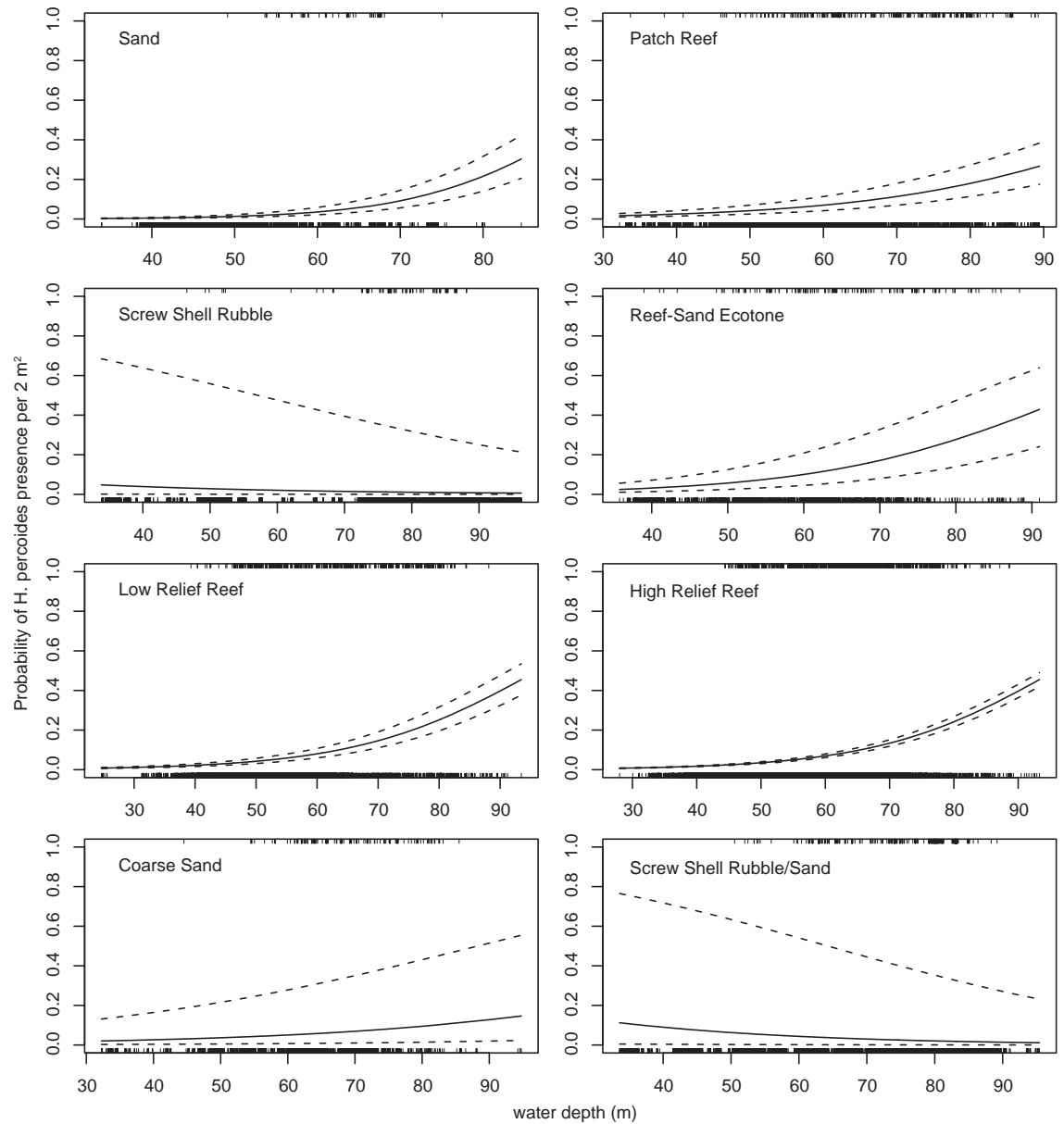


Figure 5.7: GLMM predicted probabilities of *H. percooides* presence per image (2 m<sup>2</sup>) across depth gradient for each habitat including all 14 dives (1 = presence, 0 = absence). Dashed lines represent 95% confidence interval of random intercept. Solid lines depict predicted values for *H. percooides* probability of occurrence by depth. The space in between upper and lower CI indicates variation between predictions between dives. Rug (tick marks) on top and bottom of each panel represent fish presence and absence, respectively. X-axis is water depth in m.

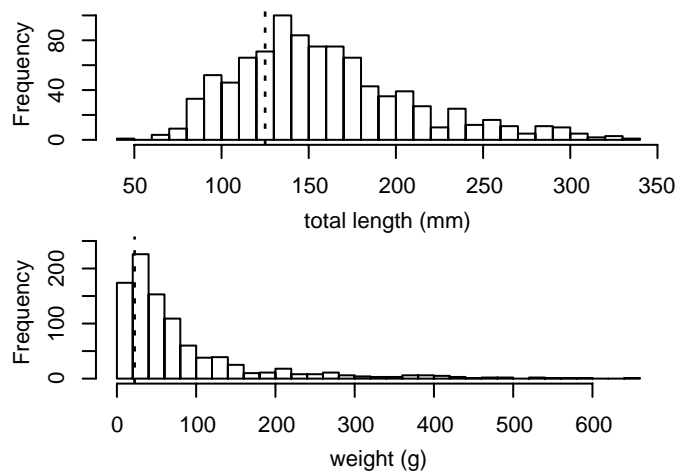


Figure 5.8: Histogram of; Top: photogrammetrically estimated tail length in mm of *H. percooides*. Vertical broken lines indicate length or weight at maturity. Bottom: histogram of calculated weight in g, ( $n = 937$ ).

rubble/sand) (Fig. 5.6). Habitat classes ‘high relief reef’ and ‘reef-sand ecotone’ had similarly high mean biomass values of  $\sim 100$  g whereas ‘sand’ scored lowest with  $\sim 35$  g. Variability among biomass values per image was highest for habitat class ‘reef-sand ecotone’ and ‘screw shell rubble/sand’.

Table 5.1: ANOVA results for fourth-root transformed *H. percooides* biomass data in response to habitat pooled over all sites and depth.

Source	df	Sum of squares	Mean Sq	$F$ value	Pr ( $> F$ )
habitat type	7	3.053	0.436	6.677	$< 0.001$
Error	296	19.333	0.065		
Total	303	22.386			

#### 5.4.4 Habitat preferences

Habitat distribution among dives was highly variable. Low and high relief reef were most abundant 17% and 29%, respectively. Reef-sand ecotone (4%) and coarse sand (5%) were the two least abundant habitat classes. Soft substratum habitat

classes (sand, coarse sand, screw shell rubble and screw shell rubble/sand) combined accounted for 39% whereas hard substratum habitat classes (high and low relief reef, patch reef and reef-sand ecotone) make up 61%. There was a clear, although non-significant, increase in frequency of occurrence with depth for habitat classes ‘screw shell rubble’ ( $t = 2.204$ ,  $p = 0.063$ ) and ‘screw shell rubble/sand’ ( $t = 2.508$ ,  $p = 0.041$ ).

The analysis to test *H. percoides* habitat preferences showed significant differences in observed numbers per habitat compared to expected numbers for each habitat (Fig. 5.9,  $G$ -test,  $G = 43.4032$ ,  $\chi^2 df = 7$ ,  $p < 0.001$ ). As indicated in Fig. 5.9, *H. percoides* prefers high relief reef (HRR) and dislikes screw shell rubble (SSR). Small deviations from zero such as coarse sand (CS) and patch reef (PR) reflected a neutral attitude towards those habitats. In general, abundance observations higher than expected occurred in rocky habitat types (high and low relief reef and patch reef). Lower abundance observations than expected occurred in sandy (sand) and rubble (screw shell rubble) habitats. The linear mixed effect model with individual fish length as response variable and habitat class and depth (interaction) as the fixed variables and three spatially nested random effects (site/dive/habitat) to test that mean biomass per image differed among habitat classes and depth were non-significant for all habitat classes and depth interactions at the 5% level. The non-significant result was equally true for the linear mixed effect model with all model components identical except weight as the response variable.

In general, adult fish ( $n_a = 687$ ) were more numerous than juvenile fish ( $n_j = 250$ ).

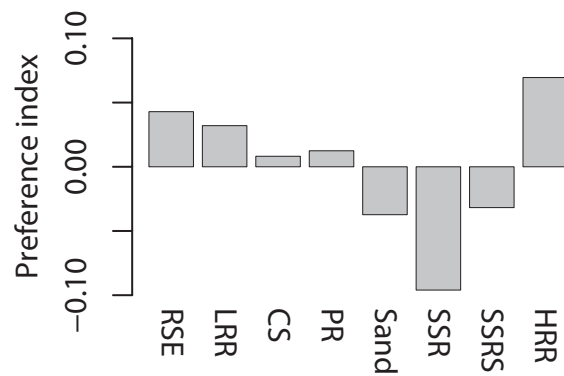


Figure 5.9: Depiction of preference index for a given habitat (observed proportion - expected proportion). RSE = reef-sand ecotone, LRR = low relief reef, CS = coarse sand, PR = patch reef, SSR = screw shell rubble, SSRS = screw shell rubble/sand, HRR = high relief reef. All results are significant using the likelihood-ratio test.

Juvenile *H. percooides* individuals preferred habitats with soft substratum (sand, screw shell rubble, screw shell rubble/sand) see Fig. 5.10, where the percentage of juveniles per habitat exceeded the mean juvenile percentage (30.5%) across all habitat classes (dashed line Fig. 5.10). The classification tree model to confirm the visual assessment showed one split with two terminal nodes distinguishing smaller (juvenile) and larger (adult) individuals. The split grouped the eight habitat classes into (1) sand, coarse sand, screw shell rubble and screw shell rubble/sand and (2) low relief reef, high relief reef, patch reef and reef-sand ecotone. Group one represents soft substratum and group two represents hard substratum. The classification tree results and the visual assessment are identical except for coarse sand being close to, but not exceeding, the mean juvenile percentage across all habitat classes (Fig. 5.10 dashed line).

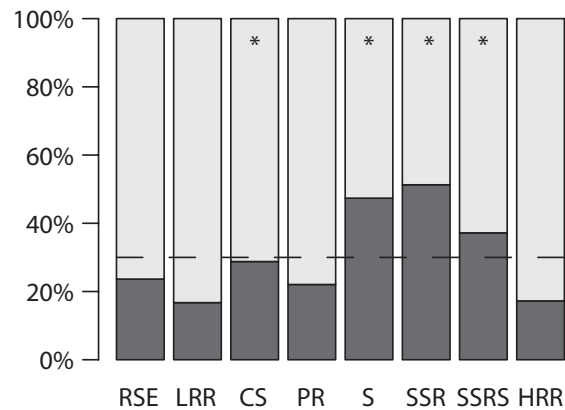


Figure 5.10: Percentage of *H. percooides* sightings considered to be mature (light bars) and juvenile (dark bars) by habitat for all dives, dashed horizontal line represents mean percentage of juveniles, \* denotes soft substrate, RSE = reef-sand ecotone, LRR = low relief reef, CS = coarse sand, PR = patch reef, S = sand, SSR = screw shell rubble, SSRS = screw shell rubble/sand, HRR = high relief reef.

## 5.5 Discussion

### 5.5.1 Distribution and size composition of *H. percooides* across habitat types

The ecological insights of interest to ocean perch assessment using image analysis included; estimates of habitat preference, greater representation of adults, compared to juveniles, in size data, and relationships between habitat type and fish size and depth and fish size. We found the ocean perch *H. percooides* used both soft and hard substrates, but generally preferred hard over soft substrate. This is consistent with habitat preferences in some other species using multiple habitat types, including rockfishes in the Sebastidae family in the NW Pacific (Tolimieri et al., 2008). However, this pattern does not apply to all sebastid rockfishes; Percy et al. (1989) found that juveniles and large adults of yellowtail rockfish

(*Sebastes flavidus*, Scorpaenidae) occurred exclusively on rocky, high-relief areas off the coast of Oregon. Pearcy et al.'s finding is opposite to our observations of juvenile ocean perch which preferred soft over hard substrate. Examining the relationship between number of juveniles and distance (classes) to nearest reef would elucidate the generality of the aforementioned finding. However, continuous reef perimeter information cannot be obtained from the imagery. We found that off Tasmania, ocean perch abundance increased with increasing depth in the range sampled (25 – 95 m) and that this was largely independent of habitat type, except for habitat classes 'screw shell rubble' and 'screw shell rubble/sand' where the trend was reversed. We do not have an adequate explanation but assume that this is an artefact of the more densely populated, deeper offshore sites and the exclusion of the shallow habitat class *Ecklonia radiata*. While the kelp cover at shallow depths excluded full interpretation of depth related patterns, diver observations in this area confirm that this species is rarely encountered at depths of 25 m or less (Barrett, personal observation and Denny et al. (2003)).

The majority of ocean perch observed in this study were between 125 mm and 175 mm long, a smaller size distribution than reported from commercial catch sampling (commonly 200 – 250 mm) off New South Wales 10 degrees further north (Rowling et al., 2010). The opposite pattern would be predicted from our observation of higher preference by small fish for sediments and the dominance of trawl-caught fish from soft substrata in the fishery data. It remains unclear whether this difference stems from a selective bias in the sampling tools, i.e., more larger fish taken by com-

mercial fishing gears, or some other factor. For example, a common life-history trait of temperate demersal fish species is the tendency to move to deeper depths when maturing (Hyndes et al., 1999). It is conceivable that *H. percoides* is also moving further offshore as it grows older. Irrespective, our finding illustrates the potential for traditional gears to be size-selective and therefore the risk of biasing assessment models sensitive to age/size structure in populations of target species (Willis et al., 2000). Because of their size-selectivity, there has been a considerable amount of research to quantify size selectivity for specific gears to mitigate bias (Millar, 1992; Millar and Walsh, 1992).

Image-based methods have drawbacks compared to physical sampling, including that it may be impossible to distinguish the sex of an individual unless there is conspicuous sexual dimorphism. This is not the case for ocean perch and it was necessary to determine sex to set a threshold for differentiating size classes, i.e., juveniles from adult ocean perch. Here we used averaged reported values for males and females, an approach that assumes a sex ratio of approximately one. Park (1993) confirms that this is a reasonable assumption in our case, but sex ratios can deviate from one due to stock exploitation or general species-specific life-history traits such as protandry or protogyny.

Collectively, these results illustrate the potential importance of data from rocky seabed for stock assessments because accurate estimates of fish abundance may require sampling of a range of habitat types, with a sampling design that considers

species-specific patterns.

### 5.5.2 Improving efficiency and quality of image-based data

Individual fish are put into a geographical context because every AUV image is geo-referenced. This requires consideration of spatial autocorrelation (SAC) because its omission in binomial (presence/absence) analysis violates assumptions of independence of errors. Incorporating SAC in statistical models is on the forefront of spatial statistical research (Dormann et al., 2007), but adequate methods are known for linear transects as well as full coverage areal census, i.e., a continuous raster where every cell is evaluated.

Length estimation: Although more than half (53%) of all fish seen ( $n = 1766$ ) could be measured, the remainder were unmeasurable due to three primary causes: (1) fish were cryptic, only partly visible hiding under ledges, crevices or benthos, (2) either snout or tail were not within the overlapping image area of the left and right camera and (3) individuals were excessively curved. Cryptic fish and fish not wholly inside the overlap area, are likely to remain elusive to measurement unless also viewed from a different angle. The equipment and data-processing costs associated with an additional, e.g., forward-looking stereo camera system, appear currently prohibitive (Stefan Williams, University of Sydney, personal communication). *Sirius* has not been specifically designed to be used as a benthic sampler but as a underwater robotic platform for robotics engineers. Adding an additional stereo camera setup with underwater housing to the current configuration would change the

buoyancy and balance of the AUV and jeopardise the functioning of emergency abort manoeuvres. The current cameras are specialised cameras that are considerable more expensive than off-the-shelf cameras, but are necessary due to the need to operate them using a Linux computer whereas consumer cameras are designed to be manually operated. However, the third problem of excessively curved fish may be addressed with a software solution that can measure arc length or take several (more than two) measurement points approximating an arc. In situations, outlined in this study, where complete census data are not available; the paramount questions are: (1) is the photogrammetrically measured length a true representation of the actual length of the fish and (2) is the photogrammetrically derived sample representative of the true size composition of the population. Question one was addressed by calibrating the camera system using well established protocols and by assessing the measurement error (see results and Fig. 5.4). With regard to question 2; since every sampling method introduces biases, the true size composition may only be obtained if several methods are used in conjunction. Watson et al. (2010) found that using two different methods of obtaining length-frequency data for reef fish in the same location produced significantly different results. Before using the AUV to complement fishery assessment data, we recommend data comparison to identify possible biases in the various data collection methods. Although length measurement error can be reduced with higher image resolution than ours (1 Megapixel resolution), by greater camera separation ( $> 70$  mm) and better calibration, we believe that improved operator accuracy is likely to be most important. Operator error is likely to decrease as image resolution increases when using PhotoMeasure. For example, higher resolution

images help to improve the precision with which the operator can place the cursor at the tip of the fish's snout or tail margin. Additional error may also result from the slightly different angle of view of both cameras where the fish is not identically depicted in both images. An automated target matching routine in PhotoMeasure defines a measurement point in a subsection of the image to reduce or even eliminate this error source by finding sharp edges and colour pattern similarities. However, because similarities are not always present in a highly complex benthic environment and because *H. percoides* is well camouflaged in its environment, the target matching failed about half the time. Measurement error was assumed to be independent of object length because no statistically significant relationship between measured object length and measurement error size was apparent.

Habitat classification: Annotation of habitat classes for each image or even a subset of images is time consuming. Tolimieri et al. (2008) report that for images collected within one hour during a dive, 5 – 10 hours of lab time are required to count and identify one fish species. Identifying habitats takes less time than identifying fish but still requires a considerable amount of time (for 3600 images, i.e., 1 image per second, the author needed on average 1.5 hours). Automated habitat classification could help to substantially reduce annotation time. Seiler et al. (in press) outline an automated habitat classification method using image features such as colour, texture and rugosity derived from a bathymetric reconstruction of the substrate using stereo imagery. After a small manually scored training set a decision tree classifier takes over and annotates the remaining images (see chapter 3 for further details).

### 5.5.3 Utility of AUV *Sirius* for fishery assessments

Our data on the size, abundance and habitat preferences of adult and juvenile reef ocean perch provide fishery-independent data for a commercially fished species and were collected simultaneously with environmental data. As such, the data overcome many shortcomings of traditional fishing gear such as size selectivity and gear avoidance behaviour (Fernandes et al., 2000) and provide information on habitat types and distributions that are important components of ecosystem-based fisheries management (EBFM) approaches, as for example, are rapidly developing in Australia (Smith et al., 2007). While currently economic costs would preclude the routine inclusion of non-extractive, imagery-yielding sampling tools in field-based fishery assessments, they have high utility in rocky reef habitats which may support a disproportionately high biomass of some fishery species and may provide structural refuges for species occupying a variety of habitat types. In many instances they are the only alternative where the use of traditional net sampling gear is impractical or impossible. One of the greatest insights for EBFM is the permanent photographic record of target species, their environments and co-occurring species. Image-based data are being used increasingly in EBFM approaches to fishery, e.g., in habitat risk assessments (Hobday et al., 2011). The historically high overheads associated with processing and storing image data are now rapidly decreasing due to the wide availability and low cost of automated options for data processing and semi-automated habitat classification (Seiler et al. in press) and efficient methods to store and retrieve data. This study analysed only one species visible in our

data set, but there is scope to also analyse the abundance and diversity of other large-bodied species of fishes, echinoderms, bivalves, crustaceans as well as benthos such as sponges, corals and ascidians, without additional data collection. We note, however, that the utility of this method to provide fishery independent data depends very much on the species in question. Currently, the downward-looking camera design excludes investigations of pelagics and some reef-associated species that can adjust their buoyancy. The five most abundant species recorded during this study were ocean perch (1766 individuals), butterfly perch (*Caesioperca lepidoptera*, 1672), rosy wrasse (*Pseudolabrus mortonii*, 302), sandpaper fish (*Paratrachichthys macleayi*, 249) and southern rocklobster (*Jasus edwardsii*, 77). Based on ranked abundance it is conceivable that highly mobile species, unless extremely abundant, are less suited for investigations using this AUV. Other commercially important reef species in Tasmanian waters such as banded morwong (*Cheilodactylidus spectabilis*), jackass morwong (*Nemadactylus macropterus*) and blue-throated wrasse (*Notolabrus tetricus*) were recorded too infrequently to provide reliable fishery data. It is highly likely that other image-based sampling tools such as baited underwater video systems are better suited to observing mobile species (Watson et al., 2010). Unfortunately, as is true for the AUV, each sampling method brings its own biases. The scope to mine additional data from image data sets is the typical situation - and will be facilitated as data formats become more standardised and data sharing and integration is encouraged by national scale observing programs, e.g., the Australian Integrated Marine Observing System (IMOS) program into which our AUV data are contributed (IMOS, 2011). We conclude that, among the variety of camera platforms

applied to provide quantitative measurements of fishery species and habitats, AUVs are a mature and cost-effective survey platform well-suited to complement future fishery-independent surveys of rocky reef species.



---

## Chapter

# 6

## A continental shelf deep-water temperate reef fish assemblage recorded by three different non-extractive image-yielding platforms – a comparison

### 6.1 Abstract

Non-extractive imagery-yielding samplers, such as baited underwater video systems (BUVS), autonomous underwater vehicles (AUV) and towed video platforms are frequently used to assess reef fish assemblages below safe SCUBA diving depths. Each platform has its strengths and weaknesses. Here, a comparative study investigates sampling bias and performance between platforms based on species richness, total number of individuals and species accumulation curves. Combined, 62 species and operational taxonomic units were identified using the three platforms. Each platform sampled a distinct component of the overall reef fish assemblage. BUVS are limited to providing a relative abundance estimate (i.e., the BUVS sample area/volume is unknown), but recorded the highest number of species. The towed video platform scored the highest total number of individuals but scored the lowest number of species. BUVS and towed video systems lack a constant field of view (sample area) and are therefore less suitable for monitoring purposes. Advantages and disadvantages of bait are discussed, as well as platform induced escape and

avoidance behaviour in fish.

## 6.2 Introduction

Fishes comprise an important component of rocky reef fauna (Kingsford and Battershill, 1998). For example, planktivorous reef fish can alter the abundance of zooplankton, are major consumers of larval forms leaving/approaching the reef to settle and enhance nutrient input into reef systems (Kingsford, 1989). The ability to reliably measure inherent attributes of reef fish assemblages, such as species diversity and species abundance is essential to ecologists, conservationists and resource managers alike. Numerous extractive and non-extractive methods to assess shallow-water reef fish assemblage attributes exist; gill netting (Hickford and Schiel, 1996), trapping (Crossland, 1976; Whitelaw et al., 1991), handline fishing (Ralston et al., 1986), underwater visual census (UVC) (Edgar et al., 2004) and baited underwater video systems (BUVS) (Willis et al., 2000). For the majority of these methods there is no depth restriction. However, UVC, the most common method to investigate reef fish assemblage structure and composition, is restricted to depths safe for divers (< 30 m, based on standard recreational SCUBA equipment commonly used in Australian scientific diving operations). Due to its non-intrusive nature, non-extractive imagery-yielding platforms such as manned submersibles are well suited to investigate vulnerable species or protected areas. Vulnerable species such as the overfished slow-growing and reef-dwelling Cowcod (*Sebastes levis*) off Southern California are now protected following the establishment of two Cowcod Conservation Areas (Yoklavich et al., 2007). The areas, also known as marine

protected areas (MPAs), are a well-established and widespread management tool to protect marine resources. They have strict restrictions on the use of extractive fishing or sampling gear. Hence, the increasing implementation of MPAs to protect the natural environment and its fauna requires alternative survey techniques that can reliably monitor MPA performance against management expectations. Alternative non-extractive sampling techniques for monitoring and to inventory fish assemblages in MPAs include BUVS (Willis et al., 2000), towed video platforms (Williams et al., 2011) and autonomous underwater vehicles (AUV) (Tolimieri et al., 2008). Each method has its intrinsic biases. For example, orange roughy (*Hoplostethus atlanticus*) disperse rapidly when towed camera systems approach (Koslow et al., 1995). Some other species have been observed to be either attracted or repelled using certain sampling tools (Watson et al., 2005). This behaviour can result in biased species composition and abundance data (Kulbicki 1998). Willis et al. (2000) compared UVC, handline fishing and baited underwater video and found that spatial variability and relative density of fishes were significantly different between methods, partly attributable to intrinsic methodological biases. Their study was conducted in depths less than 30 m and retrieving fish from such depths, by hook and line or other extractive sampling methods, is unlikely to cause physiological damage, such as swim bladder inflation to the fish. *Notolabrus tetricus* and *Cheilodactylus spectabilis* are two Tasmanian reef species that are destined for the live-fish market in Asia and are retrieved from less than 30 m to reduce mortality (Lyle 2001). However, MPAs and other conservation areas are seldom restricted to safe SCUBA diving depths. For example, only 6% of the Great Barrier Reef Marine Park can be safely monitored

using SCUBA (Cappo et al., 2003). Comparative reef fish biodiversity assessments using baited underwater video systems (BUVS) and prawn trawls are described in (Cappo et al., 2004).

Reef-fish stock assessments encompass the investigation of age structure, growth, reproduction, feeding habits and habitat preferences (Hilborn and Walters, 1992). These data are notoriously difficult to obtain due to patchy reef fish distribution and reef habitat complexity (Andrew and Mapstone, 1987). The majority of our current knowledge is based on shallow reef surveys using SCUBA. Our inability to descend below SCUBA depth limits, except inside a submersible, renders our knowledge of deep-water reef fish assemblages comparatively scarce. Some notable exceptions include Moore et al. (2009) sampling depths ranging from 26 to 110 m using BUVS and Tolimieri et al. (2008) in depths down to 250 m using an AUV.

This study targeted reef fish assemblages in depths deeper than what is considered safe for SCUBA divers and focused on non-extractive sampling techniques. We investigated the usefulness of BUVS, AUV and towed video in highly sensitive or restricted areas, such as MPAs, where extractive tools are prohibited. Each platform was assessed in their ability to measure reef fish assemblage attributes such as species richness and abundance. We compared each platform for their relative contribution in non-intrusively describing the fish assemblages present on continental shelf deep-water rocky reefs, present strengths and weaknesses of each platform and the extent to which the platforms complement each other. To our knowledge a comparison of different non-extractive, imagery-yielding platforms to investigate reef fish assemblages below safe diving depths is unprecedented.

## 6.3 Materials and methods

### 6.3.1 Study area and sites

Prior to the deployment of the three non-extractive, imagery-yielding sampling platforms described in this section, a multibeam sonar survey was conducted in order to delineate the extent of deep-water reefs in the survey area. The study area contains a representative distribution of temperate coastal to mid-shelf rocky reef systems below SCUBA diving depth ranging from 25 – 100 m. Multibeam sonar data were gathered using the 20 m research vessel R/V *Challenger* with a Simrad EM-3002 shallow water multibeam echo sounder using frequencies in the 300 kHz band. Sampling took place from 6 October 2008 to 22 August 2010 on deep-water reefs and adjacent soft substrates of the south-eastern Tasman Peninsula, Tasmania, Australia. Whereas the AUV survey and the towed video platform survey were accomplished within one fortnight, BUVS deployment dates ranged from 14 May 2009 to 22 August 2010. AUV sampling took place from 6 October to 14 October 2008 on the support vessel R/V *Challenger*. Towed video platform sampling occurred from 25 to 27 February 2009 on the same support vessel (Nichol et al., 2009). Individual AUV dives were haphazardly placed on prominent deep-water reefs focusing on rocky reef and transition zones between reef and adjacent sandy areas. All three sampling platforms targeted the same reef complexes (sites, see Fig. 6.1). The choice for BUVS sampling locations was based on georeferenced annotated AUV imagery. BUVS were deployed exclusively on rocky reefs. Towed video transects were placed to overlap AUV tracks and cover roughly the same

---

areal extent. Replication of AUV and towed video samples was insufficient around Hippolyte Rock (Fig. 6.1). Locations north and south of Hippolyte Rock were therefore combined to form sites ‘Hippolyte Rock North’ and ‘Hippolyte Rock South’. The ‘Peninsula Mapping Region’ (Barrett et al., 2001) has a dominantly easterly aspect, high vertical cliffs, deepwater reefs (to 100 m depth) and medium to high wave exposure. Geologically the coastline is composed of dolerite, sedimentary rock and to a lesser extent granite (Barrett et al., 2001).

### 6.3.2 Sampling platforms

#### AUV-borne downward-looking digital stills cameras

The AUV *Sirius* operated by the Australian Centre for Field Robotics at the University of Sydney sampled benthic fauna by means of digital photography. *Sirius* is a modified version of the *SeaBED* AUV (Singh et al., 2004a) built by the Woods Hole Oceanographic Institution. The overall dimensions of the AUV were 2.0 m (length)  $\times$  1.5 m (height)  $\times$  1.5 m (width). Its weight was  $\sim$  200 kg (depending on payload). The vehicle is rated to 700 m depth. We have chosen the AUV *Sirius* due to its ability to (1) keep a virtually constant altitude of 2 m above the seafloor which equated to an image footprint of  $1.6 \times 1.3$  m ( $\sim$  2 m<sup>2</sup>), (2) take high resolution images ( $1360 \times 1024$  pixels) and (3) provide spatially precise image location (to within 2 m). Precise image location was accomplished by re-navigating the estimated vehicle trajectories using the simultaneous localisation and mapping technique (Williams et al., 2008a). Colour images of the left camera were viewed

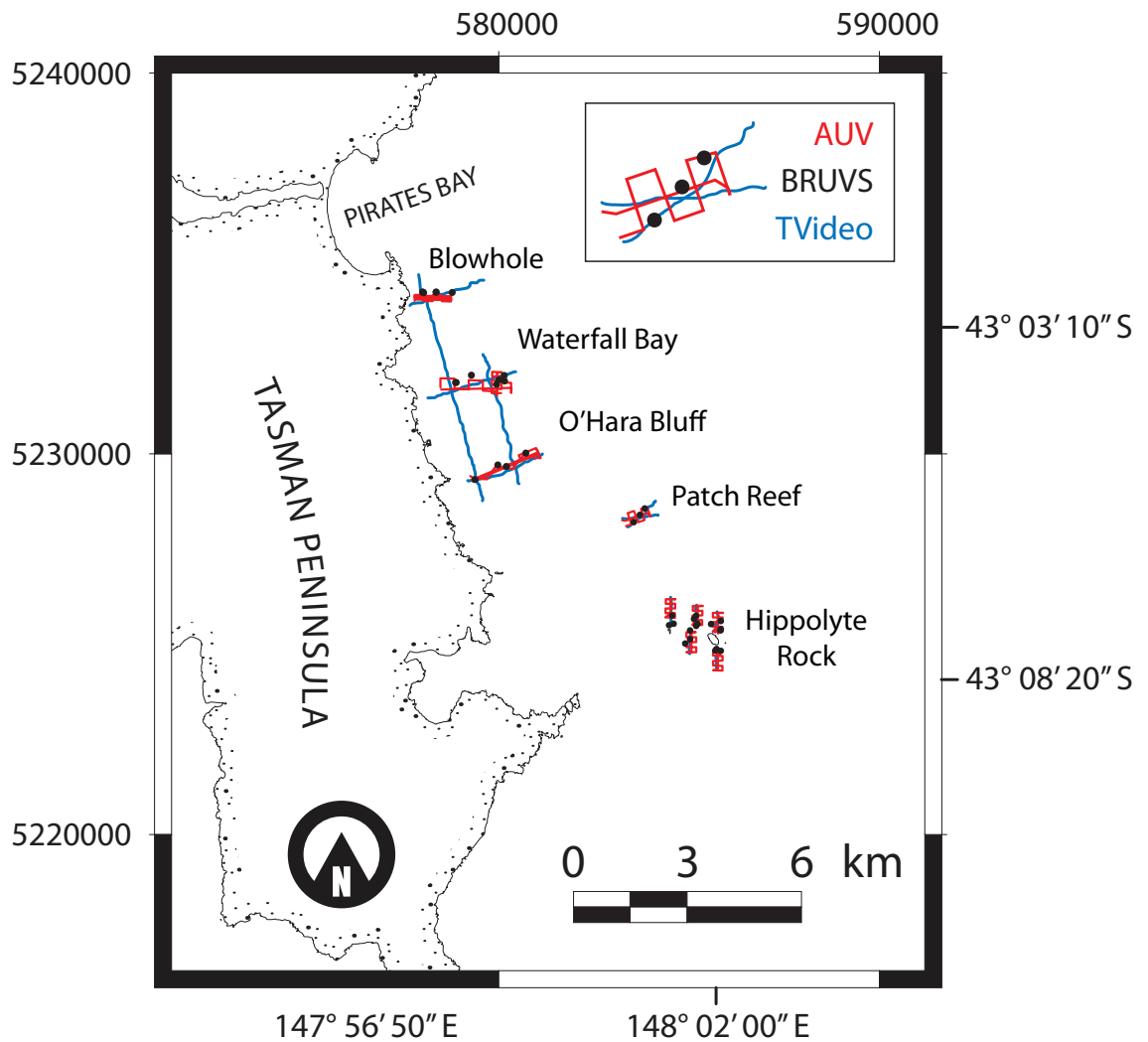


Figure 6.1: Map of south-eastern Tasman Peninsula depicting sample sites and sampling locations for each platform. Inset is the enlarged site Patch Reef to serve as an example of the spatially overlapping sampling design. Red = autonomous underwater vehicle (AUV), black = baited underwater video system (BRUVS) and blue = towed video platform (TVideo). Projected coordinates UTM 55G (WGS84).

on a large computer screen and manually annotated. Fish species identification was based on Gomon et al. (2008) and expert advice.

### **BUVS with forward-looking cameras**

The BUVS frame is shaped like a truncated pyramid with an oblong base. Frame design is identical to the design used by Harvey et al. (2002) and Watson et al. (2005). The stereo camera setup comprised of two JVC GZ-MS100 PAL (720 × 576 pixel) off-the-shelf video cameras. Raynox wide angle conversion lenses (conversion factor 0.7) were used to increase field-of-view.

Multibeam sonar mapping of the study region revealed several distinct rocky reef complexes. Each reef complex comprised one sampling site. Near-simultaneous replication (3 replicates) per site occurred over the entire depth range of a reef complex. Sampling time at the bottom was 45 min and was conducted during daylight hours using a ~ 6 m boat. The plastic mesh bait basket, attached ~ 1 m in front of the cameras, contained 800 g crushed *Sardinops sagax* (pilchard) as bait to attract fish and was re-filled before each new deployment. Sampling depth ranged from 32 – 81 m. Distance between replicates differed between sites according to reef complex size. In general, replicate distance exceeded 200 m to avoid overlapping bait plumes which compromises independent sampling. However, small reef complexes around Hippolyte Rock resulted in smaller distances between replicates. Video footage was viewed and annotated using the software package EventMeasure (Seager, 2009b). The relative abundance measure *MaxN*, maximum number of individuals of species *x* per video frame, was chosen to avoid repeated

counting of the same individual (Cappo et al., 2004).

### **Towed video platform with oblique-looking camera**

Geoscience Australia's (GA) small ( $30 \times 50 \times 40$  cm), shallow-water RayTech towed-video system consists of two steel side panels connected by rods and bars to give stability as well as attachment points for sensors (Nichol et al., 2009). A wing on the back of the platform stabilises the 'flight' path (pitch, yaw and roll). The umbilical cable serves as tether and real-time data cable to control lights and laser pointers and receive PAL video footage and positional information. The two 250 W lights can be switched on and off on demand but remained off most of the time due to adequate ambient light conditions and the high sensitivity of the digital video camera. Two laser pointers 15 cm apart underneath the lights served as an indication of scale in the video footage. An ultra-short baseline (USBL) acoustic tracking system fed back the precise geo-location of the platform during deployment. Video transects ranging from 200 m to 1.1 km ran along two directions; along depth contours and across depth gradient, i.e., perpendicular to the coastline (see Fig. 6.1). The platform was towed at 0.5 - 1.5 knots approximately 2 m above seafloor. Digital video footage was transferred from tape to hard drive and saved as an AVI-file (Audio Video Interleaved). We used the open source software package VARS (Video Annotation and Reference Software) (Schlining and Stout, 2006) for viewing and annotation. Where possible, mobile invertebrates and vertebrates were scored down to species level.

### 6.3.3 Data analysis

Whilst AUV and towed video sampled all available habitats, BUVS deployments specifically targeted hard substrate (rocky reef). For sampling platform comparison (PERMANOVA) fishes recorded in habitats other than ‘rocky reef’ were removed from analyses. To exclude camera orientation bias, pelagic species records, such as *Mola mola*, were also removed from analysis. The camera pair mounted on the AUV was unlikely to record pelagic fish species due to their downward-looking orientation. Finally, singletons, species that were recorded only once during this study, were removed from analyses. In order to establish whether the three different sampling platforms were complementary, we investigated the percentage of species unique to each platform. Since the BUVS sampling period spanned 16 months, which was comparatively long with respect to AUV and towed video platform survey time, we tested for differences in species richness (total number of species per site) and total number of individuals between years 2009 and 2010 and seasons using analysis of variance (ANOVA). Total number of individuals was  $\ln(x+1)$  transformed to comply with the normality assumption. Species richness and total number of individuals per site were analysed using ANOVA with categorical explanatory variables (factors). Factor 1 (site) was fixed with six levels (Blowhole, Waterfall Bay, O’Hara Bluff, Patch Reef North, Hippolyte Rock North and Hippolyte Rock South) and factor 2 (platform) was fixed with 3 levels (AUV, BUVS, towed video platform). The four most abundant and consistently scored species across platforms were individually analysed using univariate ANOVA or generalised linear models (GLMs) with respect

to platform and site. Prior to analysis, fish counts were tested for normality using the Shapiro-Wilk test ( $p > 0.05$ ) and transformed where appropriate using  $\ln(x + 1)$ . Where data transformation was insufficient to comply with normality assumptions, individual fish species were analysed using GLMs with quasi-Poisson error distribution.

The distribution of relative fish abundances violated general assumptions, such as independent errors, normality and common variance for traditional analyses such as MANOVA. We therefore used permutational multivariate analysis of variance (PERMANOVA), which assumes only that the observation units are exchangeable under a true null hypothesis (Anderson, 2001). PERMANOVA was used to determine whether the three sampling platforms recorded similar or different fish species assemblages. The factorial design included two factors: platform (P) with three levels; AUV, BUVS, towed video and site (S) with six levels; Blow Hole, Waterfall Bay, O'Hara Bluff, Patch Reef North, Hippolyte Rock North and South. Multivariate analyses were based on Bray-Curtis dissimilarities using fourth-root transformed relative abundance data to down-weight abundant and rare species (Clarke and Warwick, 2001). We used the stand-alone MS-DOS version of PERMANOVA with two replicates; two averaged *MaxN* pools of randomly assigned BUVS deployments per site (BUVS), two pools of towed video species abundance data (across depth gradient and along depth contour) and replicate AUV dives per site. Where replications within sites (AUV) were missing, AUV dive tracks were randomly sub-sampled. Before analysis all singletons (species occurred only once) and pelagic species were removed. Pelagic species were absent in the AUV species

list due to the downward looking cameras.

In order to be able to compare platforms with respect to effort, i.e., the time it took to derive at a certain number of species (species richness), for AUV and towed video, we split total deployment time into 45 min sampling intervals. These sampling intervals were identical to BUVS deployment times. Although, towed video platform transects were generally shorter than 45 min, across depth gradient transects and appropriate sub-sections of along depth contour transects were combined and considered replicates for each site (see Fig. 6.1). We generated species accumulation curves using EstimateS, version 8.20 (Colwell, 2006) for each platform based on 45 min sampling intervals to compare efficacy between platforms. Each of the three species accumulation curves was fitted using the Michaelis-Menten equation in the EstimateS software package. Magurran (2004) states that when the empirical species accumulation curve intersects with the one generated by the Michaelis-Menten model, sample size was sufficient and total species richness can now be estimated using a non-parametric method, such as Chao's simple estimator of the absolute number of species in an assemblage (Chao, 1984).

## **6.4 Results**

### **6.4.1 Species richness and total number of individuals**

A total of 62 species and operational taxonomic units (OTU) were identified in the imagery across all platforms. For each individual platform these were: BUVS = 49, AUV = 39 and towed video = 22 (Table 6.1), with a total of 56 species

able to be identified to species level. Finfish, with 52 species found in 34 families, comprised the majority of sightings. The two most species-rich families were Labridae and Monacanthidae each containing six species, followed by Serranidae (4) and Cheilodactylidae (3). Species that were recorded exclusively by the AUV were: *Pavoraja nitida*, *Foetorepus calauropomus*, *Neosebastes scorpaenoides*, *Solegnathus spinosissimus* and *Omegophora armilla* (Table 6.1). Species observed with BUVS and towed video but not with the AUV, excluding singletons, were: *Dinolestes lewini*, *Thyrsites atun*, *Dotalabrus aurantiacus*, *Pictilabrus laticlavus*, *Latris lineata*, *Meuschenia venusta*, *Pempheris multiradiata*, *Parapercis allporti*, *Platycephalus richardsoni*, *Scorpaena papillosa* and *Cephaloscyllium laticeps* (Table 6.1). ANOVA results, testing for differences in species richness and total number of individuals between years 2009 and 2010 and seasons were all non-significant at the 5% level.

Table 6.1: Total abundance of all mobile vertebrates (fishes) and invertebrates recorded by each platform off the Tasman Peninsula, Tasmania, Australia, † indicates cephalopods and ‡ decapods.

Family	Genus	Species	Authority	Common name	AUV	BUVS	TV
Arhynchobatidae	<i>Pavoraja</i>	<i>nitida</i>	(Günther, 1880)	Peacock skate	1	-	-
Callionymidae	<i>Foetorepus</i>	<i>calauropomus</i>	(Richardson, 1844)	Common stinkfish	27	-	-
Carangidae	<i>Trachurus</i>	<i>declivis</i>	(Jenyns, 1841)	Common Jack mackerel	-	1059	535
Centrolophidae	<i>Seriotelella</i>	<i>punctata</i>	(Forster, 1801)	Silver warehou	-	6	-
Cheilodactylidae	<i>Cheilodactylus</i>	<i>spectabilis</i>	(Hutton, 1872)	Banded morwong	6	15	25
Cheilodactylidae	<i>Nemadactylus</i>	<i>macropterus</i>	(Bloch & Schneider, 1801)	Jackass morwong	31	479	51
Cheilodactylidae	<i>Cheilodactylus</i>	<i>nigripes</i>	(Richardson, 1850)	Magpie perch	-	1	-
Congridae	<i>Conger</i>	<i>verreauxi</i>	(Kaup, 1856)	Southern conger	-	1	-
Cyttidae	<i>Cyttus</i>	<i>australis</i>	(Richardson, 1843)	Silver dory	-	23	1
Dinolestidae	<i>Dinolestes</i>	<i>lewini</i>	(Griffith, 1834)	Longfin pike	-	22	-
Diodontidae	<i>Diodon</i>	<i>nithemerus</i>	(Cuvier, 1818)	Globefish	3	2	-
family16	genus16	spp16			6	-	-
family19	genus19	spp19			1	-	-
flounder family	unidentified	unidentified			1	-	-
Gempylidae	<i>Thyrssites</i>	<i>atun</i>	(Euphrasen, 1791)	Barracouta	-	20	-
Gerreidae	<i>Parequula</i>	<i>melbournensis</i>	(Castelnau, 1872)	Silverbelly	-	31	5
Labridae	<i>Dotalabrus</i>	<i>aurantiacus</i>	(Castelnau, 1872)	Castelnau's wrasse	-	2	-
Labridae	<i>Notolabrus</i>	<i>fucicola</i>	(Richardson, 1840)	Purple wrasse	1	24	2
Labridae	<i>Notolabrus</i>	<i>tetricus</i>	(Richardson, 1840)	Blue-throated wrasse	2	104	16
Labridae	<i>Pictilabrus</i>	<i>latioclavius</i>	(Richardson, 1840)	Senator wrasse	-	16	-
Labridae	<i>Pseudolabrus</i>	<i>psittaculus</i>	(Johnston, 1885)	Rosy wrasse	302	669	564
Labridae	<i>Suezichthys</i>	<i>aylingi</i>	(Russel, 1985)	Crimson cleaner wrasse	-	64	6
Latridae	<i>Latridopsis</i>	<i>forsteri</i>	(Castelnau, 1872)	Bastard trumpeter	-	7	5

Table 6.1 – continued from previous page

Family	Genus	Species	Authority	Common name	AUV	BUVS	TV
Latridae	<i>Latris</i>	<i>lineata</i>	(Schneider, 1801)	Striped trumpeter	-	71	-
Loliginidae	<i>Septoteuthis</i>	<i>australis</i>	(Quoy & Gaimard, 1832)	Southern calamari †	5	8	-
Macroramphosidae	<i>Notopogon</i>	<i>endeavouri</i>	(Regan, 1914)	Crested bellowsfish	-	1	-
Molidae	<i>Mola</i>	<i>mola</i>	(Linnaeus, 1758)	Ocean sunfish	-	1	-
Monacanthidae	<i>Acanthaluteres</i>	<i>vittiger</i>	(Castelnau, 1873)	Toothbrush leatherjacket	6	169	-
Monacanthidae	<i>Eubalichthys</i>	<i>mosaicus</i>	(Ramsay & Ogilby, 1886)	Mosaic leatherjacket	1	9	-
Monacanthidae	<i>Meuschenia</i>	<i>scaber</i>	(Forster, 1801)	Velvet leatherjacket	31	157	1
Monacanthidae	<i>Meuschenia</i>	<i>australis</i>	(Donovan, 1824)	Brown-striped leatherjacket	-	27	1
Monacanthidae	<i>Meuschenia</i>	<i>venusta</i>	(Hutchins, 1977)	Stars-and-stripes leatherjacket	-	2	-
Monacanthidae	<i>Thamnaconus</i>	<i>degeni</i>	(Regan, 1903)	Bluefin leatherjacket	1	7	-
Moridae	<i>Lotella</i>	<i>rhacina</i>	(Forster, 1801)	Largetooth beardie	3	5	-
Moridae	<i>Pseudophycis</i>	<i>bachus</i>	(Forster, 1801)	Red cod	29	179	18
Mullidae	<i>Upeneichthys</i>	<i>vlamingii</i>	(Cuvier, 1829)	Bluespotted goatfish	3	6	1
Narcinidae	<i>Narcine</i>	<i>tasmaniensis</i>	(Richardson, 1841)	Tasmanian numbfish	19	-	2
Neosebastidae	<i>Neosebastes</i>	<i>scorpaenoides</i>	(Guichenot, 1867)	Common gurnard perch	10	-	-
Octopodidae	<i>Octopus</i>	<i>kaurua</i>	(Stanks, 1990)	Southern sand octopus †	1	-	-
Octopodidae	<i>Octopus</i>	<i>maorum</i>	(Hutton, 1880)	Maori octopus †	-	-	-
Odacidae	<i>Olisthops</i>	<i>cyanomelas</i>	(Richardson, 1850)	Herring cale	-	1	-
Ostraciidae	<i>Aracana</i>	<i>aurita</i>	(Shaw, 1798)	Shaw's cowfish	68	10	7
Palinuridae	<i>Jasus</i>	<i>edwardsii</i>	(Hutton, 1875)	Southern rock lobster ‡	77	11	-
Parascyllidae	<i>Parascyllium</i>	<i>Parascyllium</i> spp			3	-	-
Pempheridae	<i>Pempheris</i>	<i>multiradiata</i>	(Klunzinger, 1879)	Common bullseye	-	4	-
Pinguipedidae	<i>Parapercis</i>	<i>alporti</i>	(Günther, 1876)	Barred grubfish	64	2	-
Platycephalidae	<i>Platycephalus</i>	<i>richardsoni</i>	(Castelnau, 1872)	Tiger flathead	9	6	1
Pomacentridae	<i>Parna</i>	<i>microlepis</i>	(Günther, 1862)	White-ear	-	2	-
Rajidae	unidentified	unidentified			6	-	-

Table 6.1 – continued from previous page

Family	Genus	Species	Authority	Common name	AUV	BUVS	TV
Scorpaenidae	<i>Scorpaena</i>	<i>papillosa</i>	(Bloch & Schneider, 1801)	Southern red scorpionfish	1	1	-
Scyliorhinidae	<i>Cephaloscyllium</i>	<i>laticeps</i>	(Duméril, 1853)	Draughtboard shark	-	8	-
Scyliorhinidae	<i>Asymbolus</i>	<i>rubiginosus</i>	(Last, Gomon & Gledhill, 1999)	Orange spotted catshark	-	1	-
Sebastidae	<i>Helicolenus</i>	<i>percoides</i>	(Richardson, 1842)	reef ocean perch	1771	156	48
Serranidae	<i>Caesioperca</i>	<i>lepidoptera</i>	(Forster, 1801)	Butterfly perch	1672	1236	4524
Serranidae	<i>Caesioperca</i>	<i>rasor</i>	(Richardson, 1839)	Barber perch	-	72	47
Serranidae	<i>Callanthias</i>	<i>australis</i>	(Ogilby, 1899)	Splendid perch	1	23	-
Serranidae	<i>Hypoplectrodes</i>	<i>maccullochi</i>	(Whitley, 1929)	Halfbanded seaperch	37	4	-
Syngnathidae	<i>Solegnathus</i>	<i>spinosissimus</i>	(Günther, 1870)	Spiny pipehorse	26	-	-
Tetraodontidae	<i>Omegophora</i>	<i>armilla</i>	(Waite & McCulloch, 1915)	Ringed toadfish	2	-	-
Trachichthyidae	<i>Paratrachichthys</i>	<i>macleayi</i>	(Johnston, 1881)	Sandpaper fish	249	18	33
Trigidae	unidentified	unidentified			52	-	-
Urolophidae	<i>Urolophus</i>	<i>cruciatus</i>	(Lacépède, 1804)	Banded stingaree	16	-	1
Total number of species					39	49	22

To ensure that all assumptions underlying analysis of variance were satisfied residuals versus fitted values plots (heteroscedasticity), normal q-q plots (normality), scale-location plots and residuals versus factor levels plots (influential data points) were assessed visually. No pattern emerged in the residuals versus fitted values plot for each analysis (transformed total number of individuals and *C. lepidoptera* and *P. psittaculus* abundance), which attests constancy of variance. Normal q-q plots showed a few data points off the straight line but were generally well behaved, i.e., no obvious patterns such as an S-shape or J-shape could be observed. The remaining plots showed also no signs to question that any of the ANOVA assumptions have not been met. Total number of individuals, *C. lepidoptera* abundance and *P. psittaculus* abundance were  $\log(x + k)$  transformed before analysis to remove zero values (species not present) and to linearise the relationship between response and explanatory variables. Different values of  $k$  were chosen to test whether it had an effect on analysis results. Changing  $k$  to 1, 5, 10 had virtually no effect on the  $p$ -values (small changes in the third decimal place), however, q-q plots revealed that the degree of normality deteriorated with increasing  $k$  values. The site  $\times$  platform interactions for species richness and total number of individuals were non-significant and were therefore removed from the ANOVA models (Table 6.2). After removing the interaction term, species richness in response to site was non-significant ( $p = 0.075$ ) but the transformed total number of individuals in response to site was significant ( $p = 0.028$ ). In response to platform, both species richness and total number of individuals were highly significant ( $p < 0.001$ ) (Table 6.2). Average species richness recorded by the towed video platform was significantly lower than

the remaining platforms (Tukey's test,  $p < 0.001$ ) (Fig. 6.2). With respect to mean total number of individuals, all platforms differed significantly from each other (Tukey's test,  $p_{AUV-BUVS} < 0.001$ ,  $p_{BUVS-TV} < 0.001$ ,  $p_{AUV-TV} = 0.01$ ). Mean total number of individuals also differed between Waterfall Bay and the less numerous site Blowhole (Tukey's test,  $p = 0.008$ ). The towed video platform consistently scored highest average total number of individual counts (Fig. 6.2).

Table 6.2: ANOVA results for untransformed species richness and  $\ln(x + 1)$  transformed total number of individuals in response to site and platform.

Source	df	Total number of individuals			Species richness		
		Mean Sq	F value	Pr (> F)	Mean Sq	F value	Pr (> F)
site	5	0.556	2.619	0.028	11.322	2.064	0.075
platform	2	31.792	149.669	< 0.001	74.661	13.612	< 0.001
Residuals	115	0.212			5.485		

#### 6.4.2 Individual species abundances

The four most abundant and consistently scored species across all platforms were *Caesioperca lepidoptera*, *Pseudolabrus psittaculus*, *Nemadactylus macropterus* and *Helicolenus percooides*. The site  $\times$  platform interaction (ANOVA and GLM) for all four species was non-significant at the 5% level. ANOVA results for mean abundance of *P. psittaculus* and *C. lepidoptera* with respect to sampling platform and site are presented in Table 6.3. Mean *P. psittaculus* abundance was significantly different between platforms AUV and towed video (Tukey's test,  $p < 0.001$ ). Abundances recorded by BUVS and AUV did not differ significantly (Tukey's test,  $p = 0.439$ ). Site Blowhole had significantly lower mean *P. psittaculus* counts compared to all

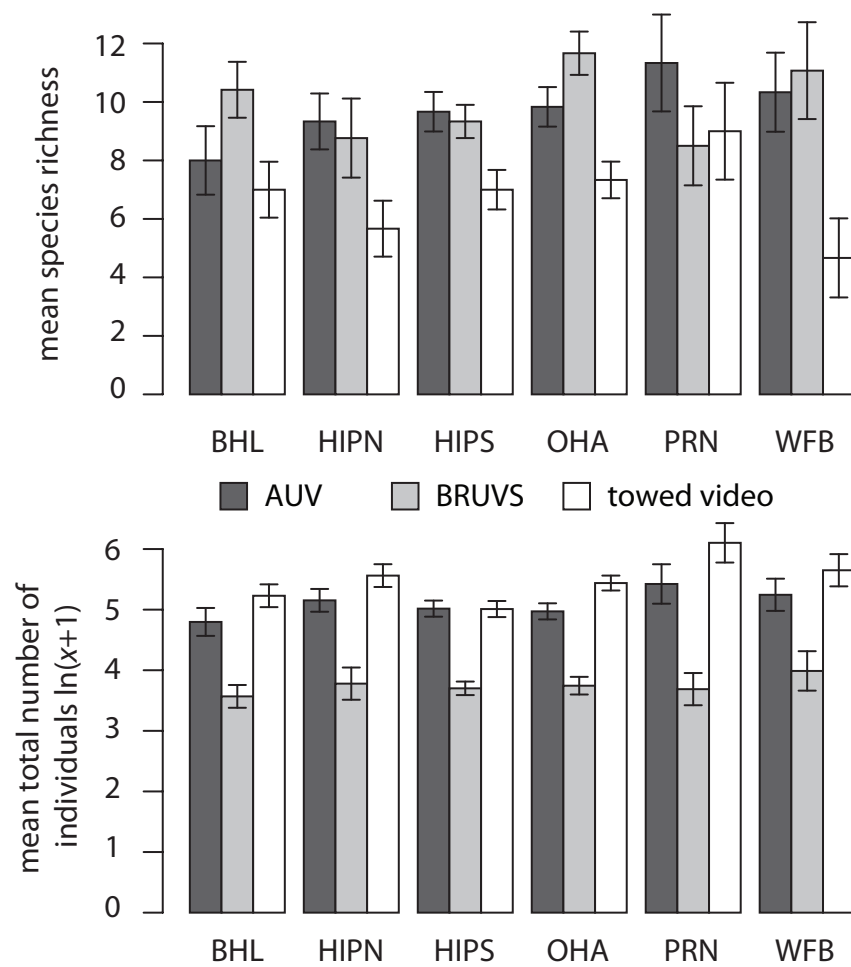


Figure 6.2: Mean species richness (top) and total number of individuals (bottom) at each site for each platform. BHL = Blowhole, HIPN = Hippolyte Rock North, HIPS = Hippolyte Rock South, OHA = O'Hara Bluff, PRN = Patch Reef, WFB = Waterfall Bay. Error bars:  $\pm 1$  SE.

other sites at the 5% level, except site Patch Reef (Tukey's test,  $p = 0.278$ ), see Fig. 6.3. *C. lepidoptera* mean abundance recorded by the AUV was significantly different from both BUVS and towed video at the 5% level (Table 6.3). *C. lepidoptera* mean abundance at site Blowhole was significantly lower than site Waterfall Bay. All other site comparisons were non-significant at the 5% level. BUVS mean abundance records for *C. lepidoptera* were consistently lowest compared to the other two sampling platforms (Fig. 6.3). GLM parameter estimates for untransformed mean abundance of *N. macropterus* and *H. percoides* with regard to sampling platform and site are presented in Table 6.4. Mean *H. percoides* abundance records from the AUV were always exceedingly higher regardless of site (Fig. 6.3), which is reflected in the significant  $p$ -value with regard to the other platforms (Table 6.4). All sites had significantly higher mean *H. percoides* abundances at the 5% level compared to site Blowhole (Fig. 6.3). Site Patch Reef North scored particularly high mean abundances regardless of platform (Fig. 6.3). *N. macropterus* mean abundance was lowest among all four selected species. It was also the only species that was not scored by the AUV in sites Blowhole and Waterfall Bay (Fig. 6.3). *N. macropterus* was, however, recorded in every BUVS deployment. This was also evident in the GLM parameter estimate for BUVS ( $p < 0.001$ ), i.e., mean abundances recorded by BUVS were significantly higher than both other platforms (Table 6.4). Again, site Patch Reef North displayed particularly high mean abundance numbers, though not significant (Fig. 3).

We analysed whether there are differences between fish assemblages recorded by the

Table 6.3: Univariate ANOVA results for *C. lepidoptera* and *P. psittaculus*  $\ln(x+1)$  transformed abundance data in response to site and platform.

Source	df	<i>Caesioperca lepidoptera</i>			<i>Pseudolabrus psittaculus</i>		
		Mean Sq	F value	Pr (> F)	Mean Sq	F value	Pr (> F)
site	5	2.086	2.553	0.031	1.817	5.906	< 0.001
platform	2	101.523	124.274	< 0.001	5.245	17.048	< 0.001
Residuals	115	0.817			0.308		

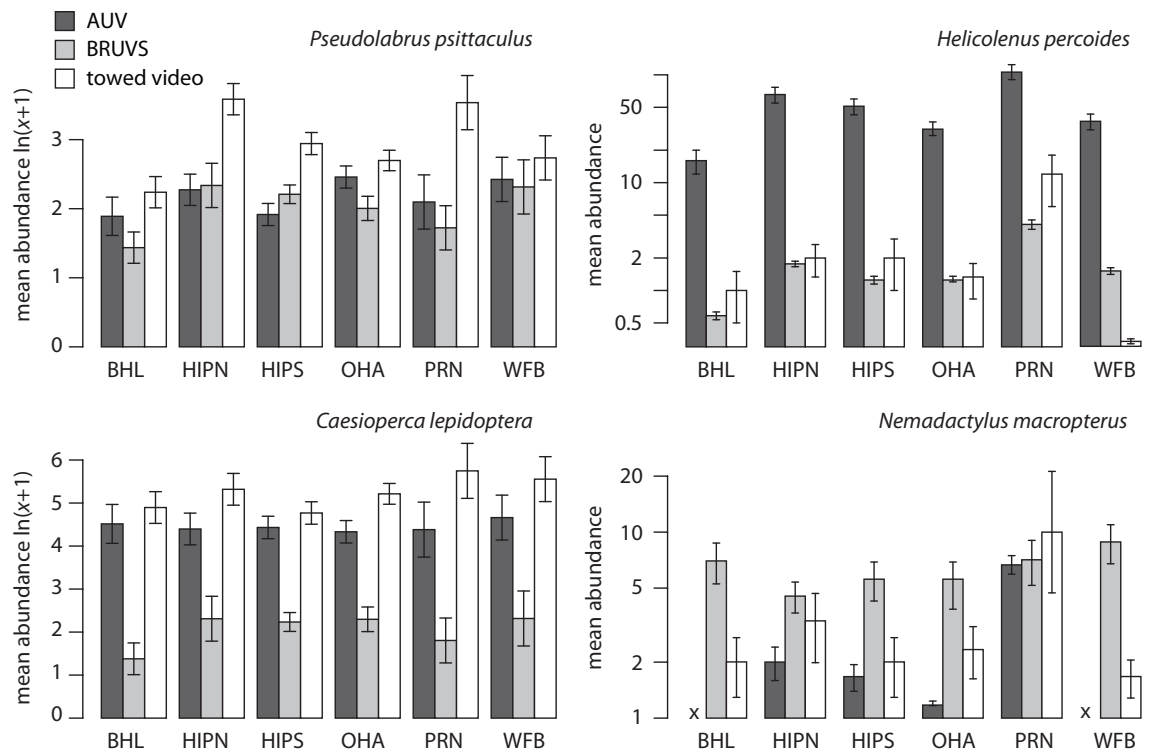


Figure 6.3: Mean ( $\pm 1$  SE) abundance of selected species (genus and species given above bar plot) recorded by each sampling platform (legend top left) and each site. x denotes species not recorded using this platform. BHL = Blowhole, HIPN = Hippolyte Rock North, HIPS = Hippolyte Rock South, OHA = O'Hara Bluff, PRN = Patch Reef North, WFB = Waterfall Bay. Note log scales for *H. percoides* and *N. macropterus* abundances

Table 6.4: GLMs parameter estimates for untransformed *Helicolenus percooides* and *Nemadactylus macropterus* counts. P = platform, S = site, parameter estimates are relative to platform AUV at site Blowhole (BHL), i.e., first line.

Factor	<i>H. percooides</i>				<i>N. macropterus</i>			
	Est	SE	<i>t</i> -value	<i>p</i>	Est	SE	<i>t</i> -value	<i>p</i>
P								
AUV <sup>BHL</sup>	2.785	0.236	11.818	< 0.001	-0.061	0.51	-0.119	0.906
BUVS	-3.405	0.185	-18.458	< 0.001	1.758	0.456	3.854	< 0.001
TV	-2.908	0.318	-9.146	< 0.001	0.918	0.592	1.551	0.124
S								
HIPN	1.373	0.254	5.403	< 0.001	-0.369	0.385	-0.958	0.340
HIPS	1.129	0.260	4.344	< 0.001	-0.218	0.404	-0.541	0.590
OHA	0.667	0.273	2.440	0.016	-0.266	0.406	-0.654	0.514
PRN	1.928	0.256	7.519	< 0.001	0.435	0.361	1.205	0.231
WFB	0.813	0.268	3.033	0.003	0.228	0.350	0.652	0.516

three sampling platforms, sites (locations) and interactions thereof; PERMANOVA results showed significant differences at the species level using relative abundance and presence/absence data (Table 6.5). Non-metric Multi-Dimensional Scaling (nMDS) plots of the Bray-Curtis dissimilarity matrices indicate distinct clusters for each platform indicating that the platforms detected distinct assemblages (Fig. 6.4, Fig. 6.5).

Comparing each of the three platforms, AUV, BUVS and towed video, with respect to total sampling duration, BUVS deployment durations accumulated to 72 hours (96 drops), followed by the AUV with 35 hours (14 dives) and lastly, the towed video platform with 11 hours (19 deployments). Sampling durations do not include travel time between sampling sites, gear loading/unloading or rebaiting.

The three sampling platforms proved to be highly additive with respect to overall

Table 6.5: PERMANOVA results based on Bray-Curtis dissimilarity of fourth-root transformed relative abundance and presence/absence data. The two factors P and S refer to platform and site, respectively.

Source	<i>df</i>	fourth root transformed relative abundance				
		SS	MS	F	<i>p</i> (perm)	<i>p</i> (MC)
P	2	30965.2	15482.6	66.8	0.001	0.001
S	5	8696.7	1739.4	7.5	0.001	0.001
P × S	10	7943	794.3	3.4	0.001	0.001
Residual	18	4173.9	231.9			
Total	35	51778.8				

Source	<i>df</i>	presence/absence				
		SS	MS	F	<i>p</i> (perm)	<i>p</i> (MC)
P	2	26252.5	13126.3	38.2775	0.001	0.001
S	5	7926.9	1585.4	4.6231	0.001	0.001
P × S	10	8593.9	859.4	2.5061	0.001	0.002
Residual	18	6172.6	342.9			
Total	35	48946.1				

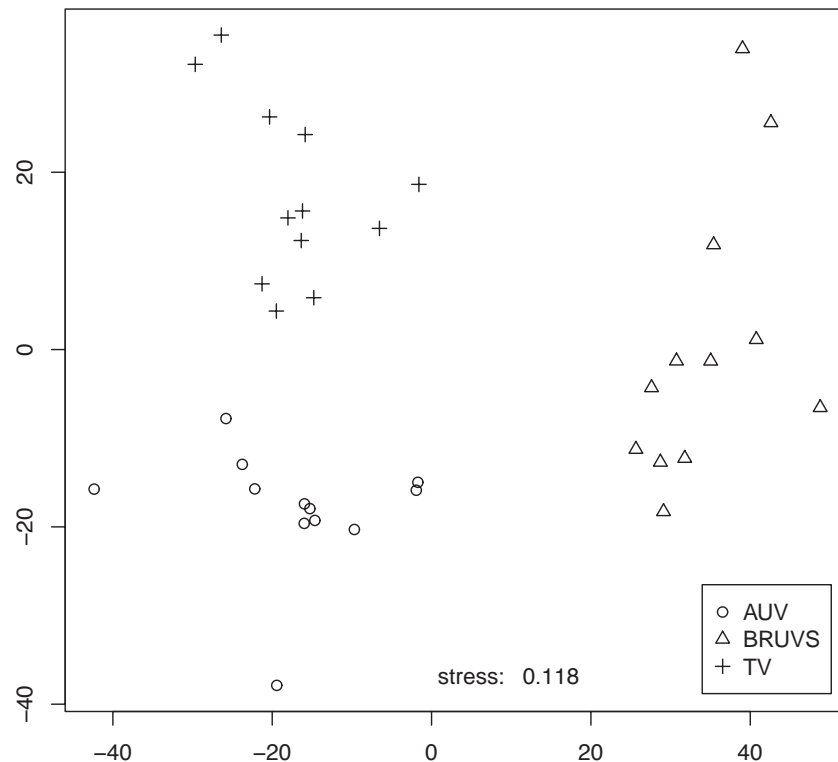


Figure 6.4: 2-dimensional nMDS plot based on fourth-root transformed abundance data of fish species recorded using AUV, BRUVS and towed video.

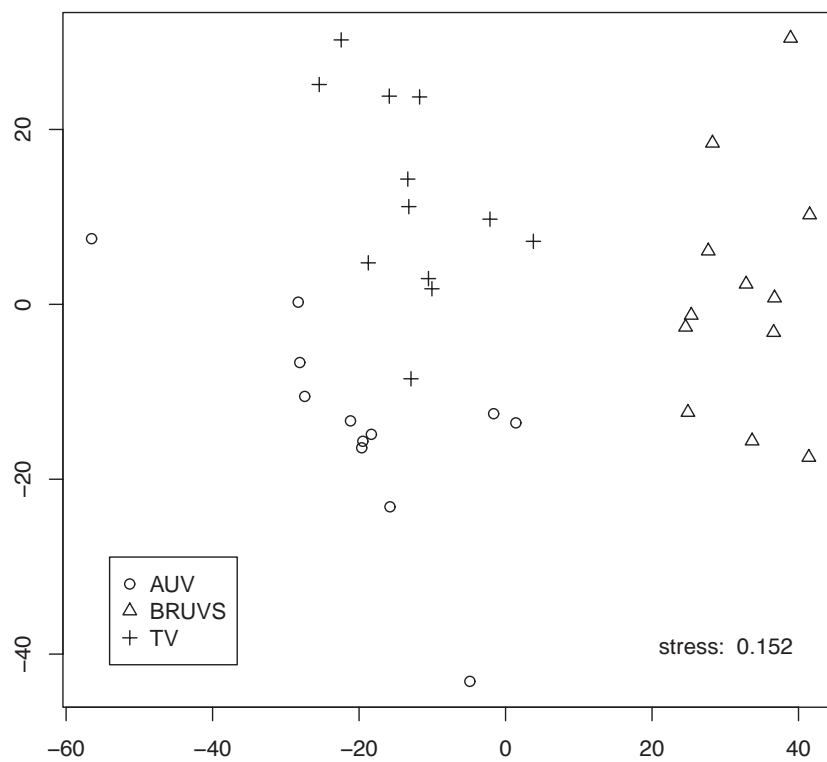


Figure 6.5: 2-dimensional nMDS plot based on presence/absence data of fish species recorded using AUV, BRUVS and towed video.

species composition. Only seven species (*C. lepidoptera*, *N. macropterus*, *C. spectabilis*, *H. percoides*, *P. macleayi*, *P. psittaculus* and *P. bachus*) were recorded by all sampling platforms (19%). Any combination of only two platforms scored fewer species numbers. The percentages of species recorded by one sampling platform and not by the remaining other two were 38% (AUV), 11% (BUVS) and 0% (towed video). The AUV recorded the largest number of species unique to this sampling platform.

We used Magurran (2004)'s rule of thumb to determine whether the sample size was sufficient to confidently estimate the absolute number of species of an assemblage using a non-parametric approach. An intersection between observed species accumulation curve (SAC) and the one generated using the Michaelis-Menten model is a positive indicator of the sample size being sufficiently large. The intersection of both curves therefore can serve as a stopping rule with respect to sampling effort. The intersection (Fig. 4.4) for the BUVS ( $n_{BUVS} = 96$ ) platform was at 87 samples, for the AUV ( $n_{AUV} = 47$ ) platform at 34. There was no intersection for the towed video platform suggesting that the sample size was too small to confidently estimate the absolute number of species. The SAC for the towed video platform showed no indication of an asymptote (Fig. 6.6). This exemplified that the number of samples taken by the towed video platform was insufficient to capture the species composition in our study area. However, Fig. 6.6 also shows that species richness for the towed video platform was slightly higher (22) after 14 deployments than for BUVS (20). Initially the AUV species accumulation curve was steeper than

any of the other curves, indicating that this platform is superior in detecting more species using fewer deployments. However, after about 45 deployments, the AUV curve followed closely the BRUVS curve, implying that these two platforms perform identically. Chao's estimate of absolute number of species for the BRUVS platform was 46 and for the AUV platform 56.

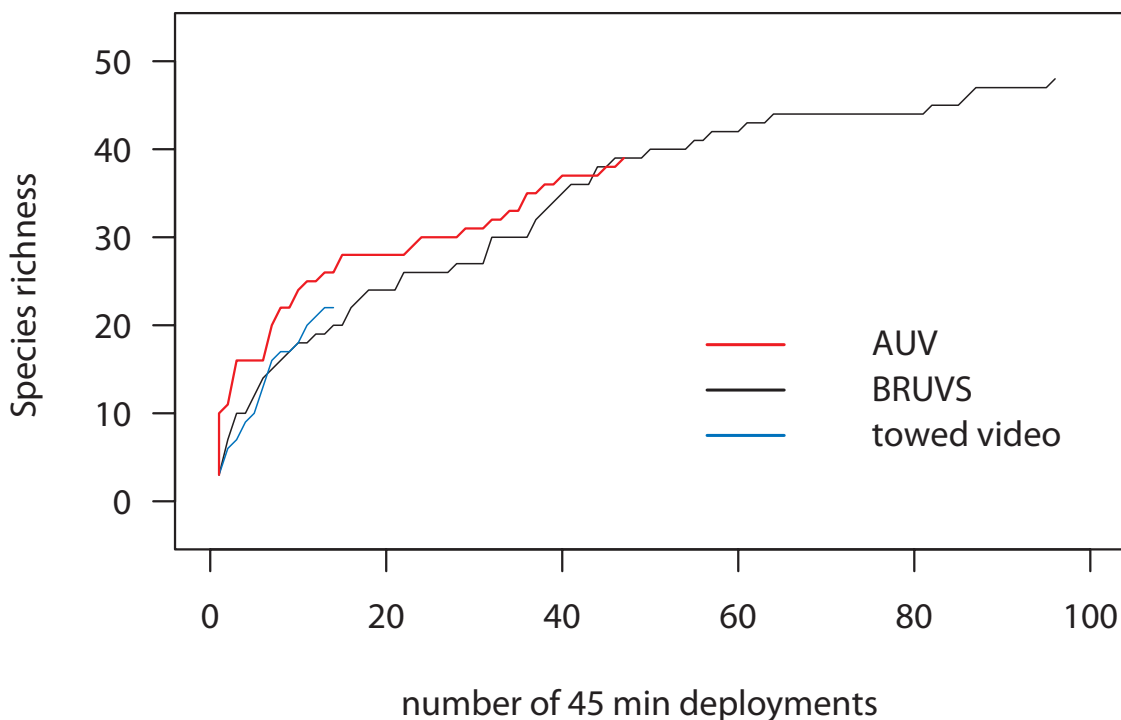


Figure 6.6: Species accumulation curve for 45 min deployments for each platform, i.e., increase in species richness with every additional deployment.

## 6.5 Discussion

This study investigated three different non-extractive, imagery-yielding sampling platforms as survey tools to describe deep-water rocky reef fish assemblages on the continental shelf. Assemblage data collected by each platform were compared with respect to total number of individuals, species richness, individual species

abundances and species accumulation curves. All platforms possess characteristics that are desirable for samplers used in monitoring programs in vulnerable and/or protected marine areas; non-extractiveness, cost-effectiveness and the ability for co-located sampling. AUV and BUVS consistently recorded several ecological key species, such as *Cheilodactylus spectabilis*, *Nemadactylus macropterus* and *Jasus edwardsii*, which emphasises their utility for monitoring MPAs in the SE Tasmanian study area.

### 6.5.1 Platform strengths and weaknesses

Each sampling platform has its strengths and weaknesses. With respect to cost-efficiency, BUVS are most affordable (set of three BUVS units cost ~AU\$15,000, purchasing price) and the AUV is most expensive, AU\$160,000. However, high prices are related to platform sophistication and some technical features are not essential for investigating fish assemblages, i.e., AUV multibeam echosounder. Besides initial platform purchasing price, deployment costs are an important consideration. BUVS can be deployed from relatively small (~ 6 m) vessels (few hundreds of dollars a day). In contrast, AUV and towed video were deployed from a 20 m research vessel (AU\$5,000 a day).

### Platform biases

Platform design-specific bias relates to (i) altered fish behaviour, such as attraction due to bait and/or commotion and avoidance/escape and (ii) species detectability

due to camera orientation and sampling mode (stationary versus mobile). We observed platform bias with regard to species richness, total number of individuals and individual species abundances.

Behavioural changes include, fish being attracted to bait (macrocarnivorous or scavenging species) and concurrent commotion (curious but non-macro-carnivorous or scavenging species), fish avoiding approaching platform (towed video, AUV) and competing for food (bait) or territory. The consequences of using bait are complex and therefore discussed in a separate section below. Attraction to concurrent commotion, increased fish activity around the bait, makes BUVS a versatile sampler able to detect a variety of species from non-macro-carnivorous feeding guilds. Watson et al. (2010) coins this attraction to commotion the “sheep-effect”. This effect was also frequently observed during this study. BUVS can therefore be used to monitor abundant species such as *Caesioperca lepidoptera* which is not attracted to bait directly but to the concurrent commotion.

Koslow et al. (1995) report rapid dispersal of orange roughy (*Hoplostethus atlanticus*) aggregations, avoidance behaviour, when the towed camera platform was approaching. Despite similar platform design, we did not observe any avoidance behaviour using the towed video platform in this study. However, based on the number of benthopelagic species recorded by the AUV compared to numbers recorded by BUVS and towed video, it is a fair assumption that these species were not indifferent to the presence of the AUV. This assumption was confirmed by comparing benthopelagic species numbers, recorded with a forward-looking video camera temporarily attached to the AUV, with those obtained from the downward-

looking AUV camera (unpublished results). The cause for the lack of benthopelagic species in the AUV images is related to species detectability and discussed further below.

Competition for food or territory was observed in *Helicolenus percooides*; this behaviour biased (underestimates) BUVS fish density estimates. For example, *MaxN* records for *H. percooides* never exceeded 4. In contrast, the AUV recorded up to 0.06 individuals per m<sup>2</sup> which is equivalent to  $MaxN = 9$ , assuming a BUVS sample area of 150 m<sup>2</sup> given in Watson et al. (2005).

Species detectability is determined by platform design. A downward-looking camera (AUV) is unlikely to detect pelagics and benthopelagic fish species. In contrast, forward-looking (BUVS) and oblique-looking (towed video) camera designs detect benthic, benthopelagic and pelagic fish species. The AUV recorded the seafloor at an altitude of  $\sim 2$  m with a downward-looking stereo camera. Hence, benthopelagic fish have to be directly underneath the AUV in order to be recorded. However, the detectability of benthic, negatively buoyant species, such as *H. percooides* and *Scorpaena papillosa*, was unaffected by the downward-looking camera design (AUV). These rockfish species seem to be indifferent to the presence of the AUV which was evident in consecutive images of the same individual (usually in 3 overlapping images), where there was no indication of escape behaviour. Stoner et al. (2008) report that of two rockfish species, *Sebastes ruberrimus* did not show escape behaviour towards the sampling platform (submersible *Alvin*) whereas *Sebastes helvomaculatus* showed signs of reduced detection. We attribute observed indifferences to the AUV's slow speed and emphasise that avoidance behaviour is

species specific.

Whereas AUV and towed video are considered line-transect methods, BUVS remain stationary for the entire sampling period. Being stationary excludes territorial species such as *C. spectabilis* if the BUVS unit is dropped outside the home range. Accordingly, this benthopelagic microcarnivore was most often recorded by the mobile towed video system as it traversed several *C. spectabilis* territories.

## **BUVS**

A major strength of BUVS is its ability to actively attract fishes. This way researchers can specifically target certain species, attracted to bait. For example, predatory species such as *Cephaloscyllium laticeps*, *Latris lineata* and *Thyrsites atun* were exclusively scored by BUVS. The BUVS cluster in the nMDS plot is tightest and most distinct, indicating that bait attracts different fish species, i.e., a different component of the entire assemblage. Major disadvantages of BUVS are (i) the relative abundance measure *MaxN* which is underestimating true density and (ii) the unknown sampling area. Conservative estimates of the visible sampling area are based on horizontal field of view, angle of circular section, multiplied by estimated underwater visibility in metres (radius of circular section). However, this estimate ignores the ability of fish to detect bait beyond the perimeter of the visible sampling area. Olfactory detection thresholds vary with species (Kleerekoper, 1969).

## AUV

Two of the AUV's advantages are (i) the unique ability to maintain a virtually constant altitude, equivalent to a consistent image footprint (sampling area) and (ii) precisely geo-referenced images. A consistent image footprint allows for precise fish density measurements (number of individuals per m<sup>2</sup>). Precisely geo-referenced images in conjunction with precise vehicle navigation allow for repeated sampling of the same area of interest. Two disadvantages of the AUV are (i) its inability to detect pelagic and benthopelagic species due to the downward-looking camera and (ii) its relatively slow survey speed, 0.4 m/s.

## Towed video

Towed video platform advantages include fast survey speed and real-time annotation capability. The species accumulation curve for the towed video platform was slightly steeper than the BUVS curve, indicating that the former platform detects more species during fewer deployments. Real-time video footage onboard the support vessel can be annotated simultaneously thereby expediting data acquisition (see Nichol et al. (2009) for details). Two disadvantages include (i) inconsistent sampling area (imagery footprint) due to relatively fast towing speed, hence delayed platform response to altitude adjustments by the winch operator, trying to follow undulating terrain and (ii) low image resolution hindering species identification.

### 6.5.2 To bait, or not to bait

Using bait is an effective way to increase the number of species in a survey (Watson et al., 2010). Willis et al. (2000) report higher abundances using non-extractive (BUVS) and extractive (line fishing) methods compared to UVC with respect to *Pagrus auratus*. Colton and Swearer (2010) found the opposite: number of individual fish was significantly higher using UVC compared to baited underwater video. Both, Willis et al. (2000) and Colton and Swearer (2010), investigated shallow reef environments suitable for UVC using SCUBA techniques. Divers are known to attract some reef fish (Shepherd et al., 2010), that are not attracted to bait. Below safe SCUBA diving depths and without the diver attraction factor, these species might not be consistently sampled using “remote” methods such as AUV or BUVS. Watson et al. (2005) compared reef fish species richness and abundance using baited and unbaited video systems and found that the latter recorded  $> 50\%$  less species. Although, bait improves efficiency of BUVS, it also introduces various factors such as behavioural changes and unknown sampling area (bait plume) that need to be quantified before drawing more robust inferences from BUVS data. For example, the assumptions about bait plume size and dispersal in this study were simplified, however, sufficiently complex for temporal and spatial comparisons. Bait plume size after 45 min (2700 s) deployment time was calculated based on predicted tidal current speed (50th percentile of hourly tidal current speed in m/s, Bureau of Meteorology, National Tidal Centre, resolution:  $0.08^\circ \times 0.08^\circ$ ) for the study area, i.e.,  $0.13 \text{ m/s} * 2700 \text{ s} = 351 \text{ m}$ . A distance of 351 m between replicate

BUVS deployments per site was considered sufficient to obtain independent samples. Treating correlated samples as independent violates assumptions of analysis of variance and inflates  $MaxN$  due to double counting the same individual. Except for sites Patch Reef North, Hippolyte Rock North and Hippolyte Rock South, distances between replicates exceeded 351 m. Due to the small reef complex sizes of the aforementioned three sites some distances between replicates were less than 351 m. In these instances BUVS units were deployed starting with the shallowest location to minimise bait plume overlap between replicates. Pilchard (*Sardinops sagax*), the most commonly used bait using BUVS in Australia has a high oil content that acts as an effective fish attractant. Since the density of (fish) oil is less than the density of seawater oil is likely to travel towards the surface rather than down to affect deeper replicates. At the same time, the effect of deeper replicates on shallower replicates was minimised due to the time difference between BUVS deployments of roughly 10 min (travel time between locations, BUVS preparation and duration of sinking to seafloor, i.e.,  $0.13 \text{ m/s} * 2100 = 273 \text{ m}$ , 78 m less). Although assumptions of the bait plume size after 45 min deployment time is a simplification it is a conservative estimate. For example, adding the swimming speed of a particular species to calculate distance of attraction reduces effective bait plume size since the fish needs to travel to the bait plume source in order to be recorded (see Ellis and DeMartini (1995)). There are two reasons why the fish swimming speed was not included in this study, (1) the lack of basic knowledge (swimming speed for most of the species encountered) and (2) the majority of species recorded are not attracted to bait but rather the commotion caused by the BUVS unit deployment (Watson et al., 2010).

The distance between replicates in this study was sufficient to obtain independent samples since bait plume size after 45 min deployment time is based on laminar flow rather than turbulent flow. Given the complex and rough topography of rocky reefs in this study it is likely that turbulence caused slower bait plume dispersal compared to laminar flow. There are several issues that need to be addressed before BUVS can be used to obtain indices of absolute fish abundance as compared to relative fish abundance (*MaxN*). (1) Bait plume dispersal models in complex terrain such as rocky reefs, (2) current meters (magnitude and direction) and (3) swimming speed and/or home range of target species. Current models that are able to predict residence time of sewage in an estuary are capable of modelling bait plume dispersal (Herzfeld et al., 2010). However, this particle tracking model assumes neutrally buoyant particles (fish oil is positively buoyant), vertical resolution is several meters (some fish are strictly benthic rendering model resolution insufficient) and “building a model is not a trivial task” (personal communication Dr Mike Herzfeld, CSIRO). Current meters, either attached to the BUVS unit (Aanderaa) or independent acoustic Doppler current profiler are both possible ways of obtaining current magnitude and direction but would increase the overheads of BUVS deployments. Finally, home ranges of a few species are available, e.g., *Notolabrus tetricus* (Barrett, 1995; Shepherd and Clarkson, 2001) and swimming speed could be estimated using stereo BUVS footage with the aid of photogrammetry.

### 6.5.3 Dissecting assemblage composition – platform-specific species detection

Non-parametric MDS plots show clearly that each platform detects different components of the assemblage. All platforms detected abundant species such as *C. lepidoptera*, *N. macropterus* and *P. psittaculus*. The assemblage component recorded by the AUV is defined by the lack of benthopelagic species. Benthopelagic species are largely excluded due to the downward-looking camera design (AUV). BUVS sample piscivorous and scavenging species such as *Thyrsites atun*, *Cephaloscyllium laticeps* and *Latris lineata* that were not recorded using both unbaited platforms.

### 6.5.4 Future research

Successful trials with a sideward-looking camera on *SeaBED* (the predecessor of AUV *Sirius*) are reported by Tolimieri et al. (2008). However, a forward-looking camera would lack a defined sampling area.

Currently, the towed video platform lacks a defined sampling area. This is due to the oblique-looking camera and variable altitude which affects image-footprint. Barker et al. (1999) provide a mechanical solution for a positively-buoyant towed video platform to maintain a constant altitude using a drag chain.

High definition video is now widely available. This provides researchers with higher resolution imagery for precision photomosaics, better species identification and video mapping (Kocak et al., 2008). All information, including full resolution HD video, can now be viewed in real-time on the support vessel through fibre optic data cable.

*MaxN*, the de facto relative abundance measure using BUVS, is underestimating true fish abundance (Cappo et al., 2004). A more reliable abundance measure is needed to extent the utility of BUVS with respect to measuring abundance.

### 6.5.5 Concluding remarks

Non-extractive imagery-yielding sampling platforms proved to be useful to investigate deep-water reef fish assemblages. However, some platforms are better suited to accomplish certain objectives. For simply monitoring biodiversity, all platforms are equally suited. More advanced monitoring objectives such as relative abundance per unit area and length estimation, AUV and BUVS are preferable given the stereo camera setup (Williams et al., 2010b). However, Barker et al. (1999) present a towed stereo video platform to assess benthic diversity of the Western Australian continental shelf. During this survey some of the large sponges were photogrammetrically measured using special software (Seager, 2009c). Another example is the use of a stereo video platform that investigated pollock behaviour when encountering trawl gear (Williams et al., 2010b). For the purpose of cataloguing or inventorying fish species for a particular area, we recommend the use of all three platforms since they are highly complementary. Where financial constraints prohibit the use of all three platforms, a combination of AUV and BUVS yields the best outcome with respect to a species inventory.

## Chapter

# 7

## Discussion and conclusion

### 7.1 Summary of achievements

#### 7.1.1 Introduction

This thesis set out to test and evaluate non-extractive sampling platforms to assess deep-water rocky reef ecosystems on the continental shelf, as alternatives to traditional sampling techniques. Alternative sampling techniques are needed as new practises, such as marine protected areas (MPAs), are adopted to manage marine resources sustainably. Most parts of MPAs are protected from extractive resource exploitation methods, including scientific sampling gear. However, there are different zones within some MPAs with different levels of protection, i.e., the Great Barrier Reef Marine Park has a General Use Zone, Habitat Protection Zone, Scientific Research Zone, Preservation Zone, etc. Trawling is prohibited in all zones except the General Use Zone. Therefore, mandatory MPA monitoring programs, to assess management strategy performance, require non-extractive sampling platforms. It is unlikely that one sampling platform will address all management requirements and it is anticipated, that a range of novel samplers will be necessary to achieve management goals. These novel sampling platforms need to meet three requirements, (i) being non-extractive to operate in vulnerable and

protected marine areas, (ii) being free from depth constraints and (iii) providing data quality as good or better than currently used sampling methods for some species such as *Nemadactylus macropterus* and *Notolabrus tetricus*. Results in this thesis reveal that largely all of those requirements are met by the platforms tested.

### **7.1.2 Mapping marine habitats – essential information for sustainable resource management**

Marine habitat mapping serves a variety of management objectives (Cogan et al., 2009), ecological risk assessment (Williams et al., 2011), monitoring of key marine ecosystems (Rees et al., 2007), MPA planning (Barrett et al., 2001; Jordan et al., 2005), coastal development and biodiversity assessment (Great Barrier Reef Marine Park Seabed Biodiversity Project). Continuing decline in fish stocks and degradation of marine environments, exacerbated by anthropogenic requirements for marine ecosystem services (Costanza et al., 1997), led to questioning existing management strategies and the search of a more integrated, ecosystem-based management (EBM) approach (Pitcher et al., 2009). In Australia, EBM has been instigated through legislation, such as Ecologically Sustainable Development (1991) and the Environmental Protection and Biodiversity Conservation Act 1999. Australia has the third largest exclusive economic zone (EEZ), however, only 12.5% have been bathymetrically mapped using sonar equipment (Bax, 2011). However, the EEZ comprises several environmental regions such as the continental shelf, continental shelf break and abyssal plains. Although interpreted bathymetry can serve as a proxy for certain habitat types at a coarse scale with varying degree of uncertainty,

accurate fine-scale habitat maps require the use of geo-referenced seafloor images. Autonomous underwater vehicles (AUV) are an effective means of collecting such images. Image processing is time-consuming and subjective when performed by a human annotator, however, computer vision techniques can curtail processing times, through automation and eliminate subjectivity (Purser et al., 2009). I explored the performance of several computer vision techniques to automatically extract image features and used these features in conjunction with a machine-learning algorithm and a training image set to semi-automatically classify seafloor images into habitat types. Results in chapter 3 suggest, that colour, texture, rugosity and patchiness features automatically extracted from stereo image pairs recorded by an AUV expedite the complex and time-consuming process of image annotation. Classification accuracy was found to be 84% (with a kappa statistic of 0.793) in this study. This exemplifies, that AUVs can effectively sample benthic habitats and the ability of automated data handling techniques to extract and reliably process large volumes of seafloor image data. Although the survey area in this study was relatively small (4.6 km transect, 5.8 km<sup>2</sup>) and targeted a particular reef system and its transition zones to surrounding soft substrates, all methods are flexible and can easily be applied to other continental shelf areas (e.g., coral reefs, seagrass beds) and used by other disciplines, such as seafloor geology. In a monitoring context it is important to know what minimum sample size (area) is required to detect changes in abundance (coverage). Norris et al. (1997) investigated subtidal seagrass coverage in a small cove and required 5.6 km total transect length, 15% of the total cove area (swathe width = 1 m), to detect a 5% change in seagrass cover. For this study

(chapter 3) this minimum required sample area could not be computed due to the lack of a finite survey area (i.e., the available substrate for seagrass to grow in Norris et al. (1997) was bounded by the shoreline and seagrass depth limit).

### **7.1.3 Beyond diver's depth – assessing reef-fish assemblages using baited underwater video systems**

Underwater visual census is commonly used to monitor marine protected areas (Barrett and Buxton, 2002). However, high quality optical surveys are needed to monitor MPAs beyond the range of safe SCUBA diving operations (Singh et al., 2004a). For example, only 6% of the Great Barrier Reef Marine Park can be safely monitored using SCUBA (Cappo et al., 2003). In a Tasmanian context, as of 2012 there are seven Marine Reserves (including Macquarie Island). Three out of these seven are partially below safe SCUBA diving depth (Kent Group, Port Davey and Macquarie Island). These three areas are also the largest reserves. Additional Commonwealth Marine Reserves in Tasmanian waters are larger than all coastal Tasmanian Marine Reserves combined and entirely beyond safe SCUBA diving depths. Within depth ranges encountered on continental shelves, remote or tethered camera platforms are free from depth restrictions. Results in chapter 4 confirm that stereo baited underwater video systems (BUVS) are reliable and effective samplers to assess reef-fish assemblages and some target species beyond safe SCUBA diving depths ( $> 30$  m) (Moore et al., 2009). Statistical power analysis of count data, that are not suitable for traditional power analysis due to non-normality, can be conducted by novel statistical techniques. This novel approach can be used to

determine the required sampling effort to detect changes in relative fish abundance in a monitoring program as well as the effect size, difference in two samples, that can be detected (i.e., can a difference of 10% between samples be detected with the current sampling effort).

#### **7.1.4 Collecting fisheries-independent stock assessment data using a stereo-vision AUV**

Many commercially important fishes and other species with high conservation significance are associated with rocky reef habitat, that is difficult to survey using conventional net-based methods. Although traditional extractive fish stock assessment techniques are widely used there is a trend to use non-extractive techniques that do not remove individuals from the population and do not destruct important habitat such as corals and sponge gardens. Extractive methods are still necessary to obtain otolith data for aging fish, gender determination and gut-content analysis, however, AUV-borne stereo camera systems can provide important small-scale fisheries-independent stock assessment data, such as size frequency distributions, abundance and habitat preferences of benthic fish species, such as *Helicolenus percoides* in Tasmanian waters (chapter 5). These data can be included in a traditional extractive stock assessment using precise densities for different habitats, i.e., rocky reef, adjacent sand, reef edge. However, this approach is only viable if a continuous habitat maps exist. Since trawls are deployed adjacent to reef rather than over rocky reef, AUV derived fish densities over rocky reef can elucidate biases associated with traditional sampling methods. *H. percoides* is mostly bycatch

using trawls. Below safe diving depths there was sparse knowledge of detailed species-habitat associations. My results show that adult *H. percooides* prefer rocky substrates over soft substrates, whereas juveniles prefer soft substrates over hard substrate. Image-based methods in general are well-suited to simultaneously provide additional quantitative measures of benthic habitats, invertebrate fauna and fishery environments.

#### **7.1.5 Observing deep-water temperate rocky reef fish assemblages on the continental shelf using three non-extractive sampling platforms**

My results showed that every platform (BUVS, AUV and towed video) sampled a different component of the reef-fish assemblage. This platform bias highlights the need for a broad range of techniques to comprehensively sample the entire assemblage. Hence, a multi-species monitoring program in a marine management context is most effective when all tested sampling platforms are combined. Measures of platform selectivity (bias) can only be obtained by comparing samples from different platforms, such as during this study. Extensive knowledge of platform biases is essential to guide marine resource managers as to what sampler can provide relevant information with respect to management objectives. For example, BUVS are unsuitable to give density estimates of fish, which, in turn, are necessary to compare two assemblage sizes (e.g., inside and outside an MPA). Several studies have shown that assemblage individuals inside MPAs are significantly larger in size and more numerous compared to adjacent unprotected areas (Barrett et al., 2007;

Willis et al., 2000). Watson et al. (2009) report that size differences can be detected, using stereo BUVS footage, by photogrammetrically measuring fish length, however, assemblage size differences can only be based on relative abundance,  $MaxN$ .  $MaxN$  is the de facto relative (due to unknown sampling area/volume) abundance measure using BUVS and is defined as the maximum number of individuals of species  $x$  in video frame  $y$  for each deployment. In chapter 4 I showed that detecting differences in relative abundance ( $MaxN$ ) between two hypothetical surveys was only feasible for certain species (*N. macropterus* and *N. tetricus*), limited to large differences between surveys ( $> 50\%$ ) and required a relatively high sampling effort ( $> 90$  replicates).

#### **7.1.6 Utilising non-extractive imagery-yielding samplers in an ecosystem-based management context**

This thesis identified the need of alternative sampling platforms, to obtain data that indicate the success or failure of management strategies, that are non-extractive and efficient. To address this need, three potential non-extractive imagery-yielding samplers (BUVS, AUV and towed video) were tested and evaluated during the course of this thesis. Currently, towed video systems are most frequently used to provide qualitative and quantitative data to resource managers. Williams et al. (2011) identified habitat types using underwater imagery collected by a towed video platform to evaluate impacts of fishing on benthic habitats in Australia. This impact assessment forms part of a hierarchical risk assessment framework — the Ecological Risk Assessment for the Effects of Fishing (ERAEF, Williams et al. (2011)). ERAEF is being applied to federally (Australia) managed fisheries as the primary scientific

evaluation tool to assess the risks that bottom-contact fishing gear pose to marine environments (Williams et al., 2011). Ecological risk assessments are mandatory for Commonwealth Fisheries to comply with Australia's environmental legislation (i.e., through the Environmental Protection and Biodiversity Conservation Act 1999).

The second example, in a sustainable resource management context, is the use of a towed video system to collect baseline data of the Huon and Freycinet Commonwealth Marine Reserve (CMR). Both CMRs are part of the National Representative System of Marine Protected Areas (NRSMPA) to ensure the conservation and sustainable use of Australia's marine and estuarine environments (DSEWPC, 2012). Australia aims to realise the establishment of the NRSMPAs by 2012. The towed video system was used to characterise seabed habitats and record distribution and abundance of biological assemblages on deep reefs of south-east Tasmania (Nichol et al. (2009) and this thesis, chapter 6). Williams et al. (2010b) used a towed stereo camera setup to study pollock reactions to trawl gear - an important requirement when assessing gear selectivity. Although BUVS have been used extensively in Australia by the scientific community to investigate reef-fish assemblages, to my knowledge, BUVS remain to be fully incorporated into fisheries management. Compared to extractive fish surveys that have been refined and rigorously tested over several decades, BUVS lack essential quantifiable parameters such as sampling area/volume and bait plume size. However, deep-water BUVS provide complementary data on the vulnerable gulper sharks (Centrophoridae), that are bycatch in the Southern and Eastern Scalefish and Shark Fishery (Alan Williams, CSIRO, personal communication) and were instrumental in assessing coral reef fish

biodiversity in the Great Barrier Reef Marine Park Seabed Biodiversity Project (Australian Institute of Marine Science, 2006).

## 7.2 Future research

### 7.2.1 AUV

#### Spatial autocorrelation

Spatial autocorrelation refers to the degree of dependency between observations. Hence, spatially autocorrelated data violate one of the fundamental assumptions in statistical analysis, independence of observations. Statistical models for line transect sampling and continuous grid data that accommodate spatial autocorrelation are widely available, for example, Hedley and Buckland (2004); Dormann et al. (2007). However, the intersecting AUV mission track (see Fig. 3.1) required to increase positional accuracy of the AUV using the simultaneous localisation and mapping technique creates data inappropriate for both line-transect and continuous data methods. *Sirius* is able to seamlessly photograph areas of up to  $50 \times 50$  m (personal communication Stefan Williams, University of Sydney) and sample using line transects, however, the former is time consuming with respect to a relatively small sampling area *cf* UVC and the latter would introduce 1.5% sensor drift (at the end of an average 5 km transect the AUV could be 75 m off course). If multibeam data are used in conjunction with AUV images to survey reef fish, positional AUV error should be similar to the sonar data resolution. In chapter 5, I treated straight

subsections of the AUV mission tracks as subsamples to determine the degree of spatial dependence between fish occurrences. Due to the lack of currently available appropriate statistical analysis techniques, I had to discard a substantial amount of data, instances where distances between observations (fish occurrences) were spatially dependent. Advanced statistical methods are needed to utilise the entire data set collected by the AUV *Sirius*.

### **Automation routines to expedite imagery annotation**

Extracting quantitative and qualitative data from imagery is the proverbial bottleneck using AUVS, BUVS and towed video platforms. Although chapter 3 describes routines to automatically extract image features such as colour and texture, that are used to classify images into habitat classes, routines that automatically identify species and measure fish lengths are unlikely to emerge in the near future. Variable lighting and fish orientation and background complexity are some of the challenges that face developers of automation routines using field data. However, given the success of automatically identifying species and measuring fish lengths in a controlled laboratory environment (White et al., 2006), it seems feasible that at least some tasks could be automated. How and to what extent available automation routines can be adapted to serve researchers using BUVS, AUVs and towed video platforms remains to be investigated.

### **Real-time image classification**

Currently the AUV is programmed to follow a pre-determined track and will only abort the mission in an emergency situation such as a failed obstacle avoidance manoeuvre. This rigid behaviour is often disadvantageous with respect to a balanced sampling design. For example, chapter 5 describes fish-habitat relationships on temperate rocky reefs. Habitat composition was unknown prior to AUV deployment and the final dataset was unbalanced with respect to habitat type, i.e., unequal sample sizes for habitat types *sand*, *high relief reef* and *Ecklonia* (Table 3.2). This is particularly likely for towed video platforms given the recent upgrade to high definition video cameras (personal communication Alan Williams, CSIRO). An AUV with the ability to classify images into habitat types in real time and make autonomous decisions would be able to continue sampling habitat types, insufficiently sampled, after completion of the pre-determined track.

### **Strength in numbers – AUV fleets**

The “flying” speed of the AUV *Sirius* is relative slow (0.4 m/s), in coastal waters its operation requires 2 – 3 highly trained personnel and a relatively large support vessel (> 12.8 m) with an A-frame or crane including crew (Singh et al., 2004b). Compared to the less sophisticated BUVS, that can be deployed by two people from small boats (~ 6 m), *Sirius* is less efficient at sampling certain components of fish assemblages. However, AUV efficiency could be greatly improved by deploying several smaller AUVs simultaneously. Deploying several AUVs would increase survey speed, require

the same amount of trained personnel and reduce expensive ship time. Currently, the high price of the AUV (\$160,000) is unlikely to promote ownership of several AUVs, however, most of the expensive sensors are unnecessary for ecological monitoring programs. Reducing the number of sensors allows for the design of smaller, lighter, cheaper AUVs that are easier to deploy. However, reduction in weight and size will affect AUV stability in pitch, roll and yaw. An unstable AUV will result in variable image footprint size and the need to rectify images. Future research should concentrate on developing multiple and less expensive AUVs by optimising sensor requirements for each AUV.

### 7.2.2 BUVS

#### *MaxN*

*MaxN*, the conservative de facto relative abundance measure using BUVS is sufficient for biodiversity assessments, e.g., species richness but insufficient to address absolute fish density estimates. Several other relative abundance estimates have been proposed; *mincount* (Gledhill et al., 2005), *Maxsna* (Willis and Babcock, 2000), *MAXNO* (Ellis and DeMartini, 1995) and *npeak* (Priede and Merrett, 1996) using baited imagery-yielding platforms but all are conservative and not absolute abundance estimates. In 2006 Cappelletti et al. (2006) proposed a BUVS index of abundance based on a combination of metrics:

$$\text{BUVS index of abundance} = (\text{mean } MaxN)(n/N)/\text{mean}(t_{arr})$$

where  $n$  = number of individuals per deployment (one replicate),  $N$  = number of individuals per station (all replicates),  $t_{arr}$  = time of first fish arrival in field of view. Six years later, no attempts at investigating the proposed BUVS index of abundance were made, so this provides another area of future research.

### **BUVS sampling area and bait plume**

Accurate density estimates are crucial parameters in managing fish populations. Simplistically, density is the number of individuals per area or volume sampled. The sampling area in single-camera horizontal (forward-looking) BUVS is largely unknown. This lack of knowledge led to the widespread use of *MaxN*, a relative abundance estimate. The advent of stereo-camera BUVS allowed the calculation of the visible sampling volume by photogrammetrically derived x-y-z coordinates. Although an improvement, this approach fails to account for the ability of a fish to sense the bait beyond the perimeter of the visible sampling volume. The use of bait, often criticised to attract predominantly scavenging and predatory fish species (Willis et al., 2000; Watson et al., 2005), provides a greater number of predatory and scavenging fish species without decreasing the number of herbivores or omnivores (Harvey et al., 2007). Harvey et al. (2007) also found that, compared to unbaited video stations, statistical power increases due to a more consistent species composition. If BUVS are to be used as a sampling platform to measure absolute abundance, it is pertinent to be able to define the sampling area or volume. A promising solution could be the combination of acoustic and optical sensors. High-resolution acoustic (sonar) technologies are able to record fish activity beyond the

perimeter of the visible sampling volume (Rose et al., 2005). Another solution to the sampling volume problem is to model bait plume dispersal. However, knowledge of the bait plume is only practical if the olfactory sensitivity of a fish species is known and its foraging strategy (i.e., random walk or counter current search – Vabø et al. (2004)). Research into four areas, combining acoustic and optical sensors, modelling bait plume dispersal in complex terrain, species-specific olfactory sensitivities and foraging strategies would provide benefits to researchers using BUVS.

### 7.2.3 Size selectivity

The propensity of certain fishing gear to select for a certain size range of fishes is known as size selectivity. Using data obtained from size-selective fishing gear to estimate population parameters such as length at age can lead to unreliable results due to the exclusion of fishes smaller than the mesh size. However, several studies to quantify gear selectivity, such as using trouser trawls (Millar and Walsh, 1992) and advanced statistics, such as selection curves using maximum likelihood estimates (Millar, 1992) exist. Apart from mesh size, behavioural traits of certain species can result in size selectivity in fishing gear. For example, Ihde et al. (2006) report that smaller lobster *Jasus edwardsii* do not enter a lobster pot when it is already occupied by a larger female individual. This can lead to overestimating recruitment strength as average length decreases in a population (Ihde et al., 2006). In chapter 4, striking differences between size distributions, obtained by extractive (i.e., line-fishing, trapping and spearfishing) and non-extractive (BUVS) are reported. Mean *Latris lineata* length recorded by BUVS was greater by 190 mm and individuals

smaller than 300 mm were not recorded using BUVS. Although my comparative study showed that extractive sampling methods are biased and this bias needs to be quantified, a mechanical explanation for mean length differences between samplers remains to be found.

### 7.3 Summary

My results show, that several challenges resource management agencies are currently facing, such as effective habitat mapping, non-extractive fisheries-independent benthic reef fish stock and biodiversity assessments can be solved using the methods presented in this thesis. Given the limited detailed knowledge of marine habitat distributions below safe SCUBA diving depths based on imagery and Australia's pledge to sustainable resource management, which includes the habitat level, AUVs, such as *Sirius*, in conjunction with automation routines can significantly curtail processing time to produce habitat maps. Currently, extensive areas of Australia's continental shelf have been mapped using sonar techniques. Bathymetry in conjunction with backscatter analysis is able to provide coarse binomial (hard/soft) sediment distributions (Nichol et al., 2009). Although, *Sirius* is able to produce fine-scale habitat maps, its survey speed and image footprint make it a more efficient tool for ground-truthing multibeam sonar data. These fine-scale habitat maps in conjunction with state-of-the-art acoustic tracking devices will enable researchers to improve our knowledge of species-habitat interactions. For example, Lucieer and Pederson (2008) linked morphometric characterisation of rocky reef with fine-scale movements of the southern rock lobster *Jasus edwardsii*. AUV *Sirius* and the

towed video system described during the course of the thesis are currently used to provide baseline data of the Huon and Freycinet Commonwealth Marine Reserves, which form part of Australia's Representative Network of Marine Protected Areas. With respect to benthic reef fish, AUV imagery is free from sampling gear bias (size selectivity) and AUVs can be deployed over rugged terrain, inaccessible to or impermissible (i.e., inside MPAs) for trawl gear. It is likely that resource managers adopt sophisticated non-extractive sampling techniques (i.e., AUVs, BUVS and towed video) in the future to assess management strategy performance (e.g., whether a catch limit resulted in population recovery). Variation on biodiversity should be monitored using reliable, preferably non-extractive, sampling platforms within a monitoring framework, such as MPAs in Australia. My results showed that BUVS are efficient and reliable samplers to monitor fish biodiversity in deep-water rocky reefs. Although, BUVS have been used to assess fish diversity in the tropics (Cappo et al., 2004; Watson et al., 2009; Langlois et al., 2010), its use in temperate deep-water reef environments is sparse, i.e., Moore et al. (2010). South-eastern Australia, including Tasmania, is one of the fastest warming regions in the southern hemisphere (Ridgway, 2007; Johnson et al., 2011) and it is anticipated that BUVS will be the preferred method of assessing flow-on effects to reef fish communities in this area.

## References

- Alexander, T., Barrett, N., Haddon, M., and G, E., 2009: Relationships between mobile macroinvertebrates and reef structure in a temperate marine reserve. *Marine Ecology Progress Series*, **389**, 31 – 44.
- Allee, W. C., 1931: *Animal aggregations: A Study in General Sociology*. University of Chicago Press, Chicago, IL, USA.
- Allmon, W. D., Jones, D., Aiello, R. L., Gowlett-Holmes, K., and Probert, P. K., 1994: Observations on the biology of *Maoricolpus roseus* (Quoy and Gaimard) (Prosobranchia: Turritellidae) from New Zealand and Tasmania. *Veliger*, **37(3)**, 267 – 279.
- Anderson, M., 2001: A new method for non-parametric multivariate analysis of variance. *Austral Ecology*, **26(1)**, 32 – 46.
- Anderson, M. J., Gorley, R. N., and Clarke, K. R., 2008: *PERMANOVA+ for PRIMER: Guide to Software and Statistical Methods*. PRIMER-E: Plymouth, UK.
- Anderson, M. J., and Willis, T. J., 2003: Canonical analysis of principal coordinates: a useful method of constrained ordination for ecology. *Ecology*, **84(2)**, 511 – 525.
- Anderson, T., Brooke, B., Radke, L., McArthur, M., and Hughes, M., 2009: Mapping and characterising soft sediment habitats, and evaluating physical variables as surrogates of biodiversity in Jervis Bay, NSW. Tech. rep., Geoscience Australia.
- Andrew, N. L., and Mapstone, B. D., 1987: Sampling and the description of spatial pattern in marine ecology. *Oceanography and Marine Biology: An Annual Review*, **25**, 39 – 90.
- Arzoumanian, Z., Holmberg, J., and Norman, B., 2005: An astronomical pattern-matching algorithm for computer-aided identification of whale sharks *Rhincodon typus*. *Journal of Applied Ecology*, **42(6)**, 999 – 1011.

- 
- Assis, J., Narváez, K., and Haroun, R., 2007: Underwater towed video: a useful tool to rapidly assess elasmobranch populations in large marine protected areas. *Journal of Coastal Conservation*, **11**, 153 – 187.
- Babcock, R. C., Shears, N. T., Alcalá, A. C., Barrett, N. S., Edgar, G. J., Lafferty, K. D., McClanahan, T. R., and Russ, G. R., 2010: Decadal trends in marine reserves reveal differential rates of change in direct and indirect effects. *Proceedings of the National Academy of Sciences*, **107(43)**, 18256 – 18261.
- Barker, B. A. J., Helmond, I., J. Bax, N., Williams, A., Davenport, S., and Wadley, V. A., 1999: A vessel-towed camera platform for surveying seafloor habitats of the continental shelf. *Continental Shelf Research*, **19(9)**, 1161 – 1170.
- Barrett, N., and Buxton, C., 2002: Examining underwater visual census techniques for the assessment of population structure and biodiversity in temperate coastal protected areas. Tech. Rep. 11, Tasmanian Aquaculture and Fisheries Institute.
- Barrett, N. S., 1995: *Aspects of the biology and ecology of six temperate reef fishes (Families: Labridae and Monacanthidae)*. Ph.D. thesis, University of Tasmania.
- Barrett, N. S., Edgar, G. J., Buxton, C. D., and Haddon, M., 2007: Changes in fish assemblages following 10 years of protection in Tasmanian marine protected areas. *Journal of Experimental Marine Biology and Ecology*, **345(2)**, 141 – 157.
- Barrett, N. S., Sanderson, J. C., Lawler, M. M., Halley, V., and Jordan, A. R., 2001: Mapping of inshore marine habitats in south-eastern Tasmania for marine protected area planning and marine management. Tech. Rep. 7, Tasmanian Aquaculture and Fisheries Institute.
- Bates, D., and Mächler, M., 2010: lme4: Linear mixed-effects models using Eigen and syntax. R package version 0.999375-35. <http://cran.r-project.org/package=lme4>.
- Bax, N. J., 2011: Marine Biodiversity Hub, Commonwealth Environment Research Facilities, Final report 2007-2010. Report to Department of Sustainability, Environment, Water, Population and Communities. Canberra, Australia. Tech. rep., CERF Marine Biodiversity Hub.
- Bjørnstad, O. N., and Falck, W., 2001: Nonparametric spatial covariance functions: Estimation and testing. *Environmental and Ecological Statistics*, **8(1)**, 53 – 70.
- Breiman, L., 2001: Random forests. *Machine learning*, **45(1)**, 5 – 32.

- Breiman, L., 2002: Manual on setting up, using, and understanding random forests v3.1.
- Breiman, L., Friedman, L. H., Olshen, R. A., and Stone, C. J., 1984: *Classification and regression trees*. Wadsworth International Group, Belmont, CA.
- Brodeur, R. D., 2001: Habitat-specific distribution of Pacific ocean perch (*Sebastes alutus*) in Pribilof Canyon, Bering Sea. *Continental Shelf Research*, **21(3)**, 207.
- Brown, C., Smith, S., Lawton, P., and Anderson, J., 2011: Benthic habitat mapping: A review of progress towards improved understanding of the spatial ecology of the seafloor using acoustic techniques. *Estuarine, Coastal and Shelf Science*, **92(3)**, 502 – 520.
- Buckland, S. T., Anderson, D. R., Burnham, K. P., Laake, J. L., Borchers, D. L., and Thomas, L., 2001: *Introduction to distance sampling: estimating abundance of biological populations*. Oxford University Press, Oxford, UK.
- Cappo, M., Harvey, E., Malcolm, H., and Speare, P., 2003: Aquatic protected areas: what works best and how do we know? J. Beumer, A. Grant, and D. Smith, Eds., *Aquatic protected areas: what works best and how do we know? 2002 World Congress on Aquatic Protected Areas, Cairns, Australia*, Australian Society for Fish Biology, North Beach, WA, Australia, 455 – 464.
- Cappo, M., Harvey, E., and Shortis, M., 2006: Counting and measuring fish with baited video techniques – an overview. *Australian Society for Fish Biology Workshop 2006*, Australian Society for Fish Biology.
- Cappo, M., Speare, P., and De'ath, G., 2004: Comparison of baited remote underwater video stations (BRUVS) and prawn (shrimp) trawls for assessments of fish biodiversity in inter-reefal areas of the Great Barrier Reef Marine Park. *Journal of Experimental Marine Biology and Ecology*, **302(2)**, 123 – 152.
- Chandrapavan, A., Gardner, C., Linnane, A., and Hobday, D., 2009: Colour variation in the southern rock lobster *Jasus edwardsii* and its economic impact on the commercial industry. *New Zealand Journal of Marine and Freshwater Research*, **43(1)**, 537 – 545.
- Chao, A., 1984: Nonparametric estimation of the number of classes in a population. *Scandinavian Journal of Statistics*, **11**, 265 – 270.

- 
- Chatfield, B. S., Van Niel, K. P., Kendrick, G. A., and Harvey, E. S., 2010: Combining environmental gradients to explain and predict the structure of demersal fish distributions. *Journal of Biogeography*, **37(4)**, 593 – 605.
- Chazdon, R. L., Colwell, R. K., Denslow, J. S., and Guariguata, M. R., 1998: Statistical methods for estimating species richness of woody regeneration in primary and secondary rain forests of Northeastern Costa Rica. *Forest biodiversity research, monitoring and modeling: conceptual background and old world case studies*, Man and the Biosphere Series, CIFOR, 285 – 309, Vol. 20.
- Clarke, K. R., and Gorley, R. N., 2006: *PRIMER v6*. PRIMER-E: Plymouth, UK.
- Clarke, K. R., and Warwick, R. M., 2001: Changes in marine communities: an approach to statistical analysis and interpretation. 2nd edition. *PRIMER-E: Plymouth, UK*.
- Cogan, C. B., Todd, B. J., Lawton, P., and Noji, T. T., 2009: The role of marine habitat mapping in ecosystem-based management. *ICES Journal of Marine Science: Journal du Conseil*, **66(9)**, 2033 – 2042.
- Colton, M. A., and Swearer, S. E., 2010: A comparison of two survey methods: differences between underwater visual census and baited remote underwater video. *Marine Ecology Progress Series*, **400**, 19 – 36.
- Colwell, R. K., 2006: EstimateS: Statistical estimation of species richness and shared species from samples. Version 8.
- Copeland, A., Edinger, E., Devillers, R., Bell, T., LeBlanc, P., and Wroblewski, J., 2011: Marine habitat mapping in support of Marine Protected Area management in a subarctic fjord: Gilbert Bay, Labrador, Canada. *Journal of Coastal Conservation*, **online**, 1 – 13.
- Costanza, R., D'Arge, R., Rudolf, D. G., Farber, S., Grasso, M., Hannon, B., Limburg, K., Naeem, S., O'Neill, R. V., Paruelo, J., Raskin, R. G., Sutton, P., and Van den Belt, M., 1997: The value of the world's ecosystem services and natural capital. *Nature*, **387**, 253 – 260.
- Courchamp, F., Berec, L., and Gascoigne, J., 2008: Allee effects in ecology and conservation. *Environmental Conservation*, **36(1)**, 80 – 85.
- Crawley, M. J., Ed., 2007: *The R Book*. John Wiley & Sons Ltd, Chichester, England.

- Crossland, J., 1976: Fish trapping experiments in northern New Zealand waters. *New Zealand Journal of Marine and Freshwater Research*, **10(3)**, 511 – 516.
- Curley, B. G., Kingsford, M. J., and Gillanders, B. M., 2002: Spatial and habitat-related patterns of temperate reef fish assemblages: implications for the design of Marine Protected Areas. *Marine and Freshwater Research*, **53**, 1197 – 1210.
- Denny, C., Willis, T., and Babcock, R., 2003: Effects of Poor Knights Islands Marine Reserve on demersal fish populations. DOC Science Internal Series 142. Tech. rep., Department of Conservation, Wellington.
- Diaz, R. J., Solan, M., and Valente, R. M., 2004: A review of approaches for classifying benthic habitats and evaluating habitat quality. *Journal of Environmental Management*, **73(3)**, 165 – 181.
- Dikau, R., 1988: The application of a digital relief model to landform analysis in geomorphology - three dimensional applications in geographical information systems. *GIS Symposium - Integrating Technology and Geoscience Applications*, United States Geological Survey, 51 – 77.
- Dormann, C. F., McPherson, J. M., Araújo, M. B., Bivand, R., Bolliger, J., Carl, G., Davies, R. G., Hirzel, A., Jetz, W., and Kissling, D. W., 2007: Methods to account for spatial autocorrelation in the analysis of species distributional data: a review. *Ecography*, **30(5)**, 609 – 628.
- DPIWE, 2000: Tasmanian marine protected areas strategy: Background report. Tech. rep., Department of Primary Industries, Water and Environment Tasmania.
- DSEWPC, 2012: National Representative System of Marine Protected Areas, Australian Government, Department of Sustainability, Environment, Water, Population and Communities. <http://www.environment.gov.au>, accessed 25 May 2012.
- Edgar, G., 1997: *Australian Marine Life*. Reed Books.
- Edgar, G. J., and Barrett, N. S., 1997: Short term monitoring of biotic change in Tasmanian marine reserves. *Journal of Experimental Marine Biology and Ecology*, **213(2)**, 261 – 279.
- Edgar, G. J., Barrett, N. S., and Morton, A. J., 2004: Biases associated with the use of underwater visual census techniques to quantify the density and size-structure

- 
- of fish populations. *Journal of Experimental Marine Biology and Ecology*, **308**(2), 269 – 290.
- Ellis, D. M., and DeMartini, E. E., 1995: Evaluation of a video camera technique for indexing abundances of juvenile pink snapper, *Pristipomoides filamentosus*, and other Hawaiian insular shelf fishes. *Fishery Bulletin*, **93**(1), 67 – 77.
- Fabricius, K., DeMath, G., McCook, L., Turak, E., and Williams, D., 2005: Changes in algal, coral and fish assemblages along water quality gradients on the inshore Great Barrier Reef. *Marine Pollution Bulletin*, **51**(1), 384 – 398.
- FAO, 2010: The state of world fisheries and aquaculture 2008. Tech. rep., Food and Agriculture Organization of the United Nations.
- Fernandes, P. G., Brierley, A. S., Simmonds, E. J., Millard, N. W., McPhail, S. D., Armstrong, F., Stevenson, P., and Squires, M., 2000: Oceanography: Fish do not avoid survey vessels. *Nature*, **404**(6773), 35 – 36.
- Friedman, A., 2010: Rugosity, slope and aspect derived from bathymetric stereo image 3D reconstructions. Ocean Engineering Society Poster Competition.
- Friedman, A., Pizarro, O., Williams, S. B., and Johnson-Roberson, M., 2012: Multi-scale measures of rugosity, slope and aspect from benthic stereo image reconstructions. *PLoS ONE*, **7**(12), e50440.
- Galparsoro, I., Borja, Á., Bald, J., Liria, P., and Chust, G., 2009: Predicting suitable habitat for the European lobster (*Homarus gammarus*), on the Basque continental shelf (Bay of Biscay), using Ecological-Niche Factor Analysis. *Ecological modelling*, **220**(4), 556 – 567.
- Garcia, S. M., Zerbi, A., Aliaume, C., Do Chi, T., and Lassere, G., 2003: The ecosystem approach to fisheries: issues, terminology, principles, institutional foundations, implementation and outlook. *FAO fisheries technical paper 443*.
- Gledhill, C. T., Ingram, G. W., Rademacher, K. R., Felts, P., and Trigg, B., 2005: SEDAR10-DW12 NOAA Fisheries Reef Fish Video Surveys: Yearly indices of abundance for Gag (*Mycteroperca microlepis*). 28pp. Tech. rep., NOAA.
- Gobi, A., 2010: Towards generalized benthic species recognition and quantification using computer vision. *OCEANS 2010 IEEE - Sydney*, 1 – 6.
- Gomon, M., Bray, D., and Kuiter, R., 2008: *Fishes of Australia's Southern Coast*. Reed New Holland.

- Greene, H. G., Yoklavich, M. M., Sullivan, D. E., and Cailliet, G. M., 1995: A geophysical approach to classifying marine benthic habitats: Monterey bay as a model. *Applications of sidescan sonar and laser-line systems in fisheries research*, Alaska Department of Fish and Game Special Publication 9, 15 – 30, Juneau, Alaska.
- Gwet, K., 2001: *Statistical tables for inter-rater agreement*. STATAXIS Publishing Company, 170 pp.
- Halpern, B., Walbridge, S., Selkoe, K., Kappel, C., Micheli, F., D'Agrosa, C., Bruno, J., Casey, K., Ebert, C., Fox, H., et al., 2008: A global map of human impact on marine ecosystems. *Science*, **319(5865)**, 948 – 952.
- Harris, B. P., and Stokesbury, K. D. E., 2006: Shell growth of sea scallops (*Placopecten magellanicus*) in the southern and northern Great South Channel, USA. *ICES Journal of Marine Science: Journal du Conseil*, **63(5)**, 811 – 821.
- Harris, P., Heap, A., Passlow, V., Sbaffi, L., Fellows, M., Porter-Smith, R., Buchanan, C., and Daniell, J., 2003: Geomorphic features of the continental margin of Australia. Tech. rep., Geoscience Australia.
- Harvey, C. J., Tolimieri, N., and Levin, P. S., 2006: Changes in body size, abundance, and energy allocation in rockfish assemblages of the northeast Pacific. *Ecological Applications*, **16(4)**, 1502 – 1515.
- Harvey, E., Cappo, M., Butler, J., Hall, N., and Kendrick, G., 2007: Bait attraction affects the performance of remote underwater video stations in assessment of demersal fish community structure. *Marine Ecology Progress Series*, **350**, 245 – 254.
- Harvey, E., Cappo, M., Shortis, M., Robson, S., Buchanan, J., and Speare, P., 2003: The accuracy and precision of underwater measurements of length and maximum body depth of southern bluefin tuna (*Thunnus maccoyii*) with a stereo-video camera system. *Fisheries Research*, **63(3)**, 315 – 326.
- Harvey, E., Fletcher, D., and Shortis, M., 2001: Improving the statistical power of length estimates of reef fish: a comparison of estimates determined visually by divers with estimates produced by a stereo-video system. *Fishery Bulletin - NOAA*, **99(1)**, 72 – 80.
- Harvey, E., Fletcher, D., and Shortis, M., 2002: Estimation of reef fish length by divers and by stereo-video: A first comparison of the accuracy and precision in

- 
- the field on living fish under operational conditions. *Fisheries Research*, **57(3)**, 255 – 265.
- Harvey, E., and Shortis, M., 1996: A system for stereo-video measurement of subtidal organisms. *Marine Technology Society Journal*, **29(4)**, 10 – 22.
- Hasan, R., Ierodiaconou, D., and Monk, J., 2012: Evaluation of four supervised learning methods for benthic habitat mapping using backscatter from multi-beam sonar. *Remote Sensing*, **4(11)**, 3427 – 3443.
- Hedley, S. L., and Buckland, S. T., 2004: Spatial models for line transect sampling. *Journal of Agricultural, Biological, and Environmental Statistics*, **9**, 181 – 199.
- Herzfeld, M., Andrewartha, J., and Sakov, P., 2010: Modelling the physical oceanography of the D'Entrecasteaux Channel and the Huon Estuary, south-eastern Tasmania. *Marine and Freshwater Research*, **61**, 568 – 586.
- Hickford, M. J. H., and Schiel, D. R., 1996: Gillnetting in southern New Zealand: duration effects of sets and entanglement modes of fish. *Fishery Bulletin*, **94(4)**, 669 – 677.
- Hilborn, R., and Walters, C. J., 1992: Quantitative fisheries stock assessment: choice, dynamics, and uncertainty. *Reviews in Fish Biology and Fisheries*, **2**, 177 – 178.
- Hobday, A. J., Smith, A. D. M., Stobutzki, I. C., Bulman, C., Daley, R., Dambacher, J. M., Deng, R. A., Dowdney, J., Fuller, M., Furlani, D., Griffiths, S. P., Johnson, D., Kenyon, R., Knuckey, I. A., Ling, S. D., Pitcher, R., Sainsbury, K. J., Sporcic, M., Smith, T., Turnbull, C., Walker, T. I., Wayte, S. E., Webb, H., Williams, A., Wise, B. S., and Zhou, S., 2011: Ecological risk assessment for the effects of fishing. *Fisheries Research*, **108(2-3)**, 372 – 384.
- Holmes, K. W., Van Niel, K. P., Radford, B., Kendrick, G. A., and Grove, S. L., 2008: Modelling distribution of marine benthos from hydroacoustics and underwater video. *Continental Shelf Research*, **28(14)**, 1800 – 1810.
- Hyndes, G. A., Platell, M. E., Potter, I. C., and Lenanton, R. C. J., 1999: Does the composition of the demersal fish assemblages in temperate coastal waters change with depth and undergo consistent seasonal changes? *Marine Biology*, **134**, 335 – 352.

- Ierodionou, D., Laurenson, L., Burq, S., and Reston, M., 2007: Marine benthic habitat mapping using multibeam data, georeferenced video and image classification techniques in victoria, australia. *Journal of spatial science*, **52(1)**, 93–104.
- Ihde, T. F., Frusher, S. D., and Hoenig, J. M., 2006: Do large rock lobsters inhibit smaller ones from entering traps? A field experiment. *Marine and Freshwater Research*, **57(7)**, 665 – 674.
- IMOS, 2011: The governance framework for the integrated marine observing system.
- Jenness, J. S., 2004: Calculating landscape surface area from digital elevation models. *Wildlife Society Bulletin*, **32(3)**, 829 – 839.
- Jensen, J. R., 2004: *Introductory Digital Image Processing*, vol. 1. Pearson Prentice Hall, 3rd edition, New Jersey.
- Johnson, C. R., Banks, S. C., Barrett, N. S., Cazassus, F., Dunstan, P. K., Edgar, G. J., Frusher, S. D., Gardner, C., Haddon, M., Helidoniotis, F., Hill, K. L., Holbrook, N. J., Hosie, G. W., Last, P. R., Ling, S. D., Melbourne-Thomas, J., Miller, K., Pecl, G. T., Richardson, A. J., Ridgway, K. R., Rintoul, S. R., Ritz, D. A., Ross, D. J., Sanderson, J. C., Shepherd, S. A., Slotwinski, A., Swadling, K. M., and Taw, N., 2011: Climate change cascades: Shifts in oceanography, species' ranges and subtidal marine community dynamics in eastern tasmania. *Journal of Experimental Marine Biology and Ecology*, **400(1-2)**, 17 – 32.
- Johnson, S. W., Murphy, M. L., and Csepp, D. J., 2003: Distribution, habitat, and behavior of rockfishes, *Sebastes* spp., in nearshore waters of southeastern Alaska: observations from a remotely operated vehicle. *Environmental Biology of Fishes*, **66(3)**, 259 – 270.
- Jordan, A., Lawler, M., Halley, V., and Barrett, N., 2005: Seabed habitat mapping in the kent group of islands and its role in marine protected area planning. *Aquatic Conservation: Marine and Freshwater Ecosystems*, **15(1)**, 51 – 70.
- Kingsford, M., and Battershill, C., 1998: *Studying temperate marine environments: a handbook for ecologists*, vol. 1. Canterbury University Press, Christchurch, New Zealand.
- Kingsford, M. J., 1989: Distribution patterns of planktivorous reef fish along the coast of northeastern new zealand. *Marine Ecology Progress Series*, **54(1)**, 13–24.

- Kleerekoper, H., 1969: *Olfaction in fishes*. Indiana University Press.
- Kocak, D., Dalgleish, F., Caimi, F., and Schechner, Y., 2008: A focus on recent developments and trends in underwater imaging. *Marine Technology Society Journal*, **42(1)**, 52 – 67.
- Koslow, J. A., Kloser, R., and Stanley, C. A., 1995: Avoidance of a camera system by a deepwater fish, the orange roughy (*Hoplostethus atlanticus*). *Deep Sea Research Part I: Oceanographic Research Papers*, **42(2)**, 233 – 244.
- Kostylev, V. E., Todd, B. J., Fader, G. B. J., Courtney, R. C., Cameron, G. D. M., and Pickrill, R. A., 2001: Benthic habitat mapping on the Scotian shelf based on multibeam bathymetry, surficial geology and sea floor photographs. *Marine Ecology Progress Series*, **219**, 121 – 137.
- Landis, J. R., and Koch, G. G., 1977: The measurement of observer agreement for categorical data. *Biometrics*, **33(1)**, 159 – 174.
- Langlois, T., Harvey, E., Fitzpatrick, B., Meeuwig, J., Shedrawi, G., and Watson, D., 2010: Cost-efficient sampling of fish assemblages: comparison of baited video stations and diver video transects. *Aquatic Biology*, **9**, 155–168.
- Lauth, R. R., McEntire, S. W., and Zenger, H., 2007: Geographic distribution, depth range, and description of Atka mackerel *Pleurogrammus monopterygius* nesting habitat in Alaska. *Alaska Fishery Research Bulletin*, **12(2)**, 165 – 186.
- Legendre, P., 1993: Spatial autocorrelation: Trouble or new paradigm? *Ecology*, **74(6)**, 1659 – 1673.
- Liaw, A., and Wiener, M., 2002: Classification and Regression by randomForest. *R News*, **2(3)**, 18 – 22.
- Ling, S. D., Johnson, C. R., Frusher, S. D., and Ridgway, K. R., 2009: Overfishing reduces resilience of kelp beds to climate-driven catastrophic phase shift. *Proceedings of the National Academy of Sciences*, **106(52)**, 22341 – 22345.
- Lucieer, V., and Pederson, H., 2008: Linking morphometric characterisation of rocky reef with fine scale lobster movement. *ISPRS Journal of Photogrammetry and Remote Sensing*, **63(5)**, 496 – 509.
- Lyle, J. M., and Hodgson, K., 2001: Tasmanian scalefish fishery assessment - 2000. Tech. rep., Tasmanian Aquaculture and Fisheries Institute.

- Lyle, J. M., and Jordan, A. R., 1999: Tasmanian scalefish fishery assessment – 1998. Tech. rep., Tasmanian Aquaculture and Fisheries Institute.
- MacArthur, R., and Wilson, E., 1967: *The theory of island biogeography*, vol. 1. Princeton University Press.
- MacLeod, N., Benfield, M., and Culverhouse, P., 2010: Time to automate identification. *Nature*, **467(7312)**, 154 – 155.
- Magurran, A. E., 2004: *Measuring Biological Diversity*. Blackwell Science Ltd.
- Malcolm, H., Gladstone, W., Lindfield, S., Wraith, J., and Lynch, T., 2007: Spatial and temporal variation in reef fish assemblages of marine parks in New South Wales, Australia-baited video observations. *Marine Ecology Progress Series*, **350**, 277 – 290.
- Mandelbrot, B., 1967: How long is the coast of Britain? Statistical self-similarity and fractional dimension. *Science*, **156(3775)**, 636 – 638.
- Millar, R. B., 1992: Estimating the size-selectivity of fishing gear by conditioning on the total catch. *Journal of the American Statistical Association*, **87(420)**, 962 – 968.
- Millar, R. B., and Walsh, S. J., 1992: Analysis of trawl selectivity studies with an application to trouser trawls. *Fisheries Research*, **13(3)**, 205 – 220.
- Min, R., and Cheng, H. D., 2009: Effective image retrieval using dominant color descriptor and fuzzy support vector machine. *Pattern Recognition*, **42**, 147 – 157.
- Monk, J., Ierodiaconou, D., Versace, V., Bellgrove, A., Harvey, E., Rattray, A., Laurenson, L., and Quinn, G., 2010: Habitat suitability for marine fishes using presence-only modelling and multibeam sonar. *Marine Ecology Progress Series*, **420**, 157 – 174.
- Moore, C. H., Harvey, E. S., and Van Niel, K. P., 2009: Spatial prediction of demersal fish distributions: enhancing our understanding of species-environment relationships. *ICES Journal of Marine Science*, **66**, 2068 – 2075.
- Moore, C. H., Harvey, E. S., and Van Niel, K. P., 2010: The application of predicted habitat models to investigate the spatial ecology of demersal fish assemblages. *Marine Biology*, **157**, 2717 – 2729.

- 
- Murawski, S. A., 2007: Ten myths concerning ecosystem approaches to marine resource management. *Marine Policy*, **31(6)**, 681 – 690.
- Nichol, S., Anderson, M., McArthur, M., Barrett, N., Heap, A. D., Siwabessy, P. J. W., and Brooke, B., 2009: Southeast Tasmanian temperate reef survey, post-survey report. Tech. Rep. Record 2009/43, Geoscience Australia, GPO Box 378, Canberra ACT 2601, Australia.
- Norris, J. G., Wyllie-Echeverria, S., Mumford, T., Bailey, A., and Turner, T., 1997: Estimating basal area coverage of subtidal seagrass beds using underwater videography. *Aquatic Botany*, **58**, 269 – 287.
- Norton, T., 2000: *Stars Beneath The Sea: The Incredible Story of the Pioneers of the Deep Sea*. Arrow, 288 pp.
- Ojala, T., Pietikäinen, M., and Mäenpää, T., 2002: Multiresolution gray-scale and rotation invariant texture classification with local binary patterns. *IEEE Transactions on Pattern Analysis and Machine Intelligence*, **24**, 971 – 987.
- Pal, M., and Mather, P. M., 2003: An assessment of the effectiveness of decision tree methods for land cover classification. *Remote sensing of environment*, **86(4)**, 554 – 565.
- Park, T. J., 1993: *A comparison of the morphology, growth and reproductive biology of two colour forms of ocean perch (Helicolenus percoides), NSW, Australia*. MSc thesis, University of Sydney.
- Pearcy, W. G., Stein, D. L., Hixon, M. A., Pikitch, E. K., Barss, W. H., and Starr, R. M., 1989: Submersible observations of deep-reef fishes of Heceta Bank, Oregon. *Fishery Bulletin*, **87(4)**, 955 – 965.
- Piepenburg, D., and Schmid, M. K., 1997: A photographic survey of the epibenthic megafauna of the Arctic Laptev Sea shelf: distribution, abundance, and estimates of biomass and organic carbon demand. *Marine Ecology Progress Series*, **147(1)**, 63 – 75.
- Pikitch, E., Santora, C., Babcock, E., Bakun, A., Bonfil, R., Conover, D., Dayton, P., Doukakis, P., Fluharty, D., Heneman, B., et al., 2004: Ecosystem-based fishery management. *Science*, **305(5682)**, 346 – 347.
- Pinheiro, J., Bates, D., DebRoy, S., Sarkar, D., and team, R. C., 2009: nlme: Linear and nonlinear mixed effects models, r package version 3.1-96.

- Pitcher, T., Kalikoski, D., Short, K., Varkey, D., and Pramod, G., 2009: An evaluation of progress in implementing ecosystem-based management of fisheries in 33 countries. *Marine Policy*, **33(2)**, 223 – 232.
- Poore, G., McCallum, A., and Taylor, J., 2008: Decapod crustacea of the continental margin of southwestern and central Western Australia: preliminary identifications of 524 species from FRV Southern Surveyor voyage SS10-2005. Tech. rep., Museum Victoria.
- Priede, I. G., and Merrett, N. R., 1996: Estimation of abundance of abyssal demersal fishes; a comparison of data from trawls and baited cameras. *Journal of Fish Biology*, **49**, 207 – 216.
- Purser, A., Bergmann, M., Lundälv, T., Ontrup, J., and Nattkemper, T. W., 2009: Use of machine-learning algorithms for the automated detection of cold-water coral habitats: a pilot study. *Marine Ecology Progress Series*, **397**, 241 – 251.
- R-Development-Core-Team, 2009: *R: A Language and Environment for Statistical Computing*. R Foundation for Statistical Computing, Vienna, Austria.
- Ralston, S., Gooding, R. M., and Ludwig, G. M., 1986: An ecological survey and comparison of bottom fish resource assessments (submersible versus handline fishing) at Johnston Atoll. *Fishery Bulletin*, **84(1)**, 141 – 156.
- Rattray, A., Ierodiaconou, D., Laurenson, L., Burq, S., and Reston, M., 2009: Hydro-acoustic remote sensing of benthic biological communities on the shallow South East Australian continental shelf. *Estuarine, Coastal and Shelf Science*, **84(2)**, 237 – 245.
- Rees, H. L., Eggleton, J. D., Rachor, E., and Vanden Berghe, E., 2007: Structure and dynamics of the north sea benthos. ices cooperative research report, 288. Tech. rep., International Council for the Exploration of the Sea.
- Rhoads, D., and Germano, J., 1982: Characterization of organism-sediment relations using sediment profile imaging: An efficient method of remote ecological monitoring of the seafloor (Remots™System). *Marine Ecology Progress Series*, **8(2)**, 115 – 128.
- Ridgway, K. R., 2007: Long-term trend and decadal variability of the southward penetration of the East Australian Current. *Geophysical Research Letters*, **34(13)**, L13613, 5 pp.

- 
- Rogers, C., 1990: Responses of coral reefs and reef organisms to sedimentation. *Marine Ecology Progress Series*, **62(1)**, 185 – 202.
- Rose, C. S., Stoner, A. W., and Matteson, K., 2005: Use of high-frequency imaging sonar to observe fish behaviour near baited fishing gears. *Fisheries Research*, **76(2)**, 291 – 304.
- Rowling, K., Hegarty, A. M., and Ives, M., 2010: Status of fisheries resources in NSW 2008/09. Tech. rep., Wild Fisheries Research Program, Cronulla Fisheries Research Centre of Excellence, PO Box 21, Cronulla, NSW 2230, Australia.
- Russell, B., 1983: The food and feeding habits of rocky reef fish of north-eastern New Zealand. *New Zealand Journal of Marine and Freshwater Research*, **17(2)**, 121 – 145.
- Schlining, B. M., and Stout, N. J., 2006: MBARI's Video Annotation and Reference System. *OCEANS 2006*, 1 – 5.
- Schofield, K. A., and Livingston, M. E., 1996: Trawl survey of hoki and middle depth species on the Chatham Rise, January 1996 (TAN9601). *New Zealand Fisheries Data Report*, **71**, 50.
- Seager, J., 2008: *EventMeasure User Guide Version 2.04*. SeaGIS Pty Ltd.
- Seager, J., 2009a: *CAL User Guide version 1.31*, vol. 1. SeaGIS Pty Ltd.
- Seager, J., 2009b: *EventMeasure Version 2.22*.
- Seager, J., 2009c: *Photomeasure version 1.61*.
- Seavy, N. E., Quader, S., Alexander, J. D., and Ralph, C. J., 2005: Generalized linear models and point count data: statistical considerations for the design and analysis of monitoring studies. *USDA Forest Service General Technical Report PSW-GTR-191*, 744 – 753.
- Shepherd, S. A., Brook, J. B., and Xiao, Y., 2010: Environmental and fishing effects on the abundance, size and sex ratio of the blue-throated wrasse, *Notolabrus tetricus*, on South Australian coastal reefs. *Fisheries Management and Ecology*, **17(3)**, 209 – 220.
- Shepherd, S. A., and Clarkson, P. S., 2001: Diet, feeding behaviour, activity and predation of the temperate blue-throated wrasse, *Notolabrus tetricus*. *Marine and Freshwater Research*, **52(3)**, 311 – 322.

- Shortis, M., Harvey, E., and Abdo, D., 2009: Cost-efficient sampling of fish assemblages: comparison of baited video stations and diver video transects. *Oceanography and Marine Biology: An Annual Review*, **47**, 257 – 292.
- Shortis, M., Harvey, E., and Seager, J., 2007: A review of the status and trends in underwater videometric measurement. *Invited paper, SPIE Conference 6491, Videometrics IX, IS&T/SPIE Electronic Imaging, San Jose, California*, 1 – 26.
- Simpson, E., 1949: Measurement of diversity. *Nature*, **163**, 688 – 688.
- Singh, H., Armstrong, R., Gilbes, F., Eustice, R., Roman, C., Pizarro, O., and Torres, J., 2004a: Imaging coral I: Imaging coral habitats with the SeaBED AUV. *Subsurface Sensing Technologies and Applications*, **5(1)**, 25 – 42.
- Singh, H., Can, A., Eustice, R., Lerner, S., McPhee, N., Pizarro, O., and Roman, C., 2004b: SeaBED AUV offers new platform for high-resolution imaging. *EOS*, **85(31)**, 294 – 295.
- Smith, A. D. M., Fulton, E. J., Hobday, A. J., Smith, D. C., and Shoulder, P., 2007: Scientific tools to support the practical implementation of ecosystem-based fisheries management. *ICES Journal of Marine Science: Journal du Conseil*, **64(4)**, 633 – 639.
- Sokal, R. R., and Rohlf, F. J., 1995: *Biometry: the principles and practice of statistics in biology research*, vol. 1. Freeman, New York, 3rd edn.
- Stoner, A. W., Ryer, C. H., Parker, S. J., Auster, P. J., and Wakefield, W. W., 2008: Evaluating the role of fish behavior in surveys conducted with underwater vehicles. *Canadian Journal of Fisheries and Aquatic Sciences*, **65(6)**, 1230 – 1243.
- Taylor, R. B., 1998: Density, biomass and productivity of animals in four subtidal rocky reef habitats: the importance of small mobile invertebrates. *Marine Ecology Progress Series*, **172**, 37 – 51.
- Thomas, L., 1997: Retrospective power analysis. *Conservation Biology*, **11(1)**, 276 – 280.
- Tolimieri, N., Clarke, M. E., Singh, H., and Goldfinger, C., 2008: Evaluating the SeaBED AUV for monitoring groundfish in untrawlable habitat. *Marine habitat mapping technology for Alaska. Alaska Sea Grant College Program, University of Alaska Fairbanks. CD-ROM*.

- Toohey, B. D., 2007: The relationship between physical variables on topographically simple and complex reefs and algal assemblage structure beneath an *Ecklonia radiata* canopy. *Estuarine, Coastal and Shelf Science*, **71**(1â€“2), 232 – 240.
- Tracey, 2007: *Assessing the population dynamics and stock viability of striped trumpeter (Latriss lineata) in a data limited situation*. Ph.D. thesis, University of Tasmania.
- Tracey, S. R., and Lyle, J. M., 2005: Age validation, growth modeling, and mortality estimates for striped trumpeter (*Latris lineata*) from southeastern Australia: making the most of patchy data. *Fisheries Bulletin*, **103**, 169 – 182.
- Vabø, R., Huse, G., Fernö, A., Jørgensen, T., Løkkeborg, S., and Skaret, G., 2004: Simulating search behaviour of fish towards bait. *ICES Journal of Marine Science: Journal du Conseil*, **61**(7), 1224 – 1232.
- Van Tienhoven, A., Den Hartog, J., Reijns, R., and Peddemors, V., 2007: A computer-aided program for pattern-matching of natural marks on the spotted raggedtooth shark *Carcharias taurus*. *Journal of Applied Ecology*, **44**(2), 273 – 280.
- Watson, D. L., Anderson, M. J., Kendrick, G. A., Nardi, K., and Harvey, E. S., 2009: Effects of protection from fishing on the lengths of targeted and non-targeted fish species at the Houtman Abrolhos Islands, Western Australia. *Marine Ecology Progress Series*, **384**, 241 – 249.
- Watson, D. L., Harvey, E. S., Anderson, M. J., and Kendrick, G. A., 2005: A comparison of temperate reef fish assemblages recorded by three underwater stereo-video techniques. *Marine Biology*, **148**(2), 415 – 425.
- Watson, D. L., Harvey, E. S., Fitzpatrick, B. M., Langlois, T. J., and Shedrawi, G., 2010: Assessing reef fish assemblage structure: how do different stereo-video techniques compare? *Marine Biology*, **157**(6), 1237 – 1250.
- Watson, D. L., Harvey, E. S., Kendrick, G. A., Nardi, K., and Anderson, M. J., 2007: Protection from fishing alters the species composition of fish assemblages in a temperate-tropical transition zone. *Marine Biology*, **152**(5), 1197 – 1206.
- White, D., Svellingen, C., and Strachan, N., 2006: Automated measurement of species and length of fish by computer vision. *Fisheries Research*, **80**, 203 – 210.

- Whitelaw, A., Sainsbury, K., Dews, G., and Campbell, R., 1991: Catching characteristics of four fish-trap types on the North West Shelf of Australia. *Marine and Freshwater Research*, **42(4)**, 369 – 382.
- Wild-Allen, K., Herzfeld, M., Thompson, P. A., Rosebrock, U., Parslow, J., and Volkman, J. K., 2010: Applied coastal biogeochemical modelling to quantify the environmental impact of fish farm nutrients and inform managers. *Journal of Marine Systems*, **81(1-2)**, 134 – 147.
- Williams, A., and Bax, N. J., 2001: Delineating fish-habitat associations for spatially based management: an example from the south-eastern Australian continental shelf. *Marine and Freshwater Research*, **52**, 513 – 536.
- Williams, A., Dowdney, J., Smith, A., Hobday, A., and Fuller, M., 2011: Evaluating impacts of fishing on benthic habitats: a risk assessment framework applied to Australian fisheries. *Fisheries Research*, **112**, 154 – 167.
- Williams, A., Schlacher, T. A., Rowden, A. A., Althaus, F., Clark, M. R., Bowden, D. A., Stewart, R., Bax, N. J., Consalvey, M., and Kloser, R. J., 2010a: Seamount megabenthic assemblages fail to recover from trawling impacts. *Marine Ecology*, **31**, 183–199.
- Williams, K., Rooper, C. N., and Towler, R., 2010b: Use of stereo camera systems for assessment of rockfish abundance in untrawlable areas and for recording pollock behavior using midwater trawls. *Fisheries Bulletin*, **108**, 352 – 362.
- Williams, S. B., Pizarro, O., Jakuba, M., and Barrett, N. S., 2010c: AUV benthic habitat mapping in south eastern Tasmania. In *Proceedings of the 7th International Conference in Field and Service Robotics*, vol. 62 of *Springer Tracts in Advanced Robotics*, Springer Berlin, 275 – 284.
- Williams, S. B., Pizarro, O., Johnson-Roberson, M., Mahon, I., Webster, J., Beaman, R., and Bridge, T., 2008a: AUV-assisted surveying of relic reef sites. *OCEANS 2008*, 1 – 7.
- Williams, S. B., Pizarro, O., Mahon, I., and Johnson-Roberson, M., 2008b: Simultaneous localisation and mapping and dense stereoscopic seafloor reconstruction using an AUV. In *Proceedings of the International Symposium on Experimental Robotics*, Athens.
- Willis, Trevor, J., Millar, R. B., and Babcock, R. C., 2003: Protection of exploited fish in temperate regions: high density and biomass of snapper *pagrus auratus*

- (sparidae) in northern new zealand marine reserves. *Journal of Applied Ecology*, **40**(2), 214 – 227, 10.1046/j.1365-2664.2003.00775.x.
- Willis, T. J., and Babcock, R. C., 2000: A baited underwater video system for the determination of relative density of carnivorous reef fish. *Marine and Freshwater Research*, **51**, 755 – 763.
- Willis, T. J., Millar, R. B., and Babcock, R. C., 2000: Detection of spatial variability in relative density of fishes: comparison of visual census, angling, and baited underwater video. *Marine Ecology Progress Series*, **198**, 249 – 260.
- Wilson, M. F. J., O'Connell, B., Brown, C., Guinan, J. C., and Grehan, A. J., 2007: Multiscale terrain analysis of multibeam bathymetry data for habitat mapping on the continental slope. *Marine Geodesy*, **30**(1), 3 – 36.
- Wood, J., 1996: *The Geomorphological Characterisation of Digital Elevation Models*. Ph.D. thesis, University of Leicester.
- Wraith, J. A., 2007: *Assessing Reef Fish Assemblages in a Temperate Marine Park Using Baited Remote Underwater Video*. Master's thesis, School of Biological Sciences, University of Wollongong.
- Yoccoz, N. G., Nichols, J. D., and Boulinier, T., 2001: Monitoring of biological diversity in space and time. *Trends in Ecology & Evolution*, **16**(8), 446 – 453.
- Yoklavich, M., Greene, H. G., Cailliet, G. M., Sullivan, D. E., Lea, R. N., and Love, M. S., 2000: Habitat associations of deep-water rockfishes in a submarine canyon: an example of a natural refuge. *Fishery Bulletin*, **98**(3), 625 – 641.
- Yoklavich, M. M., Love, M. S., and Forney, K. A., 2007: A fishery-independent assessment of an overfished rockfish stock, cowcod (*Sebastes levis*), using direct observations from an occupied submersible. *Canadian Journal of Fisheries and Aquatic Sciences*, **64**(12), 1795 – 1804.
- Ziegler, P. E., Lyle, J. M., Haddon, M., Moltschaniwskyi, N. A., and Tracey, S. R., 2006: Tasmanian scalefish fishery – 2005. Tech. rep., Tasmanian Aquaculture and Fisheries Institute.
- Zuur, A. F., Ieno, E. N., Walker, N. J., Saveliev, A. A., and Smith, G. M., Eds., 2009: *Mixed Effects Models and Extensions in Ecology in R*. Statistics for Biology and Health, Springer, New York.